Application of Efficient Frameworks for Joint Simulation of Multi-Element Mineral Deposits and Stochastic Optimization of Open Pit Mine Production Scheduling

Mário de Freitas Silva

Degree of Master of Engineering

Department of Mining and Materials Engineering

McGill University

Montreal, Quebec, Canada

Aug. 15, 2014

A thesis submitted to McGill University as a partial fulfilment of the requirements of the degree of Master of Engineering

Dedication

This document is fully dedicated to our almighty God, my parents, my sister, Vó Preta and my beloved Jessica. You are the most important thing in my life. I love you!

Acknowledgements

I would like to thank my supervisor, Dr. Roussos Dimitrakopoulos, for his valuable guidance and support during this journey and for giving me the opportunity to be part of COSMO Stochastic Mine Planning Laboratory.

I am very thankful for my whole family for all the love and care, specially my parents, sister and my beloved Jessica. Thanks to my brother Murilo Teixeira who has been always standing by my side and his omnipresent assistance. I also owe many thanks to my Canadian-Brazilian family, Ana and Vitor for all their support.

I would like also to show my great gratitude to all my research colleagues at COSMO lab and the valuable guidance and assistance received from Dr. David Machuca-Mory, Dr. Amina Lamghari, Ryan Goodfellow, Luis Montiel and James Macneil. Thanks a lot Debbie and Barbara for assisting in every administrative matter. Last but not least, I would like to thank many other individuals here and in Brazil who, in one way or the other, helped me during these years in Montreal.

For you Prof. Claudio Lucio, I will be always thankful for teaching me how to be a great man and professional.

The work in this thesis was funded by Canada Research Chair (Tier I) in "Sustainable Mineral Resource Development and Optimization under Uncertainty", NSERC Collaborative Research and Development Grant CRDPJ 411270 -10, "Developing new global stochastic optimization and high-order stochastic models for optimizing mining complexes with uncertainty" with industry collaborators: AngloGold Ashanti, Barrick Gold, BHP Billiton, De Beers, Newmont Mining and Vale and NSERC Discovery Grant 239019.

Contribution of Authors

This section states the contribution of the co-author of the papers that comprises the present work. The author is the primary author of all the work presented herein, which was done with the normal supervision, advice and orientation of his advisor Prof. Roussos Dimitrakopoulos, who is also the co-author of all the papers to be published. Moreover, Dr. Amina Lamghari is an additional co-author of the paper presented in Chapter 3.

Chapter 3: de Freitas, M., Dimitrakopoulos, R. & Lamghari, A. (2013). Solving a Large SIP Model for Production Scheduling at a Gold Mine with Multiple Processing Streams and Uncertain Geology.

Chapter 4: de Freitas, M. & Dimitrakopoulos, R. (2014). Simulation of weathered profiles coupled with multivariate block-support simulation of the Puma Nickel Laterite Deposit, Brazil.

Abstract

The optimization of open pit mine production scheduling (OPMPS) is an intricate process due to its size and uncertainty of key input parameters. Over the last decade, substantial effort has been made towards the development of new stochastic frameworks that incorporates uncertainty into the decision process. However, due to the intrinsic complexity of the mathematical programming formulation and the large size of mineral deposits, finding an exact solution for the OPMPS is likely intractable. In addition to that, modelling the joint spatial uncertainty of mineral deposits accounting for several correlated geological attributes, significantly increases the complexity of these stochastic frameworks. These observations motivate the development of new computationally efficient approaches for generating joint stochastic simulations of a deposit and for solving the OPMPS under geological uncertainty. This thesis considers both aspects in its two main parts.

In the first part of this thesis, an efficient heuristic solution approach is applied and tested to the stochastic mine production scheduling of a relatively large gold mine containing about 120 thousand blocks and considering a set of fifteen geological scenarios generated stochastically. The stochastic integer programming (SIP) formulation addresses multiple processing streams and a 'grade' stockpile which adds flexibility to the specific operation by advancing the processing of highly valuable material. The solution approach tested herein, first generates an initial feasible solution by sequentially solving the stochastic OPMPS period by period and afterwards, a network flow algorithm is used to sequentially search for further improvements. In this network graph the nodes identify candidate blocks which might have their extraction either postponed or advanced, aiming for new schedule with higher values and lower risk. The results show that production schedules with low deviations from production expectations can be generated in a reasonable time for an actual mining environment.

In the second part, an efficient joint simulation framework is demonstrated though an application to Vale's Puma deposit, a major nickel laterite asset in Brazil. To integrate the variability of the revolting profiles, their 'true' thicknesses are jointly simulated using min/max autocorrelation factor (MAF). The realizations serve as geological boundaries within which Ni, Co, Fe, SiO2, MgO and dry-tonnage factor (DTF) can be jointly simulated directly at block support scale. The

final result is a set of equiprobable representations of the deposit that incorporates both grade and tonnage uncertainty. These simulations can be used to assess the uncertainty about key aspects of the project, such as strict control of the ore's quality that feeds the metallurgical plant. The framework explored takes advantage of the MAF and direct block simulation approaches which facilitate the joint simulation of large multi-element deposits.

Résumé

Le problème d'optimisation de la production des mines à ciel ouvert (POPM) est un problème complexe en raison de sa taille et de l'incertitude associée à ses paramètres clés. Au cours de la dernière décennie, des efforts considérables ont été déployés pour élaborer des nouveaux cadres stochastiques intégrant l'incertitude dans le processus de décision. Toutefois, en raison de la complexité intrinsèque de la formulation mathématique du problème et de la grande taille des dépôts minéraux, trouver une solution exacte pour le POPM est probablement impensable vu temps de calcul induit. De plus, la modélisation de l'incertitude spatiale commune de gisements minéraux tenant compte de plusieurs attributs géologiques corrélés augmente de manière significative la complexité de ces cadres stochastiques. Ces observations motivent le développement de nouvelles approches efficaces pour générer des simulations stochastiques communes d'un dépôt et pour résoudre le POPM sous incertitude géologique. Cette thèse considère ces deux aspects dans ses deux parties principales.

Dans la première partie de cette thèse, une approche de résolution heuristique efficace est appliquée et testée pour la planification stochastique de le production d'une mine d'or relativement grande contenant environ 120 000 blocs et considérant un ensemble de quinze scénarios géologiques générés de façon stochastique. La formulation de programmation stochastique en nombres entiers tient compte de plusieurs installations de traitement et d'une « réserve » qui ajoute de la souplesse à l'opération en avançant le traitement des blocs ayant une grande teneur en minerai. L'approche de résolution testée génère d'abord une solution initiale réalisable en résolvant successivement des sous-problèmes du POPM stochastique, où chaque sous-problème est associé à une période. Par la suite, un algorithme de flot dans les réseaux est utilisé séquentiellement pour obtenir des améliorations supplémentaires. Dans le réseau associé au problème de flot, les nœuds représentent les blocs candidats qui pourraient voir leur extraction retardée ou avancée pour générer un nouveau calendrier de production de valeur plus élevée et présente un risque moindre. L'approche de résolution décrite ci-dessus a été testée dans un environnement minier réel et les résultats montrent que des calendriers de production proches des prévisions peuvent être générés en un temps de calcul raisonnable.

Dans la deuxième partie de la thèse, l'efficacité d'un cadre de simulation est démontrée à travers une application au cas du dépôt minéral Puma de Vale, une importante latérite de nickel située au Brésil. Pour intégrer la variabilité des profils révoltants, leurs épaisseurs « réelles » sont simulées conjointement en utilisant le facteur d'auto-corrélation min /max (MAF). Les réalisations servent de limites géologiques dans lesquelles Ni, Co, Fe, SiO2, MgO et le facteur de tonnage (DTF) peuvent être conjointement simulés directement à l'échelle du bloc. Le résultat final est un ensemble de représentations équiprobables du dépôt minéral qui intègrent l'incertitude associée aussi bien à la teneur du minerai qu'au tonnage. Ces simulations peuvent être utilisées pour évaluer l'incertitude liée aux aspects clés du projet, tels que le contrôle strict de la qualité du minerai qui alimente l'usine métallurgique. Le cadre exploré tire parti de la MAF et des méthodes de simulation directs à l'échelle du bloc qui facilitent la simulation de grands dépôts qui contiennent des éléments multiples.

Table of Contents

List of Figures

List of Tables

List of Abbreviations

NPV: Net present value

BEV: undiscounted block economic value

LOM: Life-of-Mine

OPMPS: Open-pit mine production scheduling

COG: Cut-off grade

SIP: Stochastic integer programming

MIP: Mixed integer programming

BC: Branch-and-cut

GH: Greedy heuristic

CPLEX: IBM ILOG CPLEX Optimization studio

RF: Random Field

PCA: Principal component analysis

MAF: Minimum/Maximum autocorrelation factors

LMC: Linear model of corregionalization

JD: Joint diagonalization

SGS: Sequential Gaussian simulation

SIS: Sequential indicator simulation

DBSIM: Direct block simulation

MPS: Multiple-point simulation

HOSIM: High-order simulation

LU: Lower/Upper

DTH: Down-the-hole

TTK: True thickness

Chapter 1

Introduction

"If you are in a shipwreck and all the boats are gone, a piano top buoyant enough to keep you afloat that comes along makes a fortuitous life preserver. But this is not to say that the best way to design a life preserver is in the form of a piano top."

Operating manual for Spaceship Earth, R. Fuller

Mining is a largely capital intensive venture, because it demands high efficiency on management decisions, which are taken under conditions of uncertainty. Over the past decades, mining has experienced important trends: increasingly complexity of mineral deposits, more strict environmental regulations, a more competitive global market and the everlasting pressure over operational costs. As a result, robust and concise methodologies are increasingly required for the assessment of mineral projects, building the basis for solid investment decisions.

Mine planning is one of the core decision making processes during mineral project evaluations and it aims to provide a realistic plan to profitably exploit the mineral resources. The uncertainty regarding several parameters, such as the orebody delineation and its metal content, or the future commodity prices, prevents the definition of a truly optimal plan. For forty years now, (David, *et al.*, 1974), it has been well known that estimated orebody models established for assessment of ore resources may not be satisfactory for planning purposes, since it is not able to reveal the spatial uncertainty and true variability of the deposit. During the last decade, several authors have proposed new stochastic driven frameworks to incorporate uncertainty into mine planning process (e.g., Godoy, 2003; Ramazan and Dimitrakopoulos, 2013). In the case of geological uncertainty, stochastic simulation techniques are used to generate multiple equally probable representations of the deposit (e.g., Journel, 1974).

Despite of the significant achievements in the field, the practical implementation of stochastic driven approaches in the mining industry is still limited. The main contributor for that is the additional complexity involved for the incorporation of multiple scenarios

and the generation of these scenarios themselves, meaning a heavy allocation of additional time and resources. This has strongly motivated the development of new efficient methods for the generation of stochastic simulations and for solving the stochastic optimization problem during the last few years.

1.1 Goal and Objectives

The goal of this thesis is to test efficient frameworks for both the generation of stochastic joint simulations of mineral deposits, and open-pit mine production scheduling under geological uncertainty. To achieve this goal, the following objectives are set:

- Review the literature concerning incorporation of uncertainty into mine planning routines, in particular to open-pit mine production scheduling, and review the literature of conditional stochastic simulation methods, focusing on joint simulation techniques.
- Apply a heuristic solution approach to solve a stochastic integer programming formulation for the open-pit mine production scheduling in a gold deposit, highlighting different options to generate an initial solution and for dealing with a stockpile.
- Apply minimum/maximum autocorrelation factor and direct block simulation techniques for the joint simulation of geological domains, and multi-elements, in a nickel laterite deposit.
- Provide conclusions and suggest further works related to the topic.

1.2 Thesis Outline

The thesis is organized according to the following chapters:

- Chapter 1 introduces the subject of the thesis, along with the goals, objectives and the thesis outline.
- Chapter 2 brings a literature review on the incorporation of uncertainty into mine planning, in particular to the life-of-mine open-pit mine production scheduling. In addition, a literature review on stochastic simulation is shown, stressing joint simulation of multivariate deposits.

- Chapter 3 describes a heuristic solution approach for solving a stochastic integer programming formulation of the open-pit mine production scheduling, with an application to a gold deposit.
- Chapter 4 describes efficient methodologies for joint simulation of multivariate deposits, and their application to a major nickel laterite deposit.
- Chapter 5 addresses the main conclusions and suggests related future work.

Chapter 2

Literature Review

"Life is uncertain. Eat dessert first"
Ernestine Ulmer

In long-term mine planning, several decisions must be taken with incomplete knowledge about key input parameters. This inherent uncertainty of mining projects may arise from different sources (e.g., technical, market prices, market costs, environmental, political, social, etc.) and their relative importance depends on several features intrinsic to each project. Nevertheless, geological uncertainty is usually seen as one of the major contributors for projects to not meet their expectations (Vallee, 2000; Baker and Giacomo, 2001; Dimitrakopoulos *et al.*, 2002). Such uncertainty is mainly associated to the characteristics of the deposit itself, for example, its intrinsic variability, and the degree of knowledge gathered from it, as the geological information about the deposit is based on sparse drilling and a limited number of samples.

In traditional open-pit mine production scheduling (OPMPS) framework, all the input parameters, including the spatial distribution of geological attributes, such as grades, is deemed to be known (Lerchs and Grossman, 1965; Johnson, 1969; Piccard, 1976; Kim, 1979; Dagdelen and Jonhson, 1986; Whittle, 1988; Tolwinski and Underwood, 1996; Cacceta and Hill, 2003; Boland *et al.* 2009). An average type representation of the deposit is used as input to a decision making process, which aims to provide a feasible sequence of extraction that maximizes the discounted economic return. However, as one may note in a later example, even if this sequencing is optimal for a given set of inputs, it might lead to very different results as the reality departs from the initial assumptions. In mine planning when uncertainty is not ignored, it is often treated in very simplistic frameworks, such as through the practice of conservatism (e.g., overestimating costs and/or underestimating grades) or sensitivity analysis. Ravenscroft (1992) calls the

attention to the deliberate use of measures for confidence limits to assess risks in mine production.

Several authors (David *et al.*, 1974; Ravenscroft, 1992; Dowd, 1994, 1997; Dimitrakopoulos, *et al.*, 2002) show the impact of geological uncertainty by means of conditional simulations, for a risk-analysis on the operational and financial performance of mining schedules. Pioneering work is carried out by David *et al.* (1974), where the authors perform a study to analyse the ability of kriging on providing an interpolated model to the definition of an ultimate pit. In their study, a simulated orebody model is used to emulate a real deposit. After sampling this simulation, a kriged model is derived and the Korobov algorithm is used to calculate the final pit boundaries at different cut-off grades. Their results show significant discrepancies between the emulated reality and forecasted returns, raising important questions about the matter. Dimitrakopoulos *et al.* (2002) perform a risk analysis, overlapping different geostatistical simulations on optimized pit shells of an Australian gold mine. Assessing the probability distributions of the net present value associated to each of those nested pits, they develop a case study which shows that the estimated model substantially overestimates the net present value. For the ultimate pit chosen in their case study, the probability is about 2-4% on achieving the same results as suggested by the ordinary kriging model and the most likely NPV is 25% smaller than the one forecasted with the kriging model. This study helps to highlight that, using an average type model as input to conventional optimizers, does not result in an average type of response.

All studies above converge to a common conclusion that, using a smoothed image representation of the geological reality may lead to unpredictable response parameters of interest, when applying non-linear transfer functions, such as optimization routines for scheduling and design. In general, interpolated orebody models reduce the intrinsic variability of the deposit and to do not reproduce its spatial pattern of variability (Goovaerts, 1997).

2.1 Moving forward from deterministic models

An intuitive introduction about how stochastic models may enrich the mathematical formulations and lead to better decisions is demonstrated by King and Wallace (2012).

They show an example of a news vendor, who has to take a decision about the total amount of newspapers to bring every day. There are three different newspaper editions: political, business and regional. He knows that the first two newspapers are among the primary preference of the customers (these are also the most profitable), but if they do not find their preferred newspaper they necessarily buy the regional one. Hence, if the news vendor knows the exact number of customers who are willing to buy either political or business newspapers in a given day, he does not need to bring regional ones, since everybody will leave happy his newspaper stall. Therefore, assuming the demands are known, the solution of the deterministic problem becomes trivial. However, if the reality is different of what he is expecting, he will not cover the demand of either political or business newspaper, and some customers will leave without a newspaper because the owner did not hedge his business by bringing any regional papers (which would be the customer's second option). This shows that the model will be actually 'infeasible' for any demand different of the one initially expected. These results highlight that optimization procedures aim to find their best with the information they have, but they might result in very poor result if the reality comes to be different.

From this news vendor example, it can be concluded that modelling the demand of each newspaper as uncertain and incorporating it in the mathematical formulation of the problem, leads to a result that the seller must always take regional papers. This should be an intuitive solution from the beginning, because it is very unlike that the vendor will correctly guess the demand for political and business papers. In the case this happens, he would still have regional papers to sell and shelter himself from major losses (get stuck with left over business/political newspapers). This observation leads to another important observation, which is related to the fact even if some property is present in every deterministic solution (for any demand forecasted, he would never take regional newspapers), it does not necessarily carry over to the optimal solution when uncertainty is incorporated, with severe effects on downstream engineering process, as for example long documented in petroleum reservoir forecasting (e.g., Wolcott and Chopra, 1993).

2.2 Incorporation of uncertainty into mine planning routines

Once several limitations regarding the use of a smoothed representation of the deposit into mine planning decision processes were understood, researches started to focus on the development of new tools which are able to incorporate such geological uncertainty. An intuitive way of accomplishing that is to independently apply a conventional optimizer to multiple simulated geological scenarios. Based on this idea, Whittle and Bozorghebrahami (2007) propose a hybrid-pit framework to find the intersection of multiple ultimate pits generated one for each conditional simulation, aiming the design of "robust" ultimate pit limits. Aiming to find robust mining phases and pit limits, Dimitrakopoulos *et al.* (2007) carry out several risk-analysis for multiple candidate mine designs, trying to find the one with high probabilities to fulfill the mill requirements and at the same time maximizes the upside potential and minimizes the downside risks relative to an economic reference point termed minimum acceptance return (MAR). Such method is tedious in as much as multiple designs must be done one for each simulated model and the solution does not correspond to the optimal one since it only considers a small set of alternatives.

The next logical step is to develop novel tools which are able to incorporate geological uncertainty directly into their formulation for the mine production scheduling. One of the avenues of research to accomplish such a goal is to formulate the problem as a mixed integer programming (MIP) model, but now taking into account the local uncertainty associated to each of the blocks. Dimitrakopoulos and Ramazan (2004) incorporate the probabilities of each block to have a quality within a desired interval through a constraint that limits the possible deviations from a production target. An important concept brought by the authors in this paper is the geological risk discounting (GRD), postponing larger risks to later periods. A major drawback of this approach, and other probabilistic based approaches that only incorporates local uncertainty through summarized probabilities is their inability to incorporate spatial uncertainty into the optimization process (Ramazan and Dimitrakopoulos, 2004b; Grieco and Dimitrakopoulos, 2007). A very simple example that shows such a limitation can be illustrated as follows. Imagine two neighboring blocks of the deposit which are likely to be mined together (given a realistic

operation which seeks minimum equipment relocation). In one simulated orebody model, the first of these blocks is ore and the other is waste, but in a second scenario their destinations are inverted (i.e., the second block is ore and the first is waste). If one limits the scheduler to look at each of those blocks individually, they are indeed very uncertain (the odds of having ore/waste are 50/50 for each block). However, if the optimizer could assess their joint uncertainty, it would be actually observed that by mining both blocks it is very likely (100% certainty, regarding the two simulated scenarios) that 50% of the material is ore and 50% is waste.

Morales and Rubio (2010) also propose a robust approach that aims to maximize the number of scenarios for which production goals are achieved. However, the effects of the "bad cases" are not well captured by such approach, which is a common problem seen in chance-constrained models.

Menabde *et al.* (2007) develop a Mixed Integer Programming model that accounts for a variable cut-off grade (COG) during the LOM and handles geological uncertainty through constraints that do not allow processing and mining capacities to be exceeded on the average of the multiple conditional simulations. In other words, the formulation simply enforces that the expected performance of the mining operation meets the desired targets, but does not minimize the deviations from production targets and hence, it cannot guarantee a robust performance under uncertainty.

2.2.1 Two-stage formulations for a stochastic OPMPS

An approach on how to incorporate uncertainty into decision problems is brought by the field of stochastic programming, which is built over the pillar that decisions can be separated in two different sets: the ones that have to be taken without full knowledge of the random process and the ones that can be taken after the random experiment takes place (King and Wallace, 2012; Birge and Louveaux, 2011). Such approach brings the idea that recourse decisions can then be made in a second stage in order to compensate for any bad effects that might have been experienced as a result of first stage decisions. Stochastic programming is based on splitting the problem in multiple stages, which are points in time where decisions are made. Usually, the information available at each of those stages is very different. In the news vendor example of King and Wallace (2012),

the first stage is the point in time when the orders are placed and the second stage corresponds to the amounts to be sold after the demand is revealed. In one way or another, the methodologies to be presented in the following paragraphs share a multi-stage structure, either incorporated into heuristic approaches or in a more explicit way, through a formal mathematical programming model.

Godoy (2003) implements a multi-stage mine production scheduling framework, adapting a combinatorial optimization algorithm based on Simulated Annealing (Kirkpatrick *et al.*, 1983; Geman and Geman, 1984). In Godoy's approach, the goal is to generate a final sequence of extraction which combines multiple mining sequences, one for each simulated orebody model, in order to minimize the risks related to deviations from production targets. This is accomplished by minimizing the following objective function:

$$Min\ O = \sum_{p=1}^{P}\left(\sum_{s=1}^{S}\left|\theta_p^*(s) - \theta_p\right| + \sum_{s=1}^{S}\left|\omega_p^*(s) - \omega_p\right|\right) \tag{2.1}$$

which consists on minimizing the differences between the ore and waste production ($\theta_p^*(s)$ and $\omega_p^*(s)$) respectively, when considering the S different geological scenarios, and the desired targets (θ_p and ω_p) over all the production periods P.

The algorithm proceeds as follows, from the initial set of mining sequences the probabilities of each block to be mined in each period (transition probability); when the same scheduling decision to a given block is the same over all the scenarios, its period is frozen; otherwise, it is considered during the annealing process which consists on randomly selecting blocks to have their period swapped to feasible candidate periods accordingly to its transition probability. Hence, the system is iteratively perturbed in order to provide a single schedule that minimizes the deviations from production targets, which is assessed through (2.1). All favourable perturbations ($O_{new} \leq O_{old}$) are accepted and unfavourable ones are accepted accordingly to an exponential distribution, $exp(O_{old} - O_{new}/T)$, which varies with time accordingly to the so-called *annealing temperature* T. The annealing starts with a high-temperature, which increases the probability of accepting unfavourable perturbations and reduces the chances of the

optimization to get trapped into local minima. Then, a cooling factor is sporadically applied to assist the process to converge into a final solution.

As one may note, in one stage, Godoy's approach explores different parts of the solution space, generating different feasible mining sequences, with "performances" assessed through different geological scenarios in a second stage, fully incorporating geological uncertainty into the mine production scheduling. Thus, the evaluation of the objective function in Eq. (2.1) works as a recourse action that guides the perturbation mechanism for the creation of new schedules. In a case study for the Fimiston pit in Western Australia, Godoy (2003) shows that the stochastic approach has a potential of increase by 28% the NPV of the project when compared to the forecasted value reported by the conventional OPMPS routine. Godoy (2003) observes that the major contribution to this difference comes from the fact that despite that the same total amount of metal is comprised in both schedules, the stochastic approach is able to advance the metal production to earlier periods and at the same time deferring the extraction of waste. Coupled to the potential economic improvements, the stochastic approach is able to provide more realistic schedules, inasmuch as risk analysis shows that the largest deviation from ore target production is expected to be no larger than 4% while for the conventional schedule the deviations are in order of 13% during several years.

As one may note, Godoy's approach provides not only a risk resilient solution to the OPMPS (by driving the schedule through zones where the risk of not achieving production targets are minimized), but it also increases the asset value by considering an inherent source of uncertainty and risk. The approach is also flexible to incorporate other sources of uncertainty and goals in Eq. (2.1). Major shortcomings are the setup process of several abstract parameters for the annealing mechanism and the definition of multiple schedules, one for each simulated model.

Leite and Dimitrakopoulos (2007) further explores the capability of the simulated annealing framework for the stochastic mine production scheduling of a disseminated copper deposit, showing that even for a deposit with relative low-variability the stochastic approach is able to improve the NPV by 26% when compared to the forecasts of a conventional scheduler. Albor and Dimitrakopoulos (2009) test the sensitivity of the

methodology regarding different parameters. In addition, a case study is performed to compare stochastically generated optimal pit limits to conventional ones, along with the related production schedules both generated stochastically. Their results show that the stochastic approach leads to larger pit limits, increasing the LOM by one year and the NPV by 10%. The authors conclude that this difference in economic performance is associated to a 'cost' on ignoring uncertainty and assuming a 'perfect knowledge' of the metal content and distribution in the deposit. In contrast to the deterministic optimization, the stochastic approach is able to aggregate value and to explore potential opportunities, such as by expanding the LOM.

More recently, Montiel and Dimitrakopoulos (2013a) implement the approach in a more complex mining environment, adapting the objective function to account for multiple processing destinations and material types. In their application, the deviations of ore and waste production from desired targets are significantly reduced. Goodfellow and Dimitrakopoulos (2013a) extend the idea of simulated annealing to generate stochastic pushbacks in multi-process operations. Their algorithm is successfully applied to BHP Billiton's Escondida Norte mine showing a reduction up to 61% of the variability in terms of quantities of material sent to the various processes with respect to the conventional design.

2.2.1.1 Stochastic Integer Programming (SIP)

In mathematical programming, the classical two-stage stochastic linear programming with fixed recourse, originally defined in Dantzig (1955) is the problem of finding:

$$\min z = c^T x + E_{\xi}[\min q(\omega)^T y(\omega)] \tag{2.2}$$

$$s.t.\ Ax = b \tag{2.3}$$

$$T(\omega)x + Wy(\omega) = h(\omega) \tag{2.4}$$

$$x, y(\omega) \geq 0 \tag{2.5}$$

In this formulation, the objective function in Eq. (2.2) contains a deterministic component, led by the vector of first stage decision variables x, and the expectation of a second-stage objective $q(\omega)^T y(\omega)$ taken over all the realizations of the random process

$\boldsymbol{\zeta}$. Therefore, for each realization ω, the second-stage decision variables $y(\omega)$ are the solution of a linear program, such that:

$$\mathrm{Q}(x,\omega) = \min_{y}\{q(\omega)^T | Wy = h(\omega) - T(\omega);\ x, y \geq 0\} \tag{2.6}$$

Therefore, for each scenario ω, optimal decisions regarding the second-stage decision variables will be taken with a prior knowledge of first-stage decision variables. The formulation (2.2)-(2.5) is the simplest form of a stochastic two-stage program and extensions can be easily modeled. For example, if some of the first-stage or second-stage decisions are to be integers, constraint (2.5) can be replaced to restrict the variables to an integer space (Birge and Louveaux, 2011). Such a formulation is called stochastic integer programming (SIP).

Ramazan and Dimitrakopoulos (2007) introduce a SIP optimization model for the OPMPS. This work was an initial start-up of a fully developed model in Ramazan and Dimitrakopoulos (2013). In this model, the NPV is maximized over the life-of-mine (LOM), accounting with a recourse action to minimize deviations in tonnage, grades, and metal production from desired targets. The objective function is:

$$\max z = \sum_{t=1}^{Np}\Bigg\{\underbrace{\sum_{i=1}^{Nblocks} E\left[(NPV)_i^t\right]x_i^t}_{\text{Part 1}} - \underbrace{\sum_{j=1}^{Nstck}\left[E\left[(NPV)_j^t\right] + MC_j^t\right]w_j^t}_{\text{Part 2}} + \underbrace{\sum_{s=1}^{nSims}(SV^t/nS)k_s^t}_{\text{Part 3}} - \underbrace{\sum_{s=1}^{nSims}\left(c_u^{to}\,d_{su}^{to} + c_l^{to}\,d_{sl}^{to} + c_u^{tg}\,d_{su}^{tg} + c_l^{tg}\,d_{sl}^{tg} + c_u^{tq}\,d_{su}^{tq} + c_l^{tq}\,d_{sl}^{tq}\right)}_{\text{Part 4}}\Bigg\} \tag{2.7}$$

The Part 1 of the objective function accounts for the total expected NPV of all blocks mined in a given period. The decision variable x_i^t represents the fraction of a block i which is mined in a period t. If such variable is binary, it is equal to one if block i is mined in period t and zero otherwise. Part 2 adjusts the total value previously accounted from Part 1, considering that a percentage of the blocks being mined (w_j^t) will be sent to the stockpile and not processed at period t. Therefore, from the total value added in Part 1, only the mining cost (MC_j^t) actually incur during that given period. Part 3 adds the value of an amount of ore (k_s^t) reclaimed from the stockpile. The unitary value

(dollars/ton) associated to this material is given by the parameter SV^t. One may note that, in contrast to the decisions in Part 1 and 2, the amount of material considered in this part is scenario dependent. First, the model must take the decision when to mine a given block, without the full information being known. However, the model assumes that at the time of the decision about the amount of material to be reclaimed from the inventory, complete information about the mined blocks is known: whether the material from the mine is enough to supply the processing plant or not, and what is the shortage. Part 4 is devoted for the management of geological risks. Such risk is assessed through lower (d_{sl}^{t*}) and upper (d_{su}^{t*}) deviations from ore tonnages (o), grades (g) and metal targets (q), for each scenario s. Associated to these deviations there are costs ($c_{u/l}^{t*}$) to be incurred at each period, in order to penalize the risk of not attending the project expectations. Usually, it is desired to meet production targets at early stages of the LOM, so that the initial capital expenditures can be recovered as earlier as possible and the financial risks minimized. To accomplish such risk management over time, the concept of geological risk discounting (GRD) is used. Therefore, the costs associated to the excess and deficient production decreases over the LOM by the application of a discounting rate.

The deviations of Part 4 are calculated through scenario-dependent constraints in the formulation. Equation (2.8) exemplifies how it is modelled for the case of ore tonnage targets (O_{tar}):

$$\sum_{i=1}^{Nblocks} O_{si} x_i^t - \sum_{j=1}^{Nstck} O_{sj}\, w_j^t + k_s^t + d_{sl}^{to} - d_{su}^{to} = O_{tar} \qquad \forall\, s,t \qquad (2.8)$$

The first two sums account for the total tonnage of material mined in period t which is sent straight to the processing plant (O_{s*} is the tonnage of a given block in a given scenario s). k_s^t accounts for the amount of ore reclaimed from the stockpile and feeding the processing plant in period t. Thus, if the total tonnage of ore feed in a given period is equal to the target (O_{tar}), no deviations are accounted for. Otherwise, the equality forces one of the deviation terms to assume a value, addressing either an excess or a shortage in ore production. It is noteworthy that, because these deviations are associated to costs in the objective function (2.7), only one of them takes place at a time. Constraints of the

same nature of (2.8) are built for assessment of grade and metal deviations from targets. An additional set of constraints is introduced for flow stream control of material associated to the stockpile; *slope constraints* guarantee geotechnical stability for the mining operation, setting predecessors of blocks that are mined to reach an underlying block; *reserve constraints* guarantee that blocks mined only once during the LOM; and *mining capacity* constraints force the total rock movement (ore and waste) to be inside a desired range. As one may note, the introduction of penalties in the objective function (2.7) adds a great flexibility for managing risks over the LOM. One may choose, for instance, to asymmetrically control the risks associated to excess or shortages, penalizing one more than the other.

The application of SIP for the OPMPS is presented in Ramazan and Dimitrakopoulos (2013) for a small gold mine (~20 000 blocks). The stochastic approach was able to reduce the risks of not meeting production targets and to increase the NPV of the project by 10% if compared to the results given by a deterministic OPMPS.

This SIP approach introduced by Ramazan and Dimitrakopoulos (2013) formed the basis for further studies. Using the same formulation, a case study is shown for a copper deposit in Leite (2008) and Leite and Dimitrakopoulos (2009), but without considering stockpiles or controlling risks over grades and metal productions. The authors report an improvement of 29% for NPV when compared to the results of a conventional deterministic framework. Albor and Dimitrakopoulos (2010) use SIP to assist on finding robust and valuable pushback designs. In their framework, a series of nested pit shells is found by a pit parameterization technique (Whittle, 1988). Then, for the different number of pushbacks desired, intermediate pits are found by grouping the nested pits that lead to maximum NPVs. In a final stage, when the problem is reduced to the decision about the optimal number of pushbacks, each design previously defined is used to guide in the generation of different LOM production schedules through SIP. In the end, the design that leads to the best performance in terms of NPV maximization and risks minimization is chosen. Although their results lead to a larger pit and an increase of 30% for NPV when compared to a conventional approach, it is a laborious workflow because a SIP model needs to be solved several times.

Benndorf (2005) and, Benndorf and Dimitrakopoulos (2013) show an application to a multivariate iron ore deposit in Australia. In their proposed framework, a joint-simulation methodology similar the one to be presented in Chapter 4, is used to model the joint spatial uncertainty of the elements considered. Then, a SIP model is used to minimize the deviations from production targets, in terms of tonnes and ore quality, and at the same time providing a smoothed schedule to facilitate equipment management and relocation during the operation. Their results demonstrate the ability of the approach to control risks of deviating from production targets for critical quality-defining elements in iron ore operations such as SiO_2 and Al_2O_3. Jewbali (2006) and, Dimitrakopoulos and Jewbali (2013) describe an application of a SIP model which integrates long and short-term planning. This is done by first extracting the spatial relationship of exploratory drill holes and grade control data from mined out areas, which serves as basis for a joint-simulation to be used as future grade control data in unexploited sites of the deposit. Secondly, a conditional simulation based on successive residuals is used in order to update existing representations of the orebody, incorporating future data that will be gathered by the time of the exploitation. Finally, the SIP approach is applied on the updated model of uncertainty, which is now coherent with the level of information available by the time of the mine operation. Their case study at Surnrise Gold Mine in Australia has shown an increase of 230M (AUD) if compared to the values reported by the conventional mine's LOM studies of the same year.

Boland *et al.* (2008a) develop a multi-stage stochastic programming approach for the OPMPS. In their formulation, the authors consider aggregates rather than blocks, modelling both mining and processing decisions through linear variables (Boland *et al.*, 2008b). The work is founded on the principle that mining is a '*learning process*,' such that new information gained through the excavation ought to influence in future mining schedule decisions. For the authors, schedules should be able to adapt over time in response to information acquired during the mining process. For that, they use non-anticipative constraints, also called *implementable* constraints, commonly used in scenario tree structured problems (King and Wallace, 2012). Because in the mine context the values are drawn from a continuous space and simulated models tend to be strictly different one from the other, the authors needed to define their own measure to quantify

how dissimilarities of two simulated orebody models, based on aggregate's properties. Based on that, non-anticipative constraints are modelled in order to ensure that, if the optimizer is not yet able to distinguish between two scenarios in a time period t or in any earlier period, the same set of decisions must be taken under both scenarios. Therefore, in theory, solving such a model with relaxed non-anticipative constraints leads to the *wait-and-see* solution (Birge and Louveaux, 2011), in which optimal sequences are found for each simulated model and then averaged out. Their case studies show an average improvement of an order of 2% in NPV if compared to the application of their deterministic formulation (out of an average 5% improvement brought by the "perfect information").

A major drawback of this multistage approach developed by Boland *et al.* (2008a) is the practicality for mining engineers, since it generates a dynamic schedule that is not directly applicable and cannot be used for subsequent studies. Moreover, the solutions might be unstable if tested with other geological simulations, and the method does not easily accommodate additional elements of a mining complex, such as stockpiles and several processing stream options.

2.2.1.1.1 Seeking for efficient solution approaches for the SIP

OPMPS models are in the class of NP-hard problems (Gleixner, 2008; Bienstock and Zuckerberg, 2010), which means that there is no known polynomial-time algorithm for this problem. In addition, because mineral deposits usually comprises thousands to several millions of blocks, it is most likely not appropriate to solve large-scale OPMPS models using exact methods for integer programing. One way to deal with the prohibitive size of the OPMPS model is to reduce the number of integer variables, for example by aggregating blocks into larger units (e.g., Ramazan, 2007; Boland *et al.*, 2008). Another way is through the development of solution approaches based on heuristic and metaheuristic methodologies for solving realistic-size instances, providing good feasible solutions in a reasonable amount of time when compared to mathematical programming solvers such as CPLEX.

In the case study presented in Ramazan and Dimitrakopoulos (2013), the authors implement the following strategies for solving the SIP model: (a) linear relaxation of binary variables associated to waste blocks (in a previous paper, Ramazan and Dimitrakopoulos (2004a) show that such approach significantly reduces the number of binary variables without generating major issues, because waste blocks are linked to ore blocks and the later forces the complete extraction of waste blocks); (b) a first stage relaxing the stochastic constraints to provide an initial solution for the second stage where the original problem is solved; (c) a divide and conquer scheme to solve the model sequentially for different group of periods.

Heuristic and metaheuristic algorithms can also be used to solve complex problems such as OPMPS more quickly than exact methods, or for at least finding an approximate solution when exact methods fail to find any feasible solution, which is the case of large mineral deposits. Focusing on providing an efficient solution method to tackle large instances of the stochastic OPMPS, Lamghari and Dimitrakopoulos (2012) propose a metaheuristic method based on tabu search (TS). The model used in their paper is similar to the two-stage SIP model with recourse from Ramazan and Dimitrakopoulos (2012) with just minor differences. Their methodology starts from an initial feasible solution, which is iteratively modified by looking for different solutions in its neighbourhood. These new solutions are generated by shifting the period of some blocks, keeping the feasibility of the problem and improving the objective value. A tabu list is used to avoid reversing short-term shifts. When the tabu search terminates (a given number of successive non-improving iterations is reached), a diversification strategy is applied to generate new starting solutions for a further tabu search. The authors test two diversification strategies: a long-term memory diversification strategy, which move blocks to periods that they have rarely been; and a variable neighbourhood strategy, which takes the best solution found so far and applies a period shifting to k different blocks while maintaining feasibility. Their results show that the first diversification strategy outperforms the second strategy and also a pure tabu search. Such variant has produced very good results with *gaps* (measured as the relative difference from the exact solution obtained for the corresponding linear relaxation) no bigger than 4% for several instances for great part of the tests.

Another metaheuristic based on a variable neighbourhood decent algorithm to solve a similar SIP formulation is proposed by Lamghari *et al.* (2013). Similar to the solution approach previously discussed (Lamghari and Dimitrakopoulos, 2012), the methodology starts by generating an initial feasible solution by two different methodologies similar to the ones discussed in Section 3.1 of this thesis. This initial solution is improved by applying an adaptation of a variable neighbourhood decent (VND) method, which consists on combining different descent heuristics based on different neighbourhood structures to escape from local optima. The schedule is iteratively modified aiming the generation of better solutions, in terms of maximizing value and minimizing risks. Three neighbourhood structures are implemented: (a) *exchanging* N^1: tries to swap two blocks scheduled in consecutive periods; (b-c) *shift-after/before*: tries to make room for new blocks in a given period by postponing/advancing the extraction of a group of blocks currently mined in such period. During the VND, a neighbourhood strategy is fully explored before starting new search using another structure. The process of looking for better solutions stops when no move in any of the three neighbourhoods improves the value of the objective function. The case studies in the paper show very promising results with solutions found in few hours within an average gap of less than 3%. In order to better explore the solution space, Lamghari and Dimitrakopoulos (2013) propose a new heuristic methodology based on very similar neighbourhood structures described before, but now using a network-flow algorithm in order to link all periods. This novel framework for solving a stochastic OPMPS, accounting with multiple processing streams and a stockpile, is the one further explored in this thesis.

2.2.1.1.2 Incorporating additional elements of the mining complex

Recent developments have been made towards more realistic frameworks through the incorporation of additional intricacies for the mine supply chain. Montiel and Dimitrakopoulos (2013b) use a multi-stage heuristic approach which starts with an initial solution and seeks for better solutions in the neighbourhood through sequential perturbation following a given outlined strategy. Their model accounts for multiple processing destinations which are able to operate under different processing options (e.g., coarse vs. low silica), blending restrictions, different material types, stockpiles, and

processing additives. A particular aspect of their methodology is the fact that processing decisions are robust regarding uncertainty (i.e., such decisions are not scenario dependent). Goodfellow and Dimitrakopoulos (2013b) assume a static multi-mine production schedule and proposed a general model to the mine supply chain, which is further tailored to a non-linear MIP formulation. Given the complexity of the problem, the authors use a clustering framework for aggregating initial block destinations (which entails that blocks with similar characteristics are sent to the same destinations across different scenarios) coupled to a metaheuristic approach called particle swarm optimization (Kennedy and Eberhart, 1995). The supply chain is modeled as a graph such that the nodes are related to different locations (e.g., mines, processing facilities, etc.) and the arcs indicate the flow of material. It is assumed that such graph is acyclic, which allows for a sequential updating when material flow is active throughout the supply chain. A key aspect is that, within a given destination, the model allows materials to be transformed to intermediate/output materials by transforming properties using non-linear expressions (e.g., metal recovery might be treated as a non-linear function of head grades). A two-stage recourse stochastic model is built with initial cluster destinations in first stage followed by recourse actions regarding processing decisions and risk assessments. An interesting feature of the framework is that the clustering scheme allows robust decisions during the actual blending operation, not limited to single cut-off values. In addition, algorithmically evaluating the supply chain gives flexibility for the model to assess expected value of recovered metal from blended material sent to the processing streams rather than assigning economic value to blocks as it is conventionally done.

2.2.2 Other stochastic approaches in mine planning: final pit and pushback design

In conventional mine planning, a common practice is to use efficient parametric maximum flow algorithms to find optimal mine designs (Picard, 1976; Hochbaum and Chen, 2000). Meagher *et al.* (2009) extend such an idea, formulating a stochastic approach to solve the ultimate pit limit and phase design, accounting for price, exchange rates and geological uncertainties. The core modification is done in the graph structure, which now supports multiple scenarios, and allows conventional parametric maximum flow methodology to be used for finding the optimal design. Asad and Dimitrakopoulos

(2012) extend such an idea by introducing production capacity constraints and by incorporating a Lagrangian relaxation of these constraints to exploit the classical structure of the maximum flow algorithm.

2.3 Assessment of spatial uncertainty

The previous section highlighted the importance of stochastic frameworks for the OPMPS. In order to incorporate the spatial geological uncertainty and intrinsic variability of the deposit, a set of geostatistical simulations are needed. This section brings a literature review on the main principles and algorithms for generation of these stochastic scenarios, focusing on joint simulation techniques.

Geostatistics is a discipline devoted to the development of Random Field (RF) models of a spatial phenomena characterized by the distribution of one (or more) attribute(s) $z(\boldsymbol{u})$ over a field $\mathcal{D}$ (Matheron, 1963; David, 1977; 1988; Journel and Huijbregts, 1978; Journel, 1989; Goovaerts, 1997; Chiles and Delfiner, 2012). In this context, stochastic simulation is the process of building alternative, equally probable models of the spatial distribution of $Z(\boldsymbol{u})$ conditioned to data values sampled at certain locations and honouring the inferred statistics of the deposit (univariate distribution(s) and spatial variability, such as measured by (cross)-variograms).

A straight way of generating equally probable realizations of the related Random Field (RF) is by directly drawing alternative realisations from its multivariate multi-point cumulative distribution function of the RF. In practice, because such complete knowledge is rarely available, simulation algorithms are mostly built upon assumptions of ergodicity and stationarity of the RF (Journel and Huijbregts, 1978).

Most of the modern geostatistical simulation methods rely on a sequential simulation paradigm, which uses the *chain rule* of probability (Rosenblatt, 1952; Kolmogorov, 1956) to write the spatial law of the RF as products of univariate conditional distribution functions as follows (Rosenblatt, 1952):

$$F(\boldsymbol{u_1}, \dots, \boldsymbol{u_N}; z_1, \dots, z_N) = F(u_1; z_1) \cdot F(u_2; z_2 | z_1(\boldsymbol{u_1})) \cdot \dots \cdot F(u_N; z_N | z_1(\boldsymbol{u_1}), \dots, z_{N-1}(\boldsymbol{u_{N-1}}))$$

Different frameworks are used to obtain these *ccdfs* (conditional cumulative distribution functions) during the sequential process. The most common algorithms based on such

framework are: sequential Gaussian simulation (SGS), which assumes multi-Gaussianity of the RF, and by consequence, the conditional expectation and variance, which are identified by the simple kriging estimator and variance (Journel, 1984), are sufficient for characterizing the ccdf; and the sequential indicator simulation (SIS), which is based on an indicator framework for estimating a non-parametric ccdf (Journel and Alabert, 1988).

2.3.1 Joint spatial simulation

In mine planning, it is very common the need of modelling multiple spatially correlated geological attributes, for example, evaluation of recoverable resources in polymetallic deposits, assessment of deleterious elements such as phosphorous in iron ore deposits, and so on. The assessment of the joint spatial variability of such corregionalized variables is done through joint simulation techniques, which aims at building realizations that reproduces both the spatial variability of each variable and their joint spatial correlation.

Initial efforts for co-simulation in multivariate geostatistics are achieved in Chiles (1984) and Dowd (1984). The first aims the co-simulation of multi-elements in a nickel laterite deposit and the second thicknesses ratios in an oil formation. Both used a non-conditional simulation algorithm based on turning bands (Matheron, 1973; Journel, 1974), but the multivariate spatial relationship of the attributes was not directly accounted, since the random fields were independently simulated and then conditioned by kriging. Carr and Myers (1985) develop a Fortran-based tool called COSIM, which attempts to explicitly account for the corregionalization by using cokriging during the conditioning step. At that time, this approach provides a better accuracy in the simulations if compared to the previous methods. Later on, the Lower/Upper (LU) decomposition algorithm described by Davis (1987) for the univariate simulation of a mutiGaussian RF, was extended by Myers (1989) for the multivariate case. However, such approach requires the decomposition of very large cross-covariance matrices, which imposes practical limitations for its application. In the same way that the original LU simulation proposed by Davis (1987) relates to the SGS approach (Dimitrakopoulos and Luo, 2004), it is natural to imagine an extension of Myers (1989) framework to sequential Gaussian cosimulation, relying on the solution of cokriging systems at each node. Such implementation is demonstrated in Gomez-Hernandez and Journel (1993) and Verly

(1993) who generalize the SGS algorithm to the vectorial simulation of multiple variables. In order to simplify such approach, Almeida and Journel (1984) further develop the idea by implementing a collocated cokriging approximation assuming a Markov type model, simulating each variable at a time, accordingly to a hierarchical outline. Under such corregionalization model, the dependence of the secondary variable on the primary is limited to the collocated primary datum, since this one screens out the contribution of the rest of the data (Goovaerts, 1997). This model assumes that the variogram of the primary variable is proportional to the cross variogram. Markov-type assumption significantly reduces the complexity of the cosimulation process (Almeida and Journel, 1984). However, such a model is most likely to be an oversimplification of the corregionalization model, and may be limited in several applications. The algorithm proposed by Almeida and Journel (1984) is later modified by Soares (2001), who uses a direct simulation algorithm without performing any normal score transformation. The basic idea is to simulate the primary variable all over the grid and then, simulate the secondary variable using this exhaustive co-located information, and so on through the outlined hierarchy.

The major drawback with these joint simulation algorithms, which explicitly considers the corregionalization model of the multivariate random field, is that they either rely on too simplistic models (e.g., Markov-type), or they require the full inference of the corregionalization models in terms of variograms and cross-variograms. In addition to that, for a large number of correlated variables on large simulation grids, joint simulation algorithms may be computationally costly, due to the solution of very large cokriging systems (e.g., iron ore deposits with several variables to be modelled, such as, Fe_2O_3, Al_2O_3, P, SiO_2, LOI, over a realization grid comprising millions of nodes).

An alternative approach consists on replacing the simulation of the K dependent variables $\boldsymbol{Z}_k(\boldsymbol{u})$ by the independent simulation of K uncorrelated factors $\boldsymbol{F}_k(\boldsymbol{u})$, from which the original Z variables can be rebuilt (David, 1988). Such framework is considerably faster than the previous frameworks proposed because no cokriging systems need to be solved, and neither $K(K-1)/2$ cross variograms need to be inferred. A series of transformation techniques can be found in the literature, where most of them are based on a linear

relationship between original variables and factors. A well-known technique in multivariate analysis is principal component analysis (PCA), which aims the transformation of correlated variables into a linear combination of orthonormal factors through spectral decomposition of the covariance matrix (Johnson and Wichern, 2007). Relying on such approach, David *et al.* (1984) use principal components to joint simulate arsenic and uranium grades and Luster (1985) for simulating the corregionalization of limestone components. However PCA is straightforward to implement, it can only guarantee decorrelation at zero lag, but not for all separation distances, except for the special case where the correlation structure of attributes does not depend on the spatial scale, such as in the case of an intrinsic model of corregionalization (Goovaerts, 1993). Therefore, such approach is not able to control the reproduction of spatial cross correlations between variables at lags different than zero. Another transformation that only guarantees decorrelation at zero lag distance is proposed by Leaungthong and Deutsch (2002). Their stepwise conditional transform (SCT) produces transformed variables following a multivariate Gaussian distribution, allowing the straight application of Gaussian based simulation algorithms. The technique is known from Rosenblat (1952) and it is very similar to the normal score transform for the univariate case. For bivariate cases, the normal scores transformation of a secondary variable is conditional to the probability class of a primary variable and so on for the higher dimensional cases. Besides not guaranteeing decorrelation for distances other than zero, SCT suffers from some major drawbacks: sparse data leads to inference of erratic and nonrepresentative conditional distributions. Therefore, a large amount of data is required for a good performance of the technique; the order in which variables are treated in the stepwise procedure affects the final result, increasing its practical complexity; as a global transformation, it does not allow the exploration of local spatial correlation. A positive feature of such transformation is the direct transformation into multiGaussian space and in contrast to PCA, it is a non-linear transform and explicitly accounts for heterocedasticity.

In order to overcome the limitations of the previous methodologies which were only able to provide uncorrelated factors at zero distances, Desbarats and Dimitrakopoulos (2000) bring to geostatistical context the approach of minimum/maximum autocorrelation

factors (MAF), which was first introduced by Switzer and Green (1984) for the minimization of noise in a remote sensing application. This technique is a linear transformation that decorrelates a set of spatially correlated variables into spatially uncorrelated factors for all lags, provided that the corregionalization model of the multivariate RF can be fully characterized by a linear model of corregionalization (LMC). The usual procedure for determining the MAF factors is through the application of two successive PCA rotations. As thoroughly reviewed in Rondon (2012), the MAF transformation matrix can be derived by either directly using the theoretical LMC or through a 'data driven' approach which only relies on the experimental covariance-variance plus a selected experimental (cross-)variograms/covariance matrices during its calculations. When the experimental approach is used, a series of MAF transformation matrices need to be derived using a number of alternative experimental variogram matrices at different lags and selecting the one that yields to the best spatial decorrelation structure.

In practice, the 'data driven' approach is often preferred to avoid the explicit inference of a theoretical LMC model. In addition, most of the frameworks used for the independent simulation of the MAF factors rely on algorithms for simulation of multiGaussian RFs (Desbarats and Dimitrakopoulos, 2000; Fonseca and Dimitrakopoulos, 2003; Eggins, 2006; Lopes *et al.*, 2011). Therefore, in such applications, the data must be firstly transformed to Gaussian space to be further decorrelated through MAF.

Observing the fact that the process of deriving MAF factors (or principal components) does not require the assumption of a multiGaussian RF, Bandarian *et al.* (2008) suggest the direct transformation of sample data into MAF factors, without any prior normal score transformation, to be further simulated through a direct simulation algorithm. Although such approach avoids problems associated to a normal score transformation (e.g., it is usually impractical to ensure and validate the assumption of multiGaussianity, possible deterioration of correlations and principle of maximum entropy), the approach suffers with the common pitfalls of common direct simulation algorithms.

Observing the principle that transformation methods such as PCA and MAF are based on diagonalization of covariance-variance and/or variogram matrices (i.e., vanishing with

off-diagonal terms to destroy correlation among original variables), Bandarian (2008) explores the idea of joint diagonalization (JD) for the joint simulation of spatially correlated variables. As in Afsari (2008), such problem can be stated as: given a set of N square symmetric matrices $\{\boldsymbol{C}_i\}_{i=1}^{N}$, the goal is to find a non-singular matrix $\boldsymbol{B}$ such that all the N products $\boldsymbol{B}\boldsymbol{C}_i\boldsymbol{B}^{\boldsymbol{T}}$ are "as diagonal" as possible. Such problem can only be exactly solved, if the symmetric matrices commute pairwise. Therefore, in practice, one is expected to find an approximate diagonalization. In his application, Bandarian (2008) tests several methods of JD, but the one that leads to the most interesting results was the ACDC approach, which stands for Alternating Columns and Diagonal Centres, introduced by Yeredor (2000). Briefly, this algorithm is designed to minimize the following objective:

$$C(\boldsymbol{B}, \boldsymbol{\Lambda_1}, \dots, \boldsymbol{\Lambda_N}) = \sum_{i=1}^{N} \mathrm{w}_i \, \|\boldsymbol{C}_i - \boldsymbol{B}\boldsymbol{\Lambda_i}\boldsymbol{B}^{\boldsymbol{T}}\|_F^2 \tag{2.9}$$

where w_i is a set of non-negative weights to give assymetric importance on the diagonalization of different matrices $\boldsymbol{C}_i$, and $\boldsymbol{\Lambda_i}$ are the set of approximate diagonal matrices produced by the diagonalization of each matrix $\boldsymbol{C}_i$. The operator $\|\cdot\|_F^2$ is the squared Frobenius Norm, which is simply the sum of the absolute squares of all elements of a given matrix. In order to test a similar algorithm but with a faster convergence, another JD algorithm called U-WEDGE is explored in Ferreira and Muller (2011). This algorithm, introduced by Tichavsky and Yeredor (2009), incorporates in the objective funtion (2.10) both ways of expressing a joint diagonalization property, either by isolating the "approximate" diagonal matrix or the original matrices, given that the optimization criterion for one way might not be optimum for the other way round.

$$C(\boldsymbol{V}, \boldsymbol{A}) = \sum_{i=1}^{N} \|\boldsymbol{V}\,\boldsymbol{C}_i\,\boldsymbol{V}^{\boldsymbol{T}} - \boldsymbol{A}\,ddiag(\boldsymbol{V}\boldsymbol{C}_i\boldsymbol{V}^{\boldsymbol{T}})\,\boldsymbol{A}^{\boldsymbol{T}}\|_F^2 \tag{2.10}$$

where the operator "$ddiag$" nullifies the off-diagonal elements of a square matrix, $ddiag(\mathbf{M}) = \mathbf{M} - \mathrm{off}(\mathbf{M})$**.** In an exact diagonalization, $\boldsymbol{V}$ would be the diagonalization (transformation) matrix and $\boldsymbol{A}$ its inverse, therefore $\boldsymbol{V}\boldsymbol{C}_i\boldsymbol{V}^{\boldsymbol{T}}$ would lead to a diagonal

matrix $\boldsymbol{\Lambda_i}$. Now, for any matrix $\mathbf{V}$ one can find a matrix $\boldsymbol{A}^*$ that minimizes (2.10) with respect to $\boldsymbol{A}$.

Such methodologies based on JD show a great freedom for the determination of the transformation matrix, in as much as one can easily incorporate different weights for the approximate diagonalization of different matrices, even splitting anisotropic directions. However, such freedom heavily relies on a set of "noisy" experimental variogram matrices, which may result in instabilities arisen from inconsistencies from one matrix to the other. As a linear transformation method, it also has same limitations of MAF in this context.

Linear transformations such the ones through PCA, MAF or JD, might find difficulties in reproducing complex multivariate relationships such as non-linearity and heteroscedasticity. A recent paper presented by Barnett and Deutsch (2012) brings a practical transformation to be applied as a pre-processing step for removal of these complex multivariate features. The approach is attractively simple: a secondary variable $\boldsymbol{Z_2}$ is conditionally standardized by a primary variable $\boldsymbol{Z_1}$, by subtracting from each value of $\boldsymbol{Z_2}$ its corresponding conditional expectation regarding the primary variable $E\{\boldsymbol{Z_2}|\boldsymbol{Z_1}\}$ and dividing the result by the standard deviation, also conditional to $\boldsymbol{Z_1}$, i.e., $\sigma\{\boldsymbol{Z_2}|\boldsymbol{Z_1}\}$. The derivation of such conditional statistics may be determined either parametrically through forms of regression or non-parametrically by discretization of the distribution of the secondary variable conditionally to the primary. The extension of such transformation is straightforward for more than two variables. This "conditional standardization" transformation heavily relies on the inference of the conditional statistics to accurately describe the non-linear and heteroscedasticity of the multivariate distribution. Therefore, as any other transformation which aims to the extraction of "deterministic trends", its practical application is limited for cases where such inference is reasonably reliable and it might also suffer with *overfitting*. Moreover, it is noteworthy that such transformation is only able to exploit multivariate relationships at co-located positions, disregarding the spatial multivariate heterocedasticity. Barnett and Deutsch (2012) also discuss the application of *logratios* transformations prior to a factorization transformation (e.g., through PCA or MAF), for the removal of stoichiometric constraints (e.g., compositional

data) as first suggested in Aitchinson (1984). Such consideration is of extreme importance to be incorporated in methods for simulation through uncorrelated factors, which do not explicitly account for stoichiometric balance of multi-elements, which might be of high relevance as in iron ore deposits.

Also aiming to tackle issues arisen by complex non-linear relationships, Barnett and Deutsch (2014) suggest the application of an exploratory projection pursuit algorithm, introduced by Friedman (1987). Barnett and Deutsch (2014) use projection pursuit to seek for non-Gaussian structures to be sequentially *gaussianized*, aiming that at some point (e.g., after M iterations) the multivariate distribution eventually approximates to a multiGaussian one. Major drawbacks found in such approach proposed by Barnett and Deutsch (2014) for the joint simulation context is that, it only considers decorrelation at zero lag distances (a way of tackling this in a linear sense, is to apply a second PCA rotation over an experimental variogram lag of the transformed variables). Moreover, the multiGaussian transformation does not ensure multiGaussianity of the RF itself, since it does not introduce any spatial multivariate relationship in the procedure. Back-transformation also appears as a major issue of the approach.

2.3.2 Efficient framework for joint spatial simulation

In mining, the stochastic simulation of orebody models usually requires very efficient methods that are able to handle a large number of nodes (thousands to several millions) to be simulated conditionally to drilling information. Efficient methods ought to provide stochastic realizations able to reproduce desired statistics and features, in a tractable time, at a low memory cost and with no laborious steps for fitting and modelling many parameters. In the last section, it has been shown a series of methodologies that by, simulating uncorrelated factors instead of directly simulating coregionalized variables significantly alleviates the computational burden of joint simulation techniques based on cokriging. However, the simulation of multiple fields related to each of the factors and the back rotation, still demands a high computational cost and complex memory management for large datasets, typical in mining applications.

Usually, the final goal is to represent these simulated orebody models at block support scales, to mimic the mining operation that works in such selectivity scale. Therefore, instead of naively simulating several nodes that will be further averaged out to provide simulated fields at point-support scale, it would be much more efficient to generate stochastic realizations directly at block-support scale. An efficient algorithm developed for such goal is presented in Godoy (2003) for the univariate simulation of multiGaussian RF. Direct block simulation (DBSim) is a sequential Gaussian simulation that uses similar principles of a generalized sequential Gaussian simulation (GSGS) (Dimitrakopoulos and Luo, 2004): a group of internal nodes discretizing a block is simulated, the block value is calculated and the simulated points are discarded; only the simulated block value is added to the set of conditioning data on the realization grid. For integrating conditioning information at both point (samples) and block supports, the algorithm is developed in terms of a joint point-block LU simulation (Myers, 1989). As pointed out by Godoy (2003), and Benndorf and Dimitrakopoulos (2007), the Direct Block Simulation framework is computationally efficient for several reasons. First, it incorporates the advantages of the GSGS algorithm, which relies on the idea that adjacent nodes tend to share common neighbourhood, performing fewer searches than pointwise simulations and accelerating the process for suitable discretization and neighbourhood size (Dimitrakopoulos and Luo, 2004). In addition, discarding the internal points of simulated blocks represents a decrease in memory allocation that is directly proportional to the number of nodes N discretizing the blocks. A key assumption of this algorithm is that the normal score transformation entails in multiGaussianity of the RF, inclusively for the joint relationship between point and block supports.

For multivariate simulation directly at block support, Boucher and Dimitrakopoulos (2009, 2012) extend DBSim to incorporate the MAF framework. Now, for the internal nodes of a given block, K univariate simulations are carried out one for each uncorrelated factor. For the back transformation step, the normal score variables are obtained by linear combination of the uncorrelated factors before they are back transformed to the data space and average out, in order to output the simulated multi-elements at block supports. This efficient procedure, couples the advantages brought by an indirect multivariate

simulation of corregionalized variables through uncorrelated factors with the efficiency of a framework of a direct block simulation technique.

2.4 Comments on multiple-point techniques for multivariate simulation

All the joint simulation frameworks presented above rely on second-order statistics, such as through the modelling and reproduction of (cross)variograms. Although second-order statistics are adequate for the complete statistical characterization of Gaussian random fields, they are inadequate for modeling geological phenomena which typically deviate from Gaussianity and exhibit complex non-linear spatial patterns (Guardiano and Srivastava, 1993; Journel, 2007). Such a limitation motivated the development of several multiple-point frameworks (MPS) for the simulation of categorical and continuous RFs (e.g., Strebelle, 2002; Arpat, 2005; Zhang *et al.*, 2006; Mustapha and Dimitrakopoulos, 2010; Honarkhah, 2011). However, the incorporation of multiple-point statistics in the context of joint simulation remains a challenge, and very few works have been developed towards this direction. Mariethoz *et al.*, (2010) show an adaptation of the direct sampling algorithm to address the joint simulation of multivariate RFs, defining multiple conditioning data events through several variables. A high order simulation algorithm, such as HOSIM (Mustapha and Dimitrakopoulos, 2010) that explicitly aims to build conditional cumulative distribution functions during the sequential simulation, can also be extended to accommodate multiple variables for joint simulation. During the analytical construction of the multivariate probability distribution, different variables can be used for the calculation of the high-order spatial cumulants. The challenges here are on how to generate training images honoring high-order joint spatial relationships of the deposit and the excessive number of high-order spatial (cross)cumulants that need to be calculated, which may represent a very large computational cost. A way of tackle such an issue is by factorizing the original variables considering their high-order spatial relationship. Techniques such as principal cumulants component analysis (Morton and Lim, 2009) and independent component analysis (Hyvärinen *et al.*, 2004) might be probably useful for extending the previous factorization frameworks (e.g., PCA and MAF) for the cases of multiple-point simulation.

Chapter 3

Solving a Large SIP Model for Production Scheduling at a Gold Mine with Multiple Processing Streams and Uncertain Geology

3.1 Introduction

Open-pit mine production scheduling (OPMPS) generates the optimal sequence of extraction of mining units over the life-of-mine (LOM), given a set of physical and technical constraints. Such a decision process needs to be made under conditions of uncertainty, however, conventional approaches for optimizing OPMPS (e.g., Johnson, 1969; Dagdelen and Jonhson, 1986; Gershon, 1987; Whittle, 1988; Tolwinski and Underwood, 1996; Cacceta and Hill, 2003; Hustrulid and Kuchta, 2006) tend to assume that parameter inputs are fully known, ignoring potential risks and opportunities that might arise from the different sources of uncertainty (Ravenscroft, 1992; Dowd, 1994, 1997). An example in Dimitrakopoulos *et al.* (2002) shows that the results in key performance indicators of a conventional mine design are misleading in the presence of geological uncertainty, highlighting the limits of deterministic optimization techniques.

Spatial uncertainty of geological attributes can be modelled through stochastic simulation techniques which are able to provide a series of equally probable scenarios of the orebody (Goovaerts, 1997; David, 1988). The availability of these models leads to the development of stochastic optimization frameworks that are able to integrate uncertainty into the decision process, minimizing downside risks and maximizing potential upsides. During the last decade, a substantial focus has been given for the development of new models and solution approaches for the stochastic version of the OPMPS. For example, Godoy (2003) introduces a stochastic framework where multiple schedules derived from each geological scenario are firstly joined up. Thereafter, a combinatorial optimization problem is solved by an algorithm based on simulated annealing in order to provide a single schedule with a higher NPV (improvements of 28%) and substantially lower deviations from production targets, when compared with the results reported by the conventional schedule. Similar conclusions are drawn in Leite and Dimitrakopoulos

(2007) for an application of the framework in a copper deposit. Albor and Dimitrakopoulos (2009) show for a specific case study that the application of this stochastic framework leads to a larger ultimate pit with an NPV 10% larger than the one obtained by constraining the schedule with a conventional pit limit.

Menabde *et al.* (2007) develop a mathematical formulation to maximize the expected NPV over several scenarios while minimizing deviations from production targets in an average sense. Dimitrakopoulos and Ramazan (2008) bring a stochastic integer programming (SIP) formulation which maximizes the expected net present value (NPV) and incorporates recourse actions to tackle the uncertainty modelled through stochastic simulations, by minimizing possible deviations from production targets over the life-of-mine. Ramazan and Dimitrakopoulos (2013) extend this SIP formulation to introduce a stockpile option, reporting an increase of 10% in the NPV if compared to the economic performance reported by a conventional schedule. In addition, the method provides more realistic schedules that minimize the chance of deviating from production targets, regarding geological uncertainty. These results highlight the ability of stochastic schedules on simultaneously maximising economic returns and driving the mining sequence through zones where the risk of not achieving the target ore production is minimised. Other variants and applications of SIP have also shown significant improvements over the deterministic OPMPS: Leite and Dimitrakopoulos (2014) show through an application to a porphyry copper deposit that, even for a low grade variability deposit, the NPV can be increased by 29%; Dimitrakopoulos and Jewbali (2013) incorporate in the SIP model simulated future data information, outperforming the NPV of the conventional mine design of a gold mine; Benndorf and Dimitrakopoulos (2013) extend the model to account for several elements of an iron-ore operation, showing that the capability of the stochastic approach to controlling risks of deviating from production targets for critical quality-defining elements. Boland *et al.* (2008) incorporate metal uncertainty via a multistage stochastic programming approach in such a way that, decisions made in later time periods might depend on observations of the properties of the material mined in earlier periods.

The stochastic models proposed by Ramazan and Dimitrakopoulos (2012), Menabde *et al.* (2007) and Boland *et al.* (2008), are all solved using a mixed integer programming solver such as CPLEX (ILOG, 1998), which limits their practical application to instances of relative small sizes, typically accounting for less than 20 thousands blocks (Lamghari and Dimitrakopoulos, 2012). As a result, over the past few years, several authors have been seeking the development of new solution approaches, which can efficiently tackle large instances of the stochastic OPMPS. Lamghari and Dimitrakopoulos (2012) introduce a metaheuristic approach based on Tabu search for solving large-scale SIP models within a few minutes up to few hours (while a commercial solver would take days for some instances), with a deviation of less than 4% from optimality for most of their runs. Comparable results are obtained in Lamghari *et al.* (2013b) who use two variants of a variable neighbourhood decent algorithm and average deviations of less than 3% from optimality for several instances.

The present paper focuses on an application of a heuristic approach introduced by Lamghari *et al.* (2013a) which incorporates geological uncertainty, multiple processors, stockpiles, and is capable of solving large-size mining schedule problems in a reasonable time. The solution approach can be seen as a very large-scale neighbourhood search method (Ahuja *et al.*, 2002) and it basically involves two stages: (i) the generation of an initial solution and (ii) the application of an improvement algorithm based on network flow. In the following sections, the SIP formulation and the solution approach are revisited, followed by the application at a gold mine employing two processing streams and one 'grade' stockpile. Discussions and conclusions follow.

3.2 Stochastic Integer Formulation Revisited

The stochastic integer formulation proposed by Lamghari *et al.* (2013a) is briefly outlined in this section. The following notation is used:

- N is the total number of blocks and i is the block index with $i = 1,\ldots,N$;
- T is the total number of periods and t is the period index with $t = 1,\ldots,T$;
- S is the total number of scenarios used to model the geological uncertainty and s is the scenario index with $s = 1,\ldots,S$;

- P is the total number of processing streams and p is the processing index with p = 1,…, P (e.g., a mill and a leaching facility).
- *Pred(i)* is the set of predecessors for a given block i, which means that all blocks in this set must be exploited before i in order to satisfy the slope constraints;
- dr is the economic discount rate over the time basis being considered;
- d_{ips} is a parameter indicating the most profitable destination for a block i under scenario s. Therefore, comparing the block grade g_{is} to the cut-off policy adopted, d_{ips} is equal to one for its most profitable destination stream for scenario s and it is equal to zero for all other destinations.
- w_i is the total tonnage of a given block i;
- $E[BEV_i]$ is the expected block economic value (BEV) of a given block i. This value is calculated for each geological scenario, considering the best destination of the block accordingly to the cut-off policy of the project, which is given by the d_{ips}.
- SC_P^t and RC_P^t are both undiscounted costs related to stockpile activities for a given process p during period t. The former cost stands for sending material to the stockpile and the latter for reclaiming material from the stockpile.
- $\tilde{r}_{ps}^t$ is the discounted revenue returned, if a tonne of ore under a given scenario s is reclaimed from the stockpile and sent to process p during production period t.
- W^t and Θ_p^t are the maximum mining and processing capacities (for each processing option p) respectively, for a given period t.
- I_p is the initial amount of material in the stockpile of processor p.
- Binary variables (x_i^t) for each block i and period t. It is considered that x_i^t is equal to one if the block i is already mined by period t, otherwise it assumes the value of zero. It means that, if a block I is mined in period t^*, $x_i^t = 0$ for all t = 1… t^*-1 and $x_i^t = 1$ for all $t = t^*$… *last period*. In consequence, $x_i^t - x_i^{t-1}$ only assumes the value of one for the period t when the block is mined. To simplify the

notation, a set of N dummy decision variables x_i^0 $(i = 1 \dots N)$ are introduced, all having a fixed value equal to zero.

- Linear variables (y_{ps}) related to processing streams. In the model proposed, y_{ps}^{t+} and y_{ps}^{t-} represent the surplus and shortage of material in a given period *t*, for a process destination *p*, regarding a specific scenario *s*. These variables are used to model the stockpile streams related to each process *p*. In case of surplus under a given scenario, y_{ps}^{t+} is the amount of material that must be stockpiled in order not to violate the processing capacity available. In case of shortage, y_{ps}^{t-} accounts for the amount reclaimed from the stockpile to fulfil the processing capacity. Finally, the variables y_{ps}^{t} denote the amount of ore in the stockpile at the end of period *t*.

The mathematical model aims to maximize the discounted cash flow (Eq. 3.1) given some physical and technical constraints related to the mining operation (Eqs. 3.2 to 3.10) as summarized below:

$$max \sum_{t=1}^{T} \frac{1}{(1+dr)^t} \left\{ \sum_{i=1}^{N} E[BEV_i](x_i^t - x_i^{t-1}) + \frac{1}{S} \sum_{s=1}^{S} \left[-\sum_{p=1}^{P} (\tilde{r}_{ps}^t + SC_P^t) y_{ps}^{t+} + \sum_{p=1}^{P} (\tilde{r}_{ps}^t - RC_P^t) y_{ps}^{t-} \right] \right\} \tag{3.1}$$

Subject to:

$$x_i^{t-1} \leq x_i^t \qquad \forall\, i,t \tag{3.2}$$

$$x_i^t \leq x_j^t \qquad \forall\, i,j \in Pred(i),t \tag{3.3}$$

$$\sum_{i=1}^{N} w_i (x_i^t - x_i^{t-1}) \leq W^t \qquad \forall\, t \tag{3.4}$$

$$\sum_{i=1}^{N} d_{ips} w_i \left(x_i^t - x_i^{t-1}\right) - y_{ps}^{t+} + y_{ps}^{t-} \leq \Theta_p^t \qquad \forall\, t,p,s \tag{3.5}$$

$$y_{ps}^{t-1} + y_{ps}^{t+} - y_{ps}^{t-} = y_{ps}^{t} \qquad \forall\, t,p,s \tag{3.6}$$

$$x_i^t = 0 \text{ or } 1 \qquad \forall\, i,t \tag{3.7}$$

$$x_i^0 = 0 \qquad \forall\, i \tag{3.8}$$

$$y_{ps}^{t+}, y_{ps}^{t-}, y_{ps}^{t} \geq 0 \qquad \forall\, t,p,s \tag{3.9}$$

$$y_{ps}^{0} = I_p \qquad \forall\, p,s \tag{3.10}$$

As per Eq. 3.1, the objective function can be separated in two major terms: the first one refers to the mining decisions, without having access to full information about the material that is underground (scenario independent); the remaining is associated to scenario dependent variables (stockpile actions), because once a block is mined, the operation can take the most suitable decision about where to send a given mined block, leading to different stockpile actions under each scenario. The first part of the stockpiling term refers to the total approximated undiscounted cost related to send exploited material from the mine to the stockpile of processor p in period t under scenario s; and the second part refers to the total approximated undiscounted net revenue after reclaiming material from the stockpile of processor p in period t under scenario s. As one may note, the option of using the stockpile incurs additional costs in the objective function. Thus, in an optimal solution the use of the stockpile is minimized, which means that the risks of overproduction regarding all geological simulations are also minimized.

The addition of a stockpile to the mathematical model adds the number of quadratic terms to the formulation of the OPMPS. The calculation of the parameters $\tilde{r}_{ps}^{t}$ in the objective function (3.1) depends on the knowledge of the average grades ($\tilde{G}_{ps}^{t}$) of the material that is sent/reclaimed in/from the stockpile. For a realistic approximation of the average grade of the stockpile in a given period, one should track the average grade of the material being extracted and sent to the stockpile up to this period. However, the notion of which blocks ought to be extracted are related to decision variables of the model, resulting in a cross relationship with the revenue generated by processing the material from the stockpile, and giving rise to a non-linear term in the objective function. To maintain the linearity of the model, Lamghari *et al.* (2013) use a single initial approximation for the average grade of the stockpile associated to each processor, which is fixed for all the scenarios and over all the periods. In this paper, the set of average grades $\tilde{G}_{ps}^{t}$ is iteratively approximated and may vary from period to period and scenario to scenario. This iterative approximation is performed in the following way: first, the schedule is solved using a approximated average grade, which might come from the average grade of all blocks in the deposit which are candidates to go to the destination related to the stockpile, or the average grade of materials within the cut-off between its processor and

the low-grade processor. After solving the OPMPS with this approximation, the optimizer outputs the amount of material going in and out of the stockpile (respectively given by the linear variables y_{ps}^{t+} and y_{ps}^{t-}), but it does not track which blocks specifically are being stockpiled. Since no blending constraints are considered, it is assumed that in each period, from the set of blocks scheduled to be sent to a given destination, the ones that go to the stockpile are the ones with the lowest grades, because in an optimal solution, due to the time value of money, the low-value material is stockpiled in order to leave room for the processing of high-value material. By doing such an analysis, it is possible to calculate the "expected" average grade of the stockpile for that given schedule. These average grades by period are then fed as input to the optimizer to generate a new schedule. The same process of approximating the grades and rerunning the solver keeps looping until the difference between the input grade and the "expected" one is less than a threshold ε (e.g., 10%). A similar approach is used by Sarker and Gunn (1997) to solve nonlinear problems, where the authors iteratively solve multiple linear programming problems approximating the quality of the blended material at different locations in terms of sulfur, ash and BTU content. The same authors show that, not only it is a simple and fast way of dealing with nonlinear problems, it is able to provide solutions near optimality after few iterations. A comparison between the approximation for the average grade of the stockpile shown herein and the one in Lamghari *et al.* (2013) is shown in the Appendix.

Constraints in Eq. (3.2) are the *reserve constraints*, which guarantee that each block is mined at most once. Constraints in Eq. (3.3) are the *slope constraints*, which entails that to access a given block, a set of predecessors must be mined before, assuring the slope angles are predefined. Constraints in Eq. (3.4) are the *mining constraints* which enforce that the total amount of material mined in a given period *t* cannot be higher than the mining capacity available for that period. Constraints in Eq. (3.5) are the *processing constraints*, which imposes an upper bound for the total material sent for a given process, in period *t* and under scenario *s*. Constraints in Eq. (3.6) are the *stockpiling constraints* which balance the mass flows of each stockpile. At the end of each period *t*, the stockpile of a processor *p* under scenario s must contain the amount of material initially available

at the end of period *t-1*, plus the amount of material stockpiled minus what was reclaimed during period *t*.

It is noteworthy that, although the model does not consider explicitly a lower bound capacity for the processing streams in order to better control the ore feeding, the optimizer always tries to use all the capacity available, mostly in earlier periods as an attempt to increase the NPV of the project. From this constraint one may also note that, in an optimal solution, either stockpiling or reclaiming is active, since both incur costs in the objective function. Thus, the surplus variable (y_{ps}^{t+}) will assume positive values when it is worthy to mine and send to a given processor more material than it can handle during that period, which is an attempt to reach as fast as possible the high-grade zones of the deposit, stockpiling low-grade material that had to be mined previously. On the other hand, the shortage variable (y_{ps}^{t-}) will only assume a positive value either if it is better to reclaim material from the stockpile than fulfilling the processor capacity with material from the ground, or when the material mined is not enough to fulfill the processor capacity. Moreover, inasmuch as the stockpile actions incur costs to the objective function (both associated to rehandling and opportunity cost of postponing the process valuable material in the stockpile), in an optimal solution the use of the stockpile is minimized, which means that the risks of overproduction regarding all geological simulations are also minimized. These features are expected to drive the optimizer to maximize value and minimize geological risk throughout the life-of-mine.

3.3 A Review of the Solution Approach

For solving the OPMPS model introduced in the previous section, a multistage heuristic algorithm described in Lamghari *et al.* (2013a) is used. It comprises two major steps: generation of an initial feasible solution and then its improvement by using a network flow based algorithm which efficiently searches for improving solutions over a large neighbourhood.

3.3.1 Generating an initial feasible solution

Two heuristics methodologies are used to test different initial solutions. Both of them are based on the "divide and conquer" principle, by solving the model period by period, and

thus, each period composes a reduced sub-problem. As soon as an earlier period is solved, the mining blocks scheduled to this period are taken out from the model to reduce the problem's size. The later periods are sequentially solved in a similar way. After this sequential process, the solutions found are merged, providing an initial feasible solution.

The differences existing between the two heuristic methods used are basically in the way each one solves the sub-problems. In the first method, the solutions are given by an exact mathematical programming method implemented in CPLEX. The second method is a greedy heuristic procedure (GH) which at each iteration tries to include in the set of mining blocks scheduled for a given production period *t*, a set of blocks represented by a base block (*i*) and its predecessors (*Pred(i)*) not mined yet, in such a way as to maximize the objective function of the sub-problem model, respecting the mining capacity constraint and at the same time postponing the extraction of waste and advancing the extraction of ore, thus, deferring costs and advancing profits to earlier periods. This greedy heuristic incorporates a *look ahead* feature, since it looks after blocks with all their unmined predecessors instead of treating blocks separately one by one. In both methods for generating initial feasible solutions, blocks that are not included in the sets of mined blocks in each period until the last one (T) are left behind. To represent these unmined blocks, they are included in a set corresponding to a fictitious period (T+1).

3.3.2 Improving the initial solution with a network flow algorithm

It is well known that sequentially solving the mine production schedule does not lead to an optimal solution of the long-term production schedule (Gershon, 1983). Therefore, in a second stage, the goal is to improve the initial solution generated by any of the two heuristic approaches explained above, providing a new schedule with a higher NPV. To achieve this, the improvement algorithm proposed basically tries to postpone the extraction of blocks responsible to decrease the objective function (3.1) and advance those which improve it.

The algorithm is based on a network-flow structure, where each problem is defined on a graph G = (V, E) (V is the set of nodes and E is the set of arcs). Different graphs are built according to the problem being solved: delaying (*backward pass*) or advancing (*forward*

pass) extraction of blocks. Only the construction of the first case is shown henceforth, since the formulation of the *forward structure* is straightforward. Thus, for the *backward structure*, the set of nodes represent blocks which matches the following characteristics:

- the total expected economic value of a given block and all its successors scheduled for the same period t is negative, since NPV increases as the costs are deferred, and;
- the total tonnage of this same group of blocks, summed to the total tonnage already scheduled for the next period (t+1), minus the total tonnage of a candidate group of blocks scheduled to period (t+1) which can be postponed to (t+2), must not exceed the mining capacity W^{t+1}. This condition ensures that the mining capacity is not violated when blocks are moved from one period to another.

Each node of the graph is associated to a block and its predecessors scheduled for the same period, respecting the conditions stated above. To complete the network, an additional node is added to the fictitious period T+1 which represents the set of blocks that will not be extracted; for each period, one extra node is added for fictitious blocks with neither weight nor costs, representing a path through where no modifications are done to the current schedule. In addition, two extra nodes must be added to the network referring to its source and sink. In this formulated graph, the set of arcs E involves all possible connection between two nodes currently scheduled in consecutive periods t and t+1. In addition, some arcs are added connecting the source to the nodes belonging to the first period and one more arc is connected from the fictitious node in T+1 to the sink. As a result, each path from the source to the sink, passing through nodes in consecutive periods, represents a new solution to the stochastic mine production schedule, where a given mining block and its successors represented in a node has their extraction delayed to the next period and so on. Blocks at the head of the arc are moved to the following period and the blocks represented by the node at the tail of the arc are mined in their place. Figure 3.1 shows a simplified illustration of graph G.

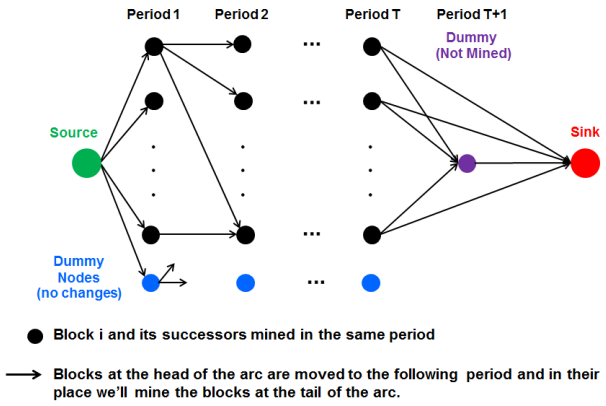

Figure 3.1 - Illustration of the graph built for the network-flow algorithm (Backward Case).

Thus, the goal is to find a single feasible path which improves the value of the objective function as in Eq. (3.1). If no such path is found, the solution given by the algorithm is the path which includes the set of fictitious nodes introduced before, and no block would be moved from one period to the other and the value of the objective function remains the same. To identify the feasible path which increases the value of the objective function the most, each arc is weighted accordingly to the feasibility of the delaying movement and the gain it brings to the objective function. After weighting each arc the model becomes a *longest path problem*, which consists in finding the simple path of maximum length, where the length in this case is represented by the sum of the weighted arcs. The weights (p_{ij}) of each arc $(i,j) \in E$ are defined as follows:

- Arcs connecting nodes associated to real blocks in each period $t = 1,\ldots,T+1$, represent movements of blocks associated in node i from their period t to $t+1$ and movements of blocks associated to node j from their period $t+1$ to $t+2$. So, if this move results in a violation of mining capacity at $(t+1)$, the weight associated to this arc (i,j) is a large negative number, which flags its infeasibility. Otherwise, a weight p_{ij} is associated to the arc, indicating the delta change in the two first parts of the objective function (Eq. 3.1). The last part, which accounts for the value of reclaimed material from the stockpile, is not considered because it cannot be evaluated in the network structure, since one needs to know what is available in the stockpile before knowing how much can be reclaimed;

- Arcs connecting the source to nodes in the first period are always feasible, (the upper bound of the mining capacity is always satisfied in period 1, because only delaying action can be taken). Thus, the p_{ij} weights are simply associated to the modifications in the two first terms of the objective function;
- A $p_{ij} = 0$ is associated to the arcs between the fictitious nodes created for each period. A null weight is also assigned to the arc from the dummy node in T+1 to the sink.

As mentioned earlier, once the graph is built, solutions are generated by solving the *longest path problem*, associating each arc to a binary variable and sending a unitary flow from the source to the sink, which guarantees that the solution provided is always a simple path. It is interesting to note that the constraint matrix (nodes-arcs incidence matrix) of this integer programming problem is *unimodular*. This property indicates that the integrality constraints can be dropped and only restricts $z_{ij} \in [0,1] \ \forall \ (i,j) \in E$. Subsequently, the problem can be efficiently solved using linear programming or network-flow techniques.

In summary, the algorithm works in an interactive way such as the following: first, it performs a *backward pass* (initial mode), trying to delay the extraction of blocks. If the solution changes, a new network is built for the new current schedule and another *backward pass* is carried out. Otherwise, if the *longest path* found identifies the set of fictitious nodes, meaning that no improvement can be made, the problem is switched to a *forward pass*, and the algorithm looks for blocks to advance their extraction. In the same way as in the first, several passes are performed until no improvement is achieved, and then the problem switches its mode again. The algorithm stops when it executes two consecutive modes, that is, *backward* and *forward passes* (and vice-versa) without any improvement in the value of the objective function.

3.4 Case Study at a Gold Mine

To demonstrate the application related aspects of the method previously described, a case study of a gold mine is presented here. The deposit being mined consists of an intensely mineralized shear system localized in mainly steeply dipping, NNW to NW striking

lodes. Gold lodes can be up to 1,800 m (5,900 ft) long, have vertical extents of 1,200 m (3,900 ft) and be up to 10 m (33 ft) wide. The mine feeds two processing streams, a mill and a leaching facility, with the first having an associated stockpile. Fixed stockpiling/reclaiming costs are used throughout the LOM and no material is in stock for the first production period.

A set of 15 stochastic simulations, discretized in about 120 thousand blocks of $20x20x20m^3$ and generated by direct block simulation (Godoy, 2003), are used to model the spatial uncertainty of grades though the deposit. This number of scenarios is used because past works, such as in Albor and Dimitrakopoulos (2009) and Leite (2008), indicate that after about such number of representations of an orebody, the stochastic schedules tend to converge to a stable final schedule and to provide stable forecasts of production performance. Such results are not surprising because, despite the spatial uncertainty modeled over blocks with few cubic meters, a production schedule of a mine represents a grouping of several hundreds to thousands of these blocks in one mining period under different constraints. Thus, with this significant increase of support (from blocks to production in mining periods), the stochastic schedules tend to be less sensitive to additional scenarios after a relatively small number of scenarios.

The general parameters for the stochastic mine production schedules are summarized in Table 3.1.

Table 3-1 - Technical and economic parameters for OPMPS

Mining Cost	$ 1.80/t	**Mining Capacity**	90 Mta
Metal Price	$ 730/oz	**Selling Price**	$5.0/oz
Discount Rate	8.0%	**Slope Angle**	45°
Mill - High Grade			
Recovery	90%	**Proc. Cost**	$ 9.50/t
Stockpiling Cost	$ 0.50/t	**Reclaiming Cost**	$ 0.85/t
Proc. Capacity	22.0 Mta	**Stockpile Capacity**	20 Mt
Leaching - Low Grade			
Recovery	50%	**Proc. Cost**	$ 5.00/t
Proc. Capacity	1.0 Mta		

The case study is split in two subsections in order to show the differences obtained when using *branch-and-cut* (Wolsey, 1998), an exact mathematical programming method implemented in CPLEX (ILOG, 2008) or a greedy heuristic to generate the initial solution. The computations are performed in a Intel Xeon 5650 (2.66GHz) with 24GB RAM. In both case studies, CPLEX is used to solve the *longest path problem* over the network during the improvement stage of the algorithm.

3.4.1 Stochastic Schedules

Two different schedules are generated, each respectively using CPLEX and the greedy heuristic (GH) to generate the initial feasible solutions. The risk profiles for the ore throughput for the mill and the material stockpiled by the end of each period are respectively shown in Fig. 3.2 and Fig. 3.3. In these graphs, the blue and red solid lines refer to the expected ore input to the mill in the schedules generated by respectively using CPLEX and GH as initial solutions. The dashed lines represent the percentiles P10 and P90 for the ore throughput over the different geological scenarios

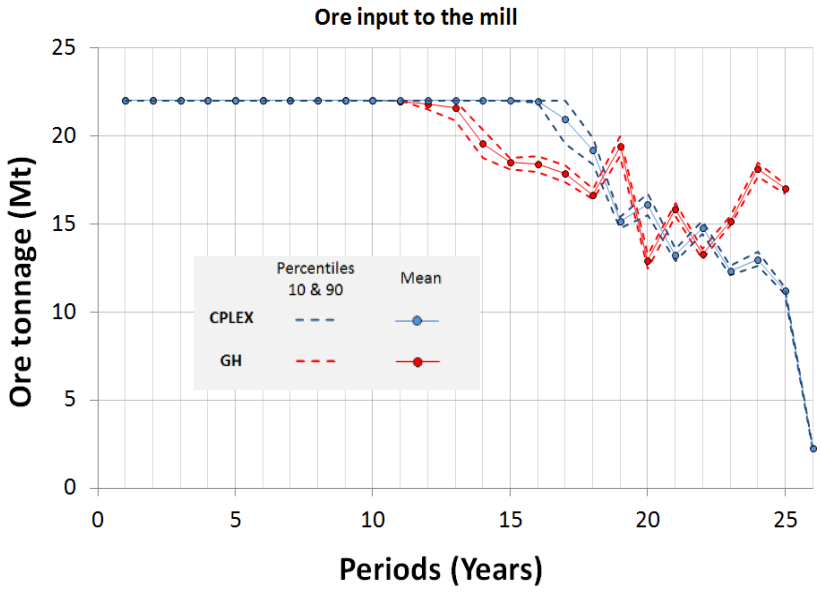

Figure 3.2 - Expected ore tonnage throughput for the mill and related risk profiles, using CPLEX (blue) and GH (red) to generate initial solutions.

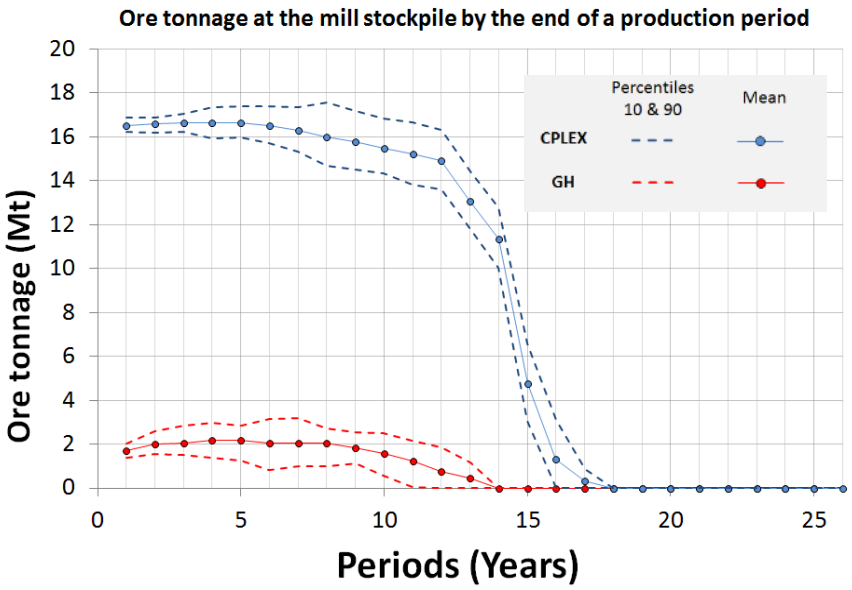

Figure 3.3 - Expected ore tonnage at the mill stockpile and related risk profiles, using CPLEX (blue) and GH (red) to generate initial solutions.

The schedule using CPLEX as initial solution considers an additional year to the LOM, shown in blue (Fig. 3.2) and an ultimate pit 1.1% bigger than the schedule using GH as initial solution. As seen in Fig. 3.2, the range of variability about the expected value of throughput for the mill is quite low, which suggests that this process is likely to operate with low uncertainty for the expected throughput. For the schedule obtained using the initial solution from CPLEX, the mill will potentially work at full capacity (22Mt) during the first sixteen years, while for the OPMPS using the GH as initial solution, this period is shortened to eleven years. During these time spans, the mill potentially works with almost no risks of over/under production. This occurs because during those periods, the tonnage uncertainty is somehow "shifted" to the stockpile, since for each scenario, the overproduction is sent to the stockpile and in case of shortages, material can be reclaimed from the stockpile. During the years for which the mill works below its capacity (Fig. 3.2), the mine operates at full mine capacity (90Mt) and not enough material is available in the stockpiles under all geological scenarios (Fig. 3.3). These factors lead the optimizer to work below the mill's maximum capacity, since the mining rate entails in a bottleneck for the operation and no penalties are incurred for underproduction in the SIP formulation presented in a previous section. A way of dealing with this would be to explicitly

incorporate penalties for idle capacity (shortage in production) in the formulation, in such a way that they do not compete with the reclaiming variables, or allow a flexibility to the mine to increase its capacity during later periods, through the acquisition of mining equipment.

Figure 3.3 shows that, for both schedules generated, the first period is when most of the material is sent to the stockpile, which allows the mill to advance the metal production, by working with a high grade material as shown in Fig 3.4. These results show, as expected, the flexibility added to the project by the use of a stockpile: (i) it allows the operation to reach high grade material earlier during the LOM and (ii) 'buffers' the risks of oversupply of ore and/or having idle processing capacity, with respect to geological uncertainty.

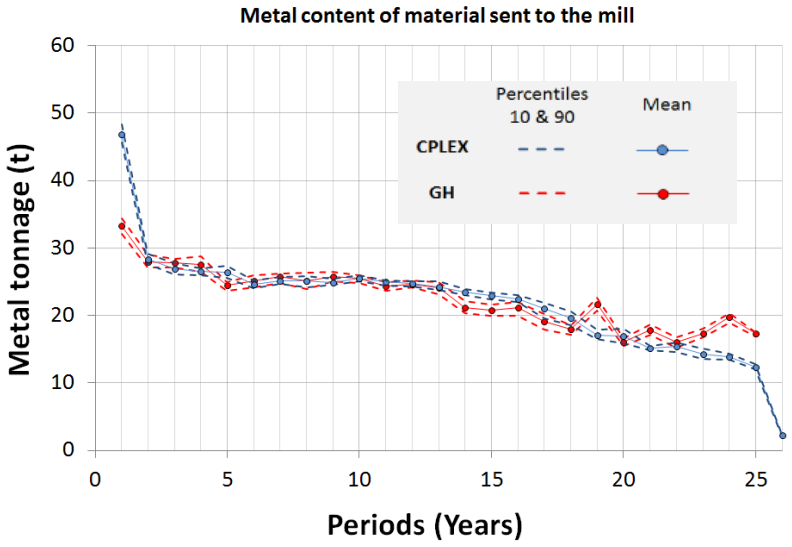

Figure 3.4 - Expected metal input to the mill and related risk profiles, using CPLEX (blue) and GH (red) to generate initial solutions.

Regarding the differences between the two schedules generated, Fig. 3.2 shows that the OPMPS using CPLEX to generate the initial solution is able to advance the production of ore (*see* years 13 to 18) and to reach high grade areas during earlier periods if compared to the solution by using the GH as initial solution. The metal content for the ore input to this processor during the first year is about 40% larger in the first production schedule than in the second. Figure 3.3 shows that these differences are mostly related to the fact

that, in the first solution approach the greater use of the stockpile provides a larger flexibility to the operation.

In contrast to the behaviour seen for the mill, Fig. 3.5 shows that the leaching process will potentially work under its nominal capacity of 1Mt and with a much more variable throughput. Such a result is expected because the SIP formulation used in this paper, controls the geological risks exclusively through the use of a stockpile associated to the mill, which is not the case for leaching. Figure 3.6 shows the risk profile for the metal production of this same processing destination.

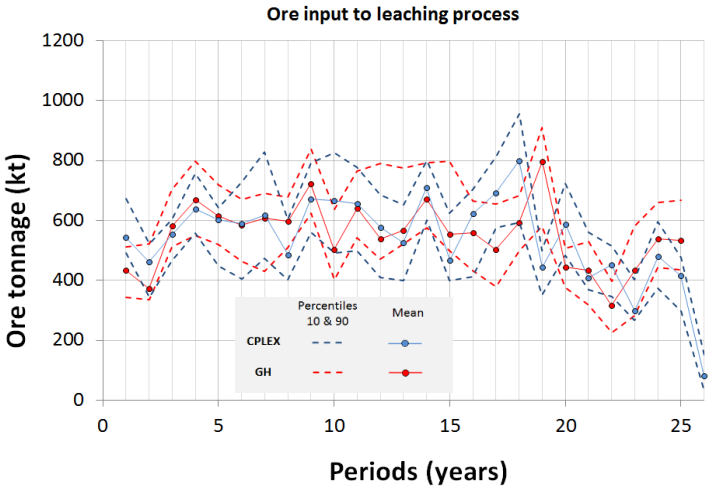

Figure 3.5 - Expected ore tonnage throughput for the leaching and related risk profiles, using CPLEX (blue) and GH (red) to generate initial solutions.

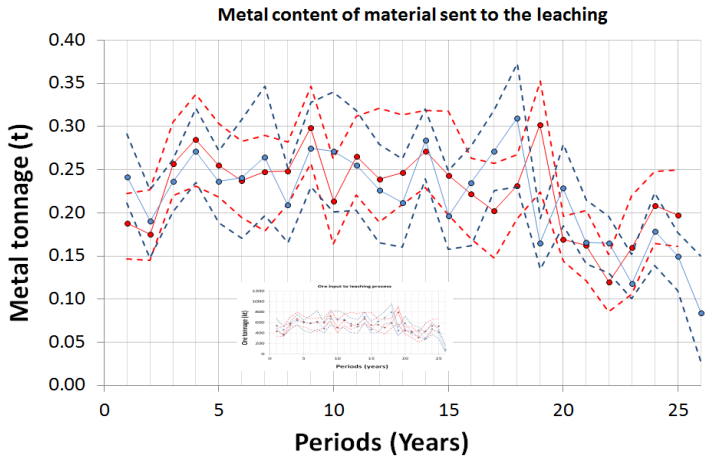

Figure 3.6 - Expected metal input to the leaching and related risk profiles, using CPLEX (blue) and GH (red) to generate initial solutions.

Regarding the economic performance of the project, the risk profiles of the cumulative NPV are shown in Fig. 3.7. These curves show a very low uncertainty about the expected NPVs for the project (less than 3% of upper/lower deviations regarding the P10 and P90). In addition, Fig. 3.7 shows that, the OPMPS using the GH as initial solution has an overall NPV 7.9% (M$215) lower than the one obtained by using CPLEX as initial solution. In this specific case study, this difference is mostly related to the ability of the latter solution to produce a larger amount of metal during the first period. In this year, its NPV is 56% (M$245) higher than the one achieved by the mine production scheduling obtained by using GH as initial solution.

While CPLEX takes hours to generate an initial solution, the GH takes only seconds. In addition, the final OPMPS using CPLEX as initial solution took a total time of 32 hours against the 38 hours required for the generation of the final solution by the approach using the GH as initial solution. This excessive time reported by this last approach is related to the size of the neighbourhood found in each iteration when it tries to make a *backward move.* In many of these iterations, the graph built has contained more than 2.7 thousands of nodes and 22 millions of arcs. This represents a very large linear programming problem, requiring more than 30 minutes to be solved. Thus, as one may observe, for this case study, besides providing a higher NPV, the final schedule generated using CPLEX's initial solution also demands a smaller computational time than the approach using GH to generate an initial solution.

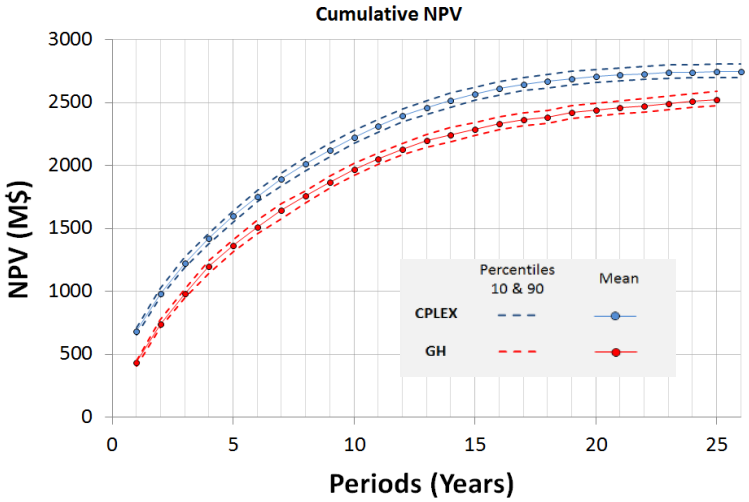

Figure 3.7 - Expected cumulative NPV and related risk profiles, using CPLEX (blue) and GH (red) to generate initial solutions.

Figure 3.8 brings South-North cross sections of the schedules, illustrating the differences in their physical sequence of extraction. Using CPLEX as initial solution produces a less smooth sequencing pattern than the one provided by employing GH as initial solution. For this case study, this latter approach tends to maintain the "clustered" structure intrinsic from its formulation

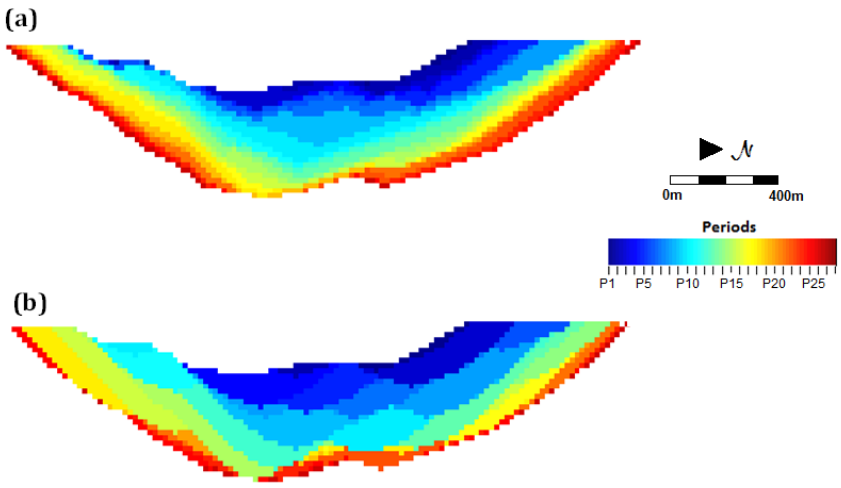

Figure 3.8 - South-North vertical cross-section of the physical sequences of extraction for the schedules using different initial solutions (a) CPLEX and (b) GH.

3.5 Conclusions

The present study highlights the practical aspects and performance of a neighborhood search method based on a network flow algorithm, developed to solve a stochastic version of the open-pit mine production scheduling. A case study was performed at a relatively large gold mine comprising about 120 thousand blocks, two processing streams and a stockpile. This consists of a very large mathematical programming model, with about 3 million integer variables. Two different ways of generating initial feasible solutions to be input to the network flow algorithm were tested. The first uses CPLEX and the second a greedy heuristic to sequentially solve the mine production schedule period-by-period. For the specific case study, although the greedy heuristic was able to find the initial solution in a few seconds and the exact method demanded hours for the same task, the improvement stage was much longer when using the greedy heuristic solution. This latter approach took 38 hours to generate a final schedule, against 32 hours required by the optimizer when the CPLEX initial solution is used. This behavior is different to the common trend observed in previous tests (Lamghari *et al*, 2013). Note that, when CPLEX was used to produce the linear relaxation of the stochastic integer programming model of this case study, it could not provide an optimal solution after two weeks, highlighting the advantages of looking for computationally efficient solutions, such as the one used in this paper.

In this case study, the production schedules generated showed that by using the initial solution from CPLEX, a better final solution can be achieved in terms of NPV (7.9% higher than starting from the initial solution generated by the GH). All results have shown that the stochastic mine production schedules have controlled deviations in ore production for the processor with a stockpile associated to it, since the SIP formulation used in this paper, considers that the recourse actions to control the geological risk are incorporated in the stockpiling actions. The overproduction under any scenario is sent to the stockpile and shortages are only controlled if there is material available in the stockpile. These actions imply costs associated to rehandling of material and the opportunity cost of leaving valuable material in the stockpile, and therefore, penalizing

deviations related to uncertainty. The shortcoming is that, if in a giving production period, no material is available at the stockpile, shortages are not explicitly penalized.

These observations highlight that the heuristic method tested in this paper is able to tackle large SIP formulations for realistic mine environments, producing mine production schedules with low deviations about expected production rates.

3.6 Chapter Appendix

To illustrate the differences of using an iterative approach to approximate the average grade of the stockpile, a third schedule is generated and shown in this Appendix. This schedule is generated using a single initial approximation for the stockpile average grades, which is the average grade of all resources that will be potentially sent to the mill accordingly to the marginal cut-off grade of the operation. For this schedule, CPLEX is also used to generate an initial feasible solution. The results have shown that, the biggest differences are related to the management of the stockpile (Fig. 3.9), given that for iterative approach, the OPMPS considers a more extensive use of the stockpile than the schedule obtained from using a single approximation. In this specific case study, this lead to a NPV of only 1.3% (M$35.66) larger for the first schedule than the one obtained by the second approach tested herein.

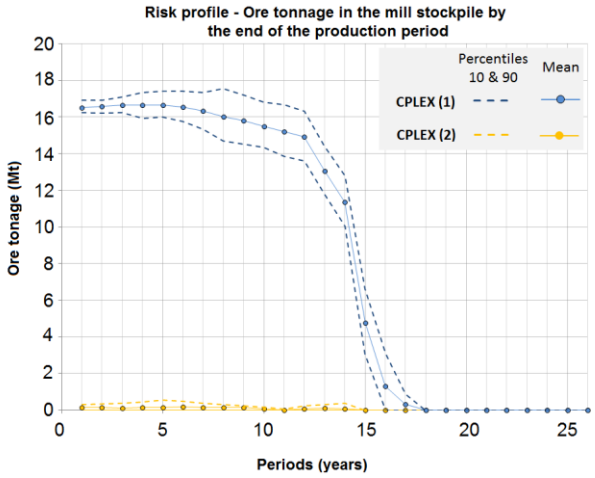

Figure 3.9 - Risk profiles for tonnage at mill stockpile - Schedules generated by iterative approximation (CPLEX(1)) and by a single approximation (CPLEX(2)) of the stockpile grade.

Chapter 4

Simulation of weathered profiles coupled with multi-element block-support simulation of the Puma Nickel Laterite Deposit, Brazil

4.1 Introduction

Over the years, stochastic simulation has been shown to be an important tool for assessment of spatial geological uncertainty in mineral deposits. Modelling uncertainty leads to a better understanding and quantification of risks at different decision levels in mining, such as in grade-tonnage curves, mine planning, grade control, etc. (e.g., Journel, 2007; Peattie and Dimitrakopoulos, 2013)

In several cases, it is of interest to model the spatial variability of not only one but a set of multiple spatially correlated variables. In contrast to the univariate case, traditional methods for multivariate simulation show cumbersome features that limit their practical use in the industrial environment (Boucher and Dimitrakopoulos, 2012). The main contributors for this complexity are the impractical computational requirements and tedious inference of an explicit model of corregionalization, which substantially increases with the number of attributes being jointly simulated (Goovaerts, 1997).

An alternative to those co-simulation frameworks is to transform the initial set of spatially correlated attributes into a new set of uncorrelated (orthogonal) factors. These factors are independently modelled and simulated, and later back-transformed to the original space of the multivariate dataset, aiming the reproduction of their cross correlations. Earlier efforts in multivariate geostatistics using such strategy are based on principal component analysis (PCA) (David, 1984, 1988). Although this methodology is simple to implement, it can only guarantee that the factors are uncorrelated at lag zero but not for all separation distances, except under very specific cases such as when assuming an intrinsic model of corregionalization (Goovaerts, 1993; Wackernagel, 2003). Leuangthong and Deutsch (2002) use a stepwise conditional transformation (SCT) to transform the data into multiGaussian variables uncorrelated at lag zero. Among the main drawbacks associated to this step-wise transformation are: the need of a large amount of

data required when dealing with several variables and the fact that, as other global transformation procedures, it may deteriorate some existing local spatial connectivity of the grades. With similar goals as SCT but solving the curse of dimensionality, Barnett and Deutsch (2014) use a projection pursuit algorithm (PPMT) to iteratively search for 'least Gaussian' structures of the multivariate distribution and sequentially "gaussianize" them. Such a process eventually transforms the multivariate data into a multivariate Gaussian distribution decorrelated at lag zero, but nevertheless that still carries a spatial structure. Tercan and Sohrabian (2013) use independent component analysis (ICA) to find *non-Gaussian* factors that are mutually independent (hence uncorrelated) at lag zero. In a different way than in previous frameworks (SCT and PPMT) that rely on a multiGaussian based algorithm to independently simulate the factors, here the authors use a direct simulation algorithm.

Aiming to find factors that are uncorrelated not only for lag zero but also at any other distance, Desbarats and Dimitrakopoulos (2000) utilize minimum/maximum autocorrelation factors (Switzer and Green, 1984) in a geostatistical context. Relying on the linear model of corregionalization (LMC) for the multivariate random field, MAF is able to provide a set of factors uncorrelated at any distance. Stochastic simulations through MAF has been increasingly used in a series of other geostatistical studies, mostly using a multiGaussian framework for the independent simulation of the uncorrelated factors (Dimitrakopoulos and Fonseca, 2003; Eggins, 2006; Lopes *et al.* 2011; Goodfellow *et al.*, 2012). Observing the fact that the orthogonalization does not relies on multinormality of the random field, in Bandarian *et al.* (2008) MAF transformation is directly applied to the dataset, without prior transformation to Gaussian space, and proceeding with a direct simulation algorithm afterwards. Although the approach reduces reliance on the multiGaussian paradigm, it suffers with the pitfalls related to direct simulation techniques. Rondon (2012) provides a thorough review about the MAF transformation.

An alternative methodology is suggested by Mueller and Ferreira (2011), who explore the application of an approximate joint diagonalization technique (AJD) called U-WEDGE. This method sets out to find a rotation matrix which is able to simultaneously diagonalize

(approximately) a set of symmetric matrices corresponding to the series of cross-variograms at different lags.

For mineral deposits, the target support to be simulated (selective mining unit) is usually much larger than the available drilling data (typically considered as point support). Thus, the common practice consists on simulating the entire deposit at point support followed by a post-processing step to average the point grades inside each mining block. Such approach can be cumbersome in practical terms when large deposits are simulated, comprising several millions of blocks. A simulation alternative for univariate multiGaussian random fields directly at block support is proposed in Godoy (2002) and extended to the joint simulation with MAF in Boucher and Dimitrakopoulos (2009, 2012), significantly increasing efficiency and reducing memory requirements during the simulation.

This paper details the application of MAF and direct block simulation for modelling the joint spatial uncertainty of multiple geological attributes of Puma, a major nickel laterite deposit in Brazil. The nickel enrichment is result of intensive weathering and laterization of ultramafic ridge complexes within the Amazon Craton of the Brazilian Precambrian Shield. Above the bed rock, a saprolitic zone is found, characterized by high content of Nickel, relatively high silica and magnesia and low iron contents. Near to the surface, an iron-rich unit is formed, with a lower nickel, silica and magnesia contents. The supergene enrichment of the regolith, leaching and erosional processes result in a highly complex environment, which accounts with a large spatial variability of thicknesses and grades.

Due to the great disparity of their chemical composition, very different metallurgical routes are needed to process limonitic or saprolitic ore. In its current operation, the mine produces ferronickel from the saprolitic ore, while the limonitic ore type is treated as an opportunity material. The process efficiency is extremely sensitive to the head grades, requiring a strict control over the quality of the ore feed, which reinforces the necessity of jointly modelling the spatial variability of multiple elements.

The following sections include a summary of the joint simulation framework through MAF and its extension for direct block simulation; a thorough description of the deposit and available data; joint simulation of bottom layers of limonite and saprolite domains,

by means of modelling their respective thicknesses, followed by subsequent joint simulation of Ni, Co, Fe, SiO_2, MgO and Dry-Tonnage Factor (DTF), aiming to a geological plausibility of the complex orebody and control over operational quality required by the ferronickel plant. Thereafter, the results from the generated grade-tonnage curves are discussed, followed by conclusions.

4.2 A recall on joint simulation of multiple correlated attributes through min/max autocorrelation factors (MAF)

Let $\boldsymbol{Z}(\boldsymbol{u}) = [Z_1(\boldsymbol{u}), Z_2(\boldsymbol{u}), \dots, Z_K(\boldsymbol{u})]^T$ denote a stationary and ergodic random field (RF) over a region D, representing K correlated continuous attributes of a natural phenomenon measured on isotopic point support samples. Now, consider its pointwise normal score transformation $\boldsymbol{Y}(\boldsymbol{u}) = [Y_1(\boldsymbol{u}), \dots, Y_K(\boldsymbol{u})]^T = [\varphi_1(Z_1(\boldsymbol{u})), \dots, \varphi_K(Z_K(\boldsymbol{u}))]^T$, which is deemed a multiGaussian RF with zero mean and unit variance. The minimum/maximum autocorrelation factors $\mathbf{M}_{\boldsymbol{MAF}}(\boldsymbol{u})$ are defined as pairwise orthogonal linear combinations of the Gaussian variable $\boldsymbol{Y}(\boldsymbol{u})$ as following (Desbarts and Dimitrakopoulos, 2000):

$$\mathbf{M}_{\boldsymbol{MAF}}(\boldsymbol{u}) = \boldsymbol{A}^{\boldsymbol{T}}\boldsymbol{Y}(\boldsymbol{u}) \tag{4.1}$$

For which the coefficients of the transformation matrix $\boldsymbol{A}$ are obtained from:

$$\boldsymbol{A}^{\boldsymbol{T}} = \boldsymbol{Q}_2^T \boldsymbol{\Lambda}_{\mathbf{1}}^{-1/2} \boldsymbol{Q}_1^T \tag{4.2}$$

where $\boldsymbol{Q}_1$ and $\boldsymbol{\Lambda_1}$ are respectively the matrices of eigenvectors and eigenvalues obtained from the spectral decomposition of the symmetric covariance-variance matrix $\boldsymbol{B}$ of the RF $\boldsymbol{Y}(\boldsymbol{u})$ at zero lag distance. Matrix $\boldsymbol{Q}_2$ is the matrix of eigenvectors resulted from the following spectral decomposition:

$$\boldsymbol{\Lambda}_2 = \boldsymbol{Q}_2 \boldsymbol{\Gamma}_{\boldsymbol{P_{PCA}}}(\Delta) \mathbf{Q}_2^T \tag{4.3}$$

where matrix $\boldsymbol{\Gamma}_{\boldsymbol{P_{PCA}}}(\Delta)$ is an experimental variogram matrix at lag Δ for PCA factors derived from:

$$\boldsymbol{P_{PCA}}(\boldsymbol{u}) = \boldsymbol{\Lambda}_{\mathbf{1}}^{-1/2} \boldsymbol{Q}_1^T \boldsymbol{Y}(\boldsymbol{u}) \tag{4.4}$$

In practice, to ensure that the transformed variables are orthogonal at all distances, several experimental lags Δ must be tested, selecting the one which provides the best decorrelation of the factors. This 'data-driven' approach of MAF avoids the tedious modelling and fitting of a linear model of corregionalization, since the transformation matrix is directly derived from the experimental data.

These new defined factors $\mathbf{M}_{\boldsymbol{MAF}}(\boldsymbol{u})$ can be independently modelled and simulated since they are spatially uncorrelated for any distance. Moreover, because of the initial multiGaussian assumption, they also follow the same distribution law, which allows the use of sequential Gaussian simulation (SGS) to provide point support realizations for each factor. More general and efficient frameworks can also be applied such as direct block simulation.

4.2.1 Direct Block Simulation

Aiming to increase efficiency and to alleviate computational requirements associated to memory and data management during geostatistical simulation, Godoy (2002) has proposed a direct block simulation framework (DBSim). This method produces univariate simulations of multiGaussian random fields. Boucher and Dimitrakopoulos (2009) have extended the idea for direct block simulation of multiple correlated variables, independently simulating the MAF factors for each of the blocks inside the domain. Thus, the simulation at block-support scale using MAF calls for the block support RF $\boldsymbol{Z}_V(\boldsymbol{v})$ defined as following:

$$\boldsymbol{Z}_V(\boldsymbol{v}) = \frac{1}{N}\sum_{i=1}^{N} \phi^{-1}[(\boldsymbol{A}^T)^{-1}\boldsymbol{M}_{MAF}(\boldsymbol{u}_i)]\,, \quad \boldsymbol{u}_i \in \boldsymbol{v}, \forall i \tag{4.5}$$

where each block $V \in D$ is discretized by a set of N points indexed by $\boldsymbol{u}_i$.

The algorithm follows a random path to visit each of the blocks inside the domain and, for each one of the factors (indexed by $l = 1 \ldots k$), the N discretizing points are simulated by performing a joint LU simulation (Myers, 1989). Intuitively, it can be seen as a pointwise simulation using an extension of the generalized group sequential Gaussian simulation (Dimitrakopoulos and Luo, 2004), implementing joint LU to

incorporate conditioning information at different supports (samples and internal nodes at point support plus previously simulated blocks). Let $\boldsymbol{C}_{IIVV}^{l}$ be the covariance matrix of all conditioning information and $\boldsymbol{C}_{pIV}^{l}$ the covariance matrix between the discretizing nodes and the neighboring information at point and block supports for the l^{th} factor. Those can be expanded as:

$$\boldsymbol{C}_{IIVV}^{l} = \begin{bmatrix} \boldsymbol{C}_{II}{}^{l} & \boldsymbol{C}_{IV}{}^{l} \\ \boldsymbol{C}_{VI}{}^{l} & \boldsymbol{C}_{VV}{}^{l} \end{bmatrix} \quad \text{and} \quad \boldsymbol{C}_{pIV}^{l} = \begin{bmatrix} \boldsymbol{C}_{pI}{}^{l} & \boldsymbol{C}_{pV}{}^{l} \end{bmatrix} \tag{4.6}$$

where $\boldsymbol{C}_{II}{}^{l}$, $\boldsymbol{C}_{IV}{}^{l}$ and $\boldsymbol{C}_{VV}{}^{l}$ are point-to-point covariance matrices, point-to-block, and block-to-block covariances, respectively for the l^{th} factor; $\boldsymbol{C}_{pI}{}^{l}$ and $\boldsymbol{C}_{pV}{}^{l}$ are the covariances between the discretizing nodes and the neighboring information at point and block supports respectively.

Finally, the vector of N simulated factors $\boldsymbol{m}_{p}{}^{l*}$ inside a given block for each factor l, is obtained by solving the following system of equations (Godoy, 2002; Boucher and Dimitrakopoulos, 2009):

$$\boldsymbol{m}_{p}{}^{l*} = \boldsymbol{L}_{21}{}^{l}\left(\boldsymbol{L}_{11}{}^{l}\right)^{-1}\boldsymbol{m}_{IV}{}^{l} + \boldsymbol{L}_{22}{}^{l}\boldsymbol{w} \tag{4.7}$$

where $\boldsymbol{m}_{IV}{}^{l}$ is the vector containing neighboring samples at point support and previously simulated blocks for the factor l, $\boldsymbol{w}$ is a vector of random numbers following a standard normal distribution and $\boldsymbol{L}_{21}{}^{l}$, $\boldsymbol{L}_{11}{}^{l}$ and $\boldsymbol{L}_{22}$ are obtained from the following Cholesky decomposition:

$$\begin{bmatrix} \boldsymbol{C}_{IIVV}{}^{l} & \boldsymbol{C}_{IVp}{}^{l} \\ \boldsymbol{C}_{pIV}{}^{l} & \boldsymbol{C}_{PP}{}^{l} \end{bmatrix} = \begin{bmatrix} \boldsymbol{L}_{11}{}^{l} & \boldsymbol{0} \\ \boldsymbol{L}_{21}{}^{l} & \boldsymbol{L}_{22}{}^{l} \end{bmatrix} \begin{bmatrix} \boldsymbol{L}_{11}{}^{l^T} & \boldsymbol{L}_{21}{}^{l^T} \\ \boldsymbol{0} & \boldsymbol{L}_{22}{}^{l^T} \end{bmatrix} \tag{4.8}$$

One may note that, once the conditioning neighbourhood is retrieved, the system of equations shown in (4.7) and (4.8) must be solved k times, one for each factor l. Moreover, it is important to note that, because the simulation process is conditioned by previously simulated blocks at MAF space and that, there is no direct transformation from this orthogonal space to the original space of the multivariate attributes at block support, after the simulation of internal nodes, the process must be split in two parts: (i) the block values $\boldsymbol{M}_{\boldsymbol{V}}^{\boldsymbol{l*}}(\boldsymbol{v})$ for each one of the factors are obtained by averaging the

simulated factors $\boldsymbol{m}_p{}^{l*}$ at point supports, and (ii) the internal nodes are back rotated to the data space and averaged to generate the desired block values as previously shown in Eq. (4.5).

The direct block MAF simulation algorithm (Boucher and Dimitrakopoulos, 2009) proceeds as following:

1. Transform the data $\boldsymbol{Z}(\boldsymbol{u})$ to normal scores $\boldsymbol{Y}(\boldsymbol{u})$.
2. Orthogonalize $\boldsymbol{Y}(\boldsymbol{u})$ through MAF transformation to obtain $\boldsymbol{M}_{MAF}(\boldsymbol{u})$.
3. Define a random path visiting each block.
4. For each block V, simulate for each factor l the discretizing N internal points $\boldsymbol{m}_p{}^{l*}(\boldsymbol{u}_i),\ i = 1, \dots, N$, using the LU decomposition as shown in Eq. (4.8). Afterwards:
    a. For each factor l, average $\boldsymbol{m}_p{}^{l*}(\boldsymbol{u}_i)$ over the block to obtain the simulated block values $\boldsymbol{M}_{\boldsymbol{V}}^{\boldsymbol{l}*}(\boldsymbol{v})$ for each corresponding factor.
    b. Back-transform of $\boldsymbol{m}_p{}^{l*}(\boldsymbol{u}_i)$ at all discretizing nodes and for all factors, in order to obtain the simulated block value $\boldsymbol{Z}_{\boldsymbol{V}}^{*}(\boldsymbol{v})$ as in Eq. (4.5).
5. Repeat step 4 until all blocks are simulated.

4.3 Simulation of the Puma Nickel Laterite Deposit

4.3.1 Deposit description and data available

The lateritic deposit studied herein (Puma) is located in northern Brazil and it has developed from layered ultramafic complexes intruding Pre-Cambrian Brazilian shield. Supergene and residual concentrations of nickel have developed along an elongated ridge for some 23km, for which only 3.5 km are comprised in this study. The ridge is an elevated area with its northerly slopes range up to 30°-45° and its southerly slopes 10°-15°. An important characteristic of the deposit are extensive silica caps on the ridges, which was likely responsible to preserve saprolitic ores from erosion (Canico Resources Corporation [CRC], 2005). The main structures of variability of the deposit are controlled

by the geometry of the ridge, which was aligned along East-West. The vertical direction comprises the direction of major variability.

The data set used in this study comprises 1 938 drill holes with 59 821 core samples regularized in interval lengths of 1m, assayed for Ni, Co, Fe, SiO_2, MgO and Dry-Tonnage-Factor (DTF). For confidentiality reasons the grades and DTF were modified by a constant factor. The vertical drill holes retrieved for this study cover an area of approximately 4.8 km^2 (Fig. 4.1). The holes are at shallow depths (mode of approximately 9.0m) and the sampling grid spacing is approximately 25 m in most of the areas of the ridge. In some denser areas, the separation can be as close as 6m and approximately 100 m in more external parts of the deposit.

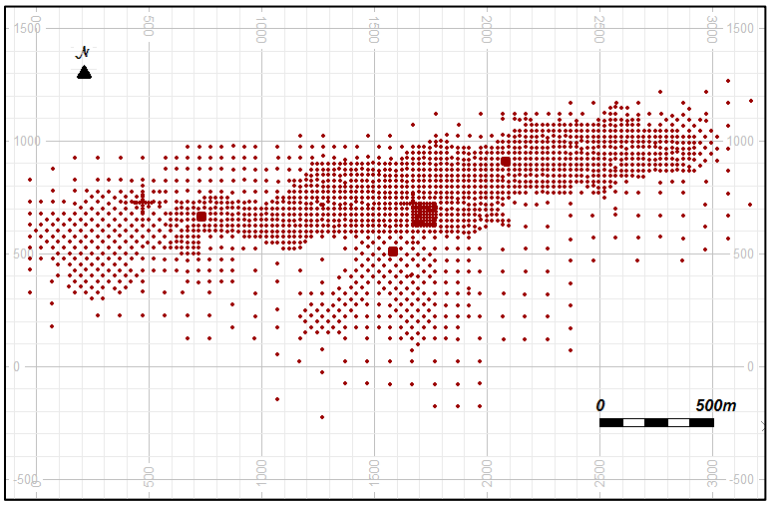

Figure 4.1 - Plan view showing the drill hole locations along the deposit ridge.

The lithologies are grouped according to their characteristics and they can be simplified into three distinct layers:

a. Limonite (Rock Code = 0), which is the uppermost horizon and has been completely altered by chemical weathering. Primary textures are absent, with iron-rich minerals increasing to the top, becoming pisolitic. It contains some nickel, low MgO and high Fe.

b. Saprolite (Rock Code = 1), which is the primary source of nickel for the ferronickel process in the actual mine. Zone with somewhat altered bed rock, with

preserved structures and textures of minerals. It is rich in hydrous Mg silicates. Shows a low content of Fe and high MgO.

c. Bedrock (Rock Code = 2), which is the parental rock lightly weathered. It can be characterized by low nickel grades, high MgO and low Fe.

4.3.2 Joint Simulation of Weathered Profiles

In this section, the main goal is to simulate the geometry of the main lateritic units in order to model their joint spatial uncertainty. This is accomplished by jointly simulating the bottom surfaces of limonite and saprolite. It is noteworthy that the weathering and leaching mechanisms in lateritic deposits, usually act in a way that bottom layers of the lateritic domains are well correlated to the topography. This reference level can be treated as a regional trend, thus, each bottom layer is modelled in terms of its residual part, which corresponds to the thickness. In other words, to obtain the simulated elevations of each geological unit, the thicknesses of the different profiles of the regolith are stochastically modelled and subtracted from the topography.

In addition, one may recall that the vertical drillholes do not directly capture the true thicknesses of the geological units, hence, the sample thicknesses are calculated after applying an *unwrinkle* process to the bottom levels using the topography level as reference (Deutsch, 2005). After simulating, the thicknesses are added back to the "flattened" topography in order to generate the bottom layers' elevations of each unit. Then, those layers are "folded" back to the original space of the deposit, and they are taken as reference levels to build the categorical orebody models at block support of $12x12x3m^3$.

In order to extract representative univariate statistics of the thickness for both limonite and saprolite units, declustering cells of 25m are used. Table 4.1 brings a summary of these declustered statistics. As one may note, both distributions are positively skewed, with limonite showing a higher variability. One important feature from the distributions is the remarkable discontinuity at the origin. This is shown in Table 4.1 as the percentage of missing thicknesses, which relates to the percentage of locations where each profile is absent. These "missing thicknesses" are mostly associated with eroded locations, mainly

located at steep slopes. As mentioned above, besides the fact that it is the uppermost geological unit, the limonite is also more easily eroded than the saprolite, because the latter is protected by a siliceous cap over it.

Tabela 4.1 - Summary of declustered statistics for true thickness (TTK) of main units

	Mean (m)	CV	Skewness	Kurtosis	Min (m)	P 25 (m)	P 50 (m)	P 75 (m)	Max (m)	Missing TTK (%)
Limonite	2.41	1.23	2.73	12.15	0	0	1.98	3.02	28	35.55
Saprolite	9.22	0.72	1.27	2.04	0	4.52	7.67	12.52	45	2.44

The global correlation between the thicknesses of both units is practically absent ($\rho < 0.1$). At first glance, as the thicknesses showed no correlation, they could be simulated independently on the basis of their individual regionalization, but nevertheless this could lead to some geological inconsistencies where local correlations exist. For example, information such as absence of limonite actually increases the probability of also eroded saprolite. In this study, it has been decided to jointly simulate saprolite and total thicknesses, with the limonite being indirectly obtained by subtracting the saprolite from the total thickness. Figure 4.2 brings a scatterplot showing the correlation between those variables:

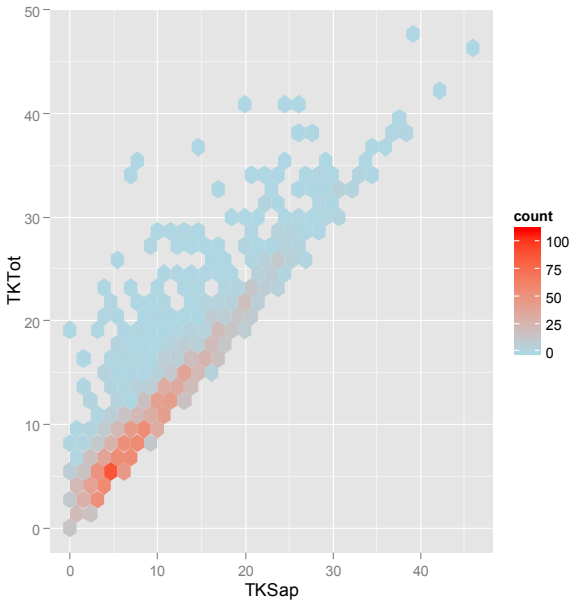

Figure 4.2 - Scatterplot for Saprolite and Total thicknesses ($\rho = 0.92$).

4.3.2.1 Normal score and MAF transformations of thicknesses

Prior to applying MAF transformations to the spatially correlated variables, each of them are transformed to a standard normal distribution. It is noteworthy that, the correlation between the normal score variables are kept very similar to the ones in the data space ($\rho = 0.90$), which suggests that the correlation is well preserved after the transformation. The lag distance (Δ) used in Eq. (4.3) is 25m and is derived after experimentally testing several distances to assure suitable decorrelation of the MAF factors. The omnidirectional correlogram between them is depicted in Fig. 4.3, showing the absence of correlation over all distances.

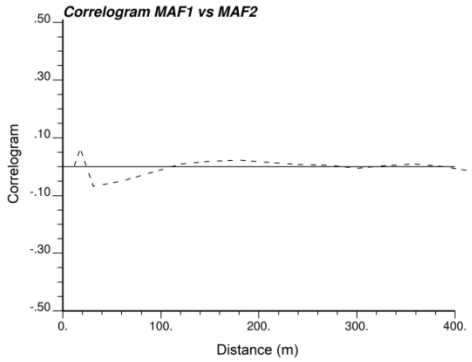

Figure 4.3 - Correlogram between MAF1 and MAF2.

Fig. 4.4 shows the experimental variograms of each factor fitted by their respective models. They both are assumed to contain a nugget and a spherical structure. One may note that MAF1, which has the larger eigenvalue associated to it, absorbs great part of the variance, which is revealed by its smaller spatial continuity if compared to MAF2.

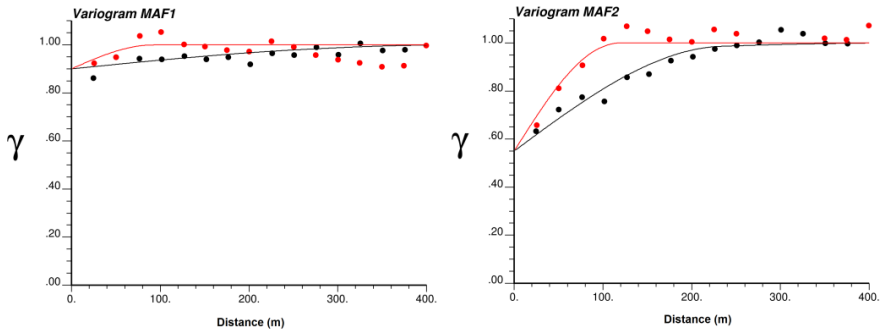

Figure 4.4 - Experimental variogram (dotted) and fitted models (lines) of each MAF factor for the main directions, NS (red) and EW (black).

4.3.2.2 Conditional simulation of MAF factors

Conditional simulation is independently performed on the two MAF factors using the pointwise sequential Gaussian simulation (SGS) on a grid of $3x3m^2$, resulting in a total of approximately 400,000 nodes. Five simulations are generated for each factor. The validation of MAF simulations is not presented herein since the subsequent sections show the validation of realizations directly in data space.

4.3.2.3 Validation of simulated thicknesses

In addition to a visual inspection, validation of jointly simulated variables involves the calculation of univariate distributions, experimental variograms and cross-variograms of the simulated realization in the data space to ensure the reproduction of statistics inferred from the original data. Fig. 4.5 shows that both declustered cumulative distributions of saprolite and total thicknesses are well reproduced by the simulated models.

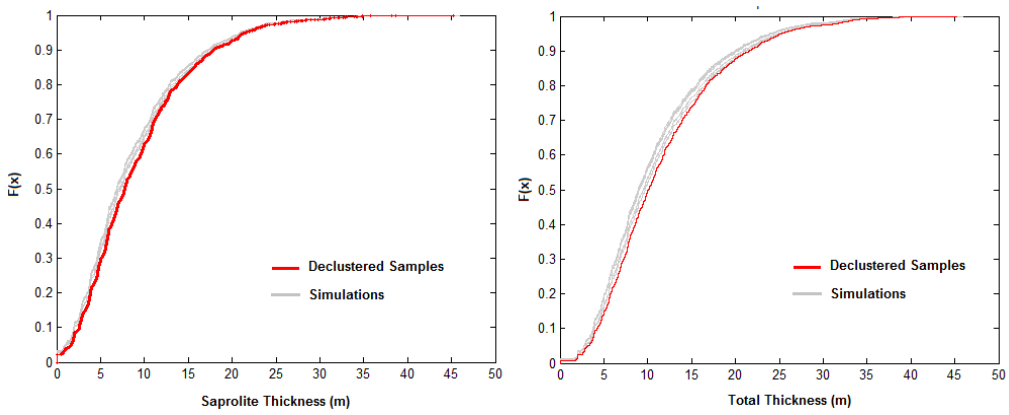

Figure 4.5 - Cumulative distributions of declustered data in red and simulated models in gray for saprolite (left) and total thickness (right).

Figures 4.6 to 4.8 show that the conditional simulations honour the variograms and cross-variograms of the original drillhole data. Recall that the variograms and cross variograms of the original variables are not directly used during the simulation, since it only requires the variograms of the uncorrelated MAF factors.

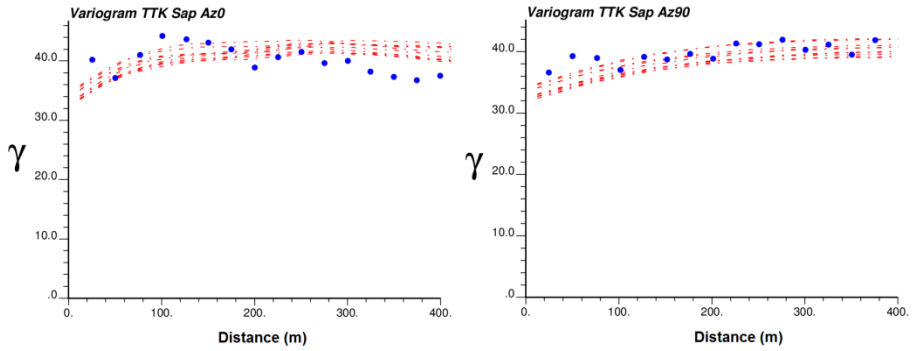

Figure 4.6 - Experimental variogram (blue dots) and simulated models (red dashed lines) for Saprolite thickness along the main directions NS and EW.

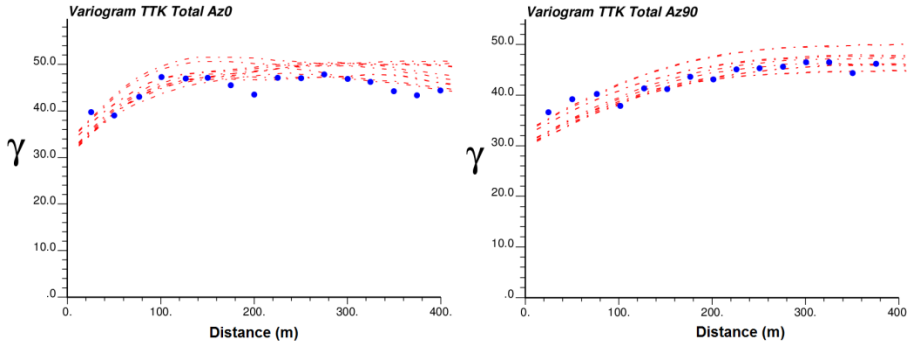

Figure 4.7 - Experimental variogram (blue dots) and simulated models (red dashed lines) for Total thickness along the main directions NS and EW.

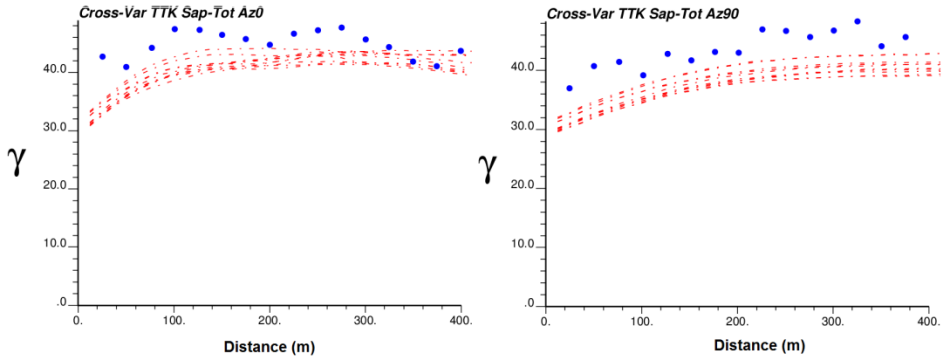

Figure 4.8 - Experimental cross-variograms (blue dots) and simulated models (red dashed lines) between Saprolite and Total thicknesses along the main directions NS and EW.

In a post-processing step, the limonite thicknesses are derived from the subtraction of the saprolite from the total thickness. The validation of its spatial variability and univariate distribution are depicted in the Chapter Appendix A. In addition to this, the indicator variograms of the categorical model generated after back transforming the simulated bottom layers of the mineralized units, are also well reproduced.

4.3.3 Multivariate block-support simulation of grades and Dry-Tonnage factor

Joint simulations directly on the block support ($12x12x3m^3$) for Ni, Co, Fe, MgO, SiO_2 and Dry-Tonnage-Factor, are constrained by previously simulated saprolite and limonite units. Although the actual mine operates a pyrometallurgical plant and only saprolitic ore is processed, the joint simulation of the elements inside the limonitic horizon is motivated by the fact that it is actually enriched in nickel and that such approach may lead to a better model of dilution. As mentioned previously, a strict control of the silica (SiO_2) to magnesia (MgO) ratio and iron (Fe) content is required to ensure minimal disruptions of the ferronickel plant.

Fig. 4.9 shows the declustered distribution of the main attributes of interest for the processing plant (Nickel, Iron, SiO_2:MgO ratio), inside the different lithological units.

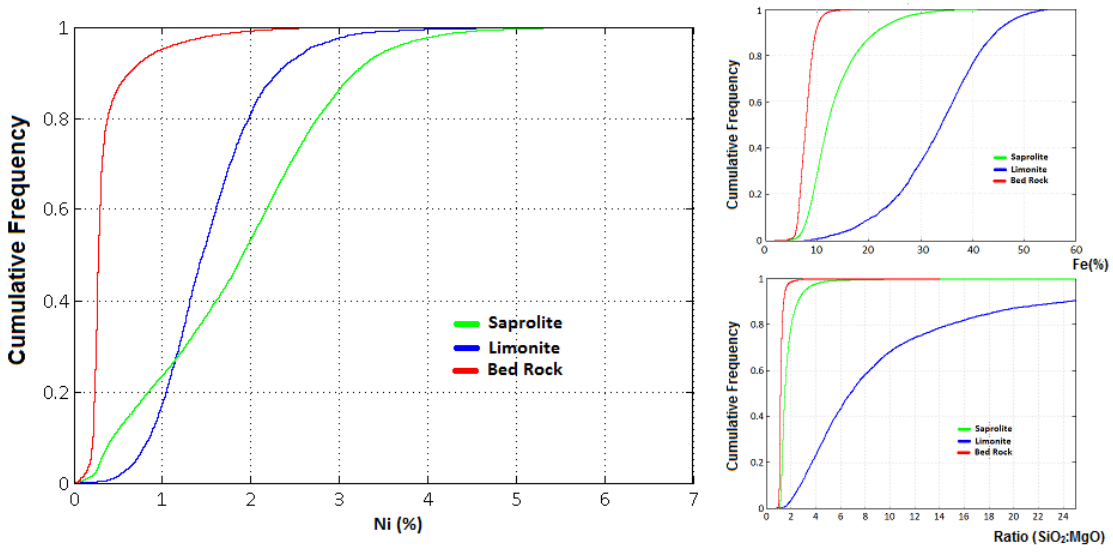

Figure 4.9 - Distribution of the samples' Ni grades over the different lithological horizons.

These curves highlight the dissimilarities of the populations inside the different weathered profiles of the Ni laterite. It clearly shows that limonite and saprolite are the main horizons enriched in Nickel. Saprolite shows a higher Ni average grade and variability than the limonite. The opposite behavior is verified for the iron content and Si:Mg ratio.

Vertical trends are commonly seen in laterite nickel studies. For this case study in particular, trends inside the saprolitic unit are not as significant as the ones found for the limonite. Therefore, inside this latter unit, the simulation is carried out on the residuals of each attribute after modeling their respective trends. The scatterplot matrix showing their multivariate correlation between the elements inside each domain are depicted in Fig. 4.10, also highlighting both Pearson and Spearman (ranked) correlation coefficients.

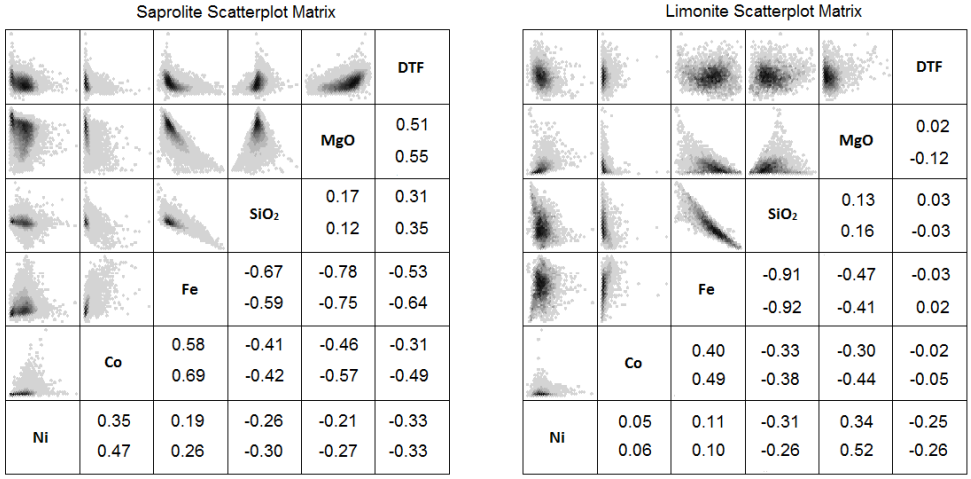

Figure 4.10 - Scatterplots of elements modeled (upper diagonal pannel) and correlation coefficients in lower diagonal pannel, with Pearson above and Spearman below, for both geolocial units, Saprolite and Limonite.

As expected, Fig. 4.10 shows that the correlations between the elements may significantly vary from one geological unit to the other. For instance, even though nickel shows a moderate correlation to most of the other elements inside the saprolite horizon, it shows very low correlations with Co and Fe for the limonite.

4.3.3.1 Normal score and MAF transformations of multi-elements

Similar to the steps carried out for the simulation of thicknesses, each of the attributes modeled herein is transformed to normal score space. Recall that for the limonite, the variables considered are the residuals obtained for each element after subtracting their modelled trends.

For deriving the loading matrix of the MAF transformations, a lag distance (Δ) of 25m is used in Eq. (4.3), i.e. the same values as in the joint simulation of thicknesses. Fig. 4.11 shows that, there are no spatial cross-correlations between the six different factors inside each geological unit, suggesting that the MAF factors have been reasonably well decorrelated.

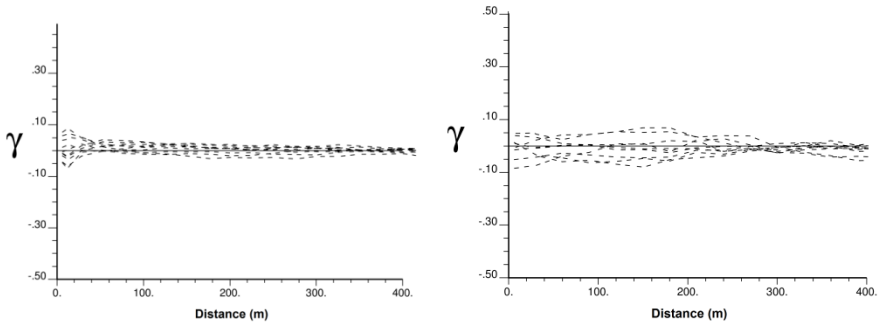

Figure 4.11 - Omnidirectional correlogram between MAF factors taken in pairs for saprolite (left) and limonite (right).

The variography on each factor are performed and the experimental variograms are fitted using exponential models. Those variograms are shown in Chapter Appendix B.

4.3.3.2 Conditional simulation of MAF factors

Conditional simulations for each of the factors in each of the domains previoulsy simulated are performed independently using Eq. 4.7 and averaged into blocks using Eq. 4.5. Five simulations are generated inside each geological unit (total of 5 x 5 = 25 simulations) using blocks of 12x12x3m^3 and a 4x4x3 node discretization, resulting in an an average of 50 and 20 thousand blocks inside saprolite and limonite units, respectively. For comparison, at point support scale, this corresponds to a simulation of about 900,000 and 2,500,000 nodes inside each of these geological units.

It is noteworthy that, for the case of limonite, an additional step is needed during the direct simulation at block support. In Eq. 4.5, besides the back transformations from MAF and normal score spaces, the trend also need to be added back to the simulated residuals at the discretizing nodes, before their average is calculated to obtain the simulated block value in data space. Once again, the validation of MAF simulations is not presented herein since the subsequent sections show the validation of realizations directly in data space.

4.3.3.3 Validation of multi-elements simulation

For validations purposes, the point-scale simulated values for some simulations in both saprolite and limonite units are retrieved. Then, the same validations performed for the simulation of thicknesses in Section 4.3.2 are repeated herein in the data space. Fig. 4.12 shows that the cumulative distributions of each simulated attribute honour the declustered statistics infered from the drillholes with some ergodic fluctuations.

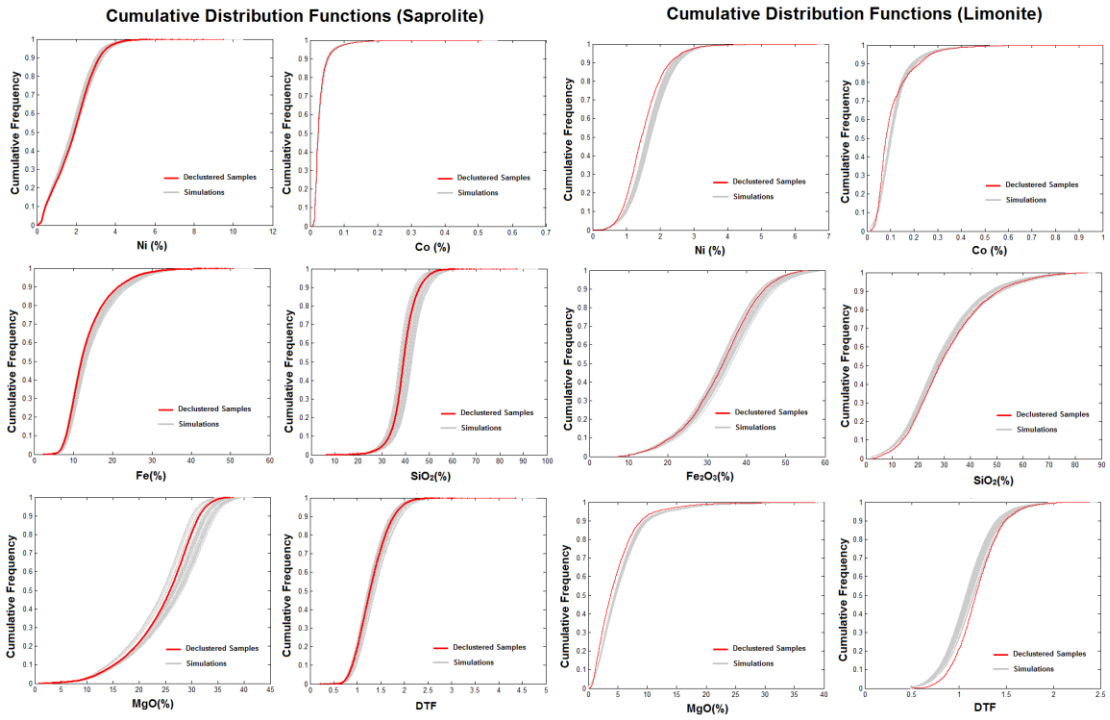

Figure 4.12 - Experimental cumulative distribution functions of declustered samples (red) and simulated models at point supports (gray) for saprolite (left) and limonite (right).

Figures 4.13 to 4.16 show some plots of variograms and cross-variograms for drillhole samples and conditional simulations at point support scales inside the saprolite unit. All results suggest that geostatistical realizations are able to reproduce the main spatial features seen for the original data.

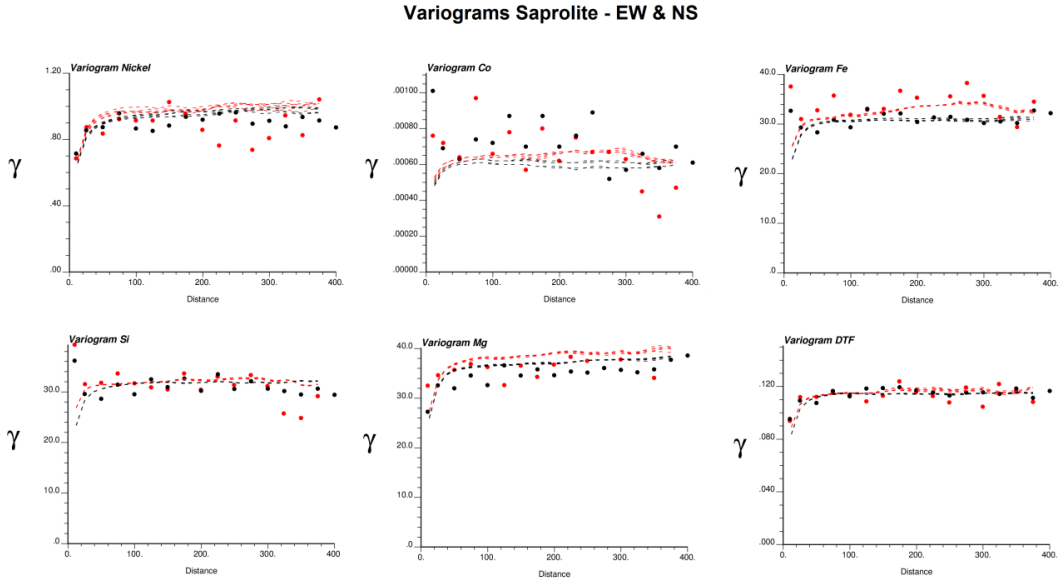

Figure 4.13 - Saprolite - Experimental direct variograms (dotted) and point-support simulated models (lines) for each element in data space over the horizontal direction (NS in red and EW in black).

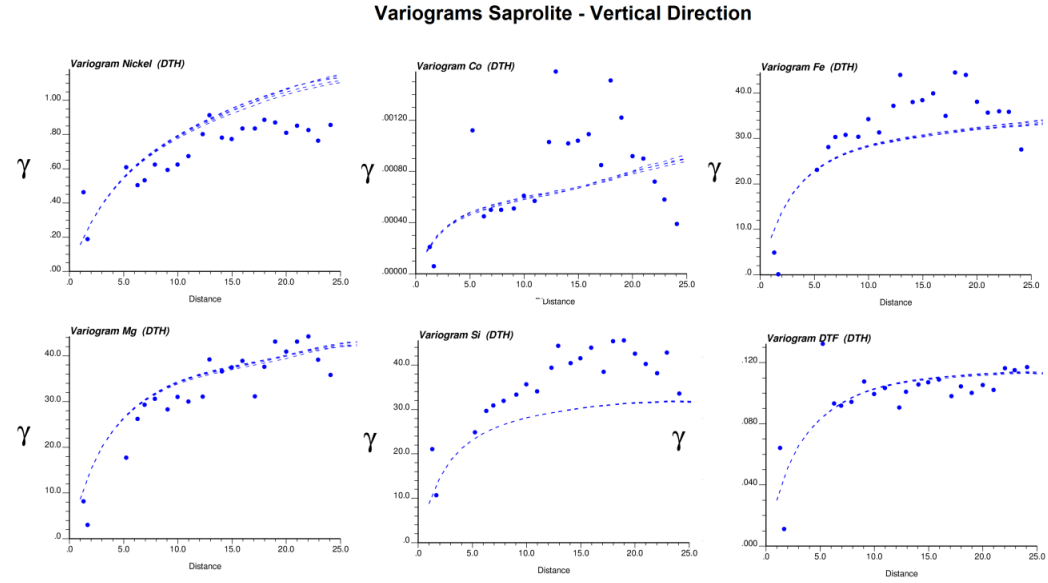

Figure 4.14 - Saprolite - Experimental direct variograms (dotted) and (point-support) simulated models (lines) for each element in data space along the vertical direction.

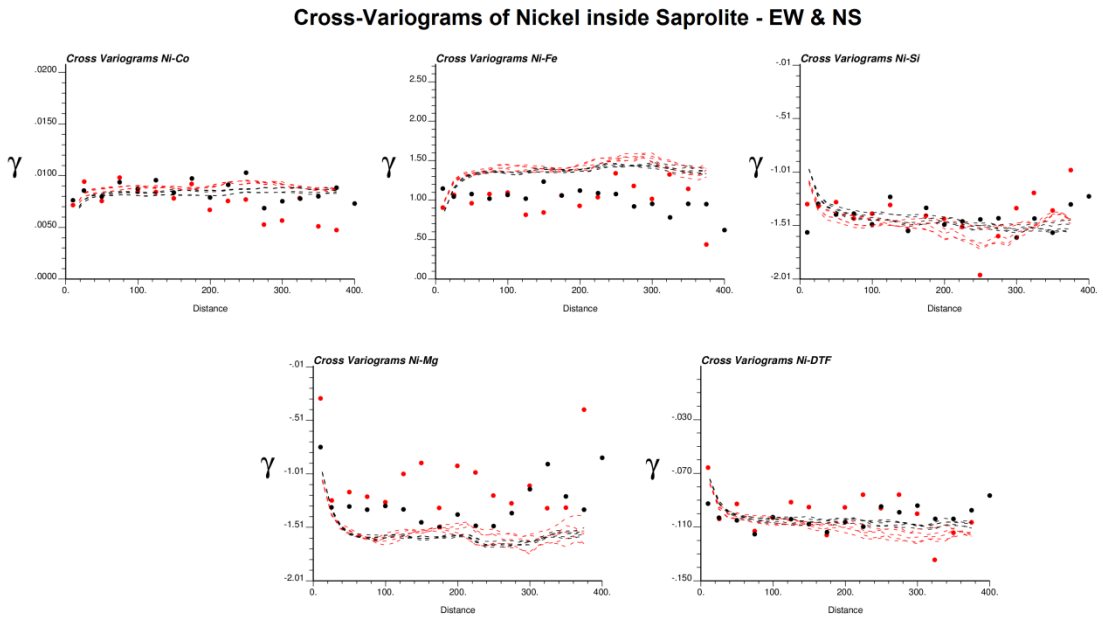

Figure 4.15 - Saprolite - Experimental cross-variograms (dotted) and point-support simulated models (dashed lines) for nickel and other five elements, in data space, over the horizontal direction (NS in red and EW in black).

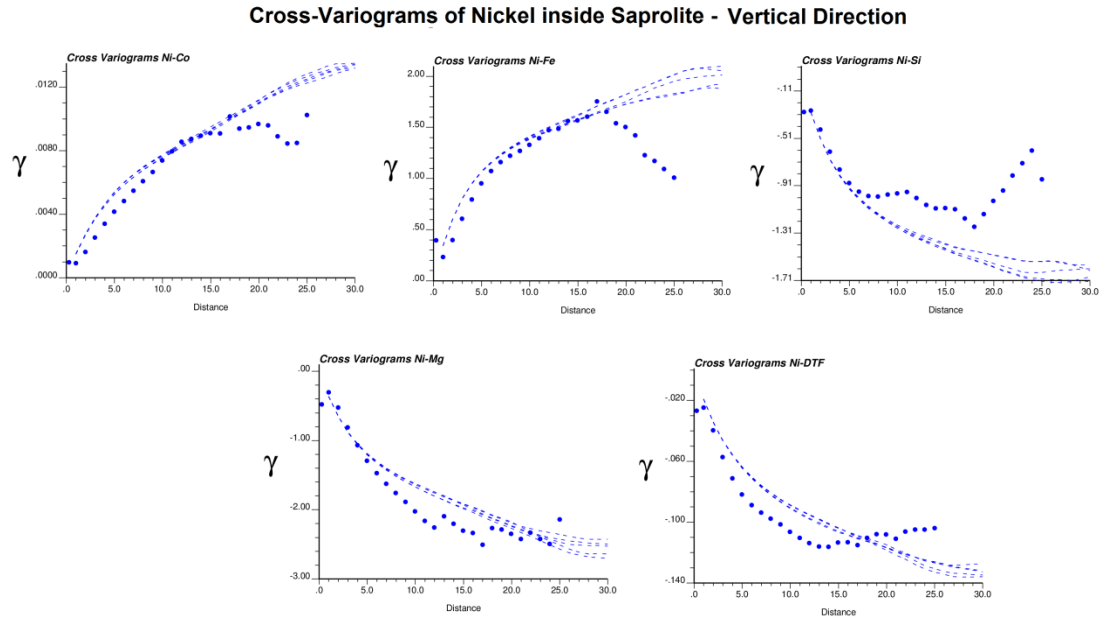

Figure 4.16 - Saprolite - Experimental cross-variograms (dotted) and point-support simulated models (dashed lines) for nickel and other five elements, in data space, along the vertical direction.

The reproduction of spatial statistics for the limonite are also very good, but for the sake of brevity[1], only the vertical variogram of nickel and its cross variogram with MgO are shown in Fig. 4.17, in order to highlight the reproduction of vertical trends seen in these experimental variograms of the data.

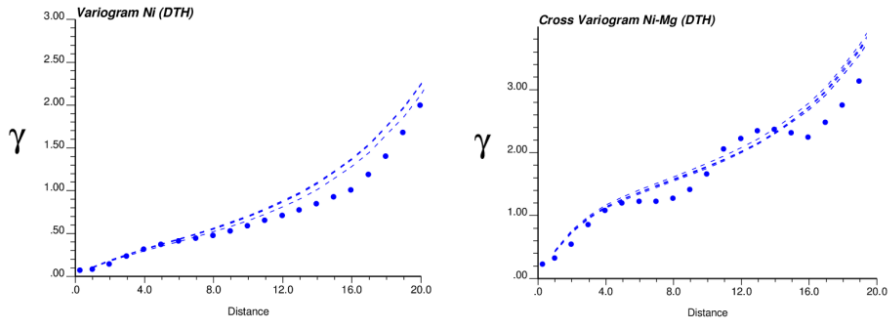

Figure 4.17 - Limonite - Experimental Ni variograms and Ni-Mg cross-variograms (dotted) and point-support simulated models (dashed lines), in data space, along the vertical direction.

4.3.3.4 Validation of high-order spatial statistics

The joint simulation framework used in this thesis relies on two-point simulation techniques, which are not able to incorportate complex, non-linear and non-Gaussian, geological features of the deposit. In order to assess the reproduction of high-order statistics by the simulated models, high-order spatial cumulants can be used (De Iaco and Maggio, 2011). These high-order statistics provides a way to characterize non-Gaussian random fields, and they have been shown to carry important information about the in situ behavior of geological entities or processes (Dimitrakopoulos *et al.*, 2010). Third-order cumulant maps were calculated for samples and simulations using different spatial templates. Figs. 4.18 and 4.19 respectively show the third-order cumulant maps for nickel and iron for two different spatial templates. The first comprising the vertical and East-West directions, and the second oriented to follow the structure of the ridge (in which the supergene and residual concentrations of nickel have developed), dipping 15 degrees to north and south directions.

[1] All (cross)-variograms for both saprolite and limonite domains are shown in the Appendix A,B of this thesis.

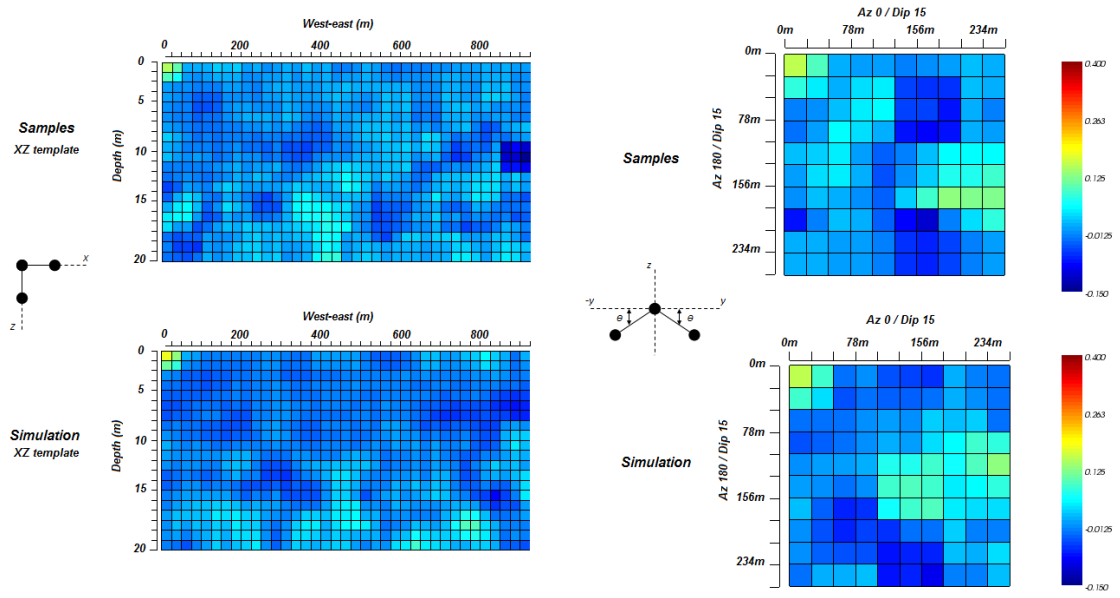

Figure 4.18 – Third-order cumulants maps of nickel for both samples (top) and simulated models (bottom), with their respective spatial templates on the left.

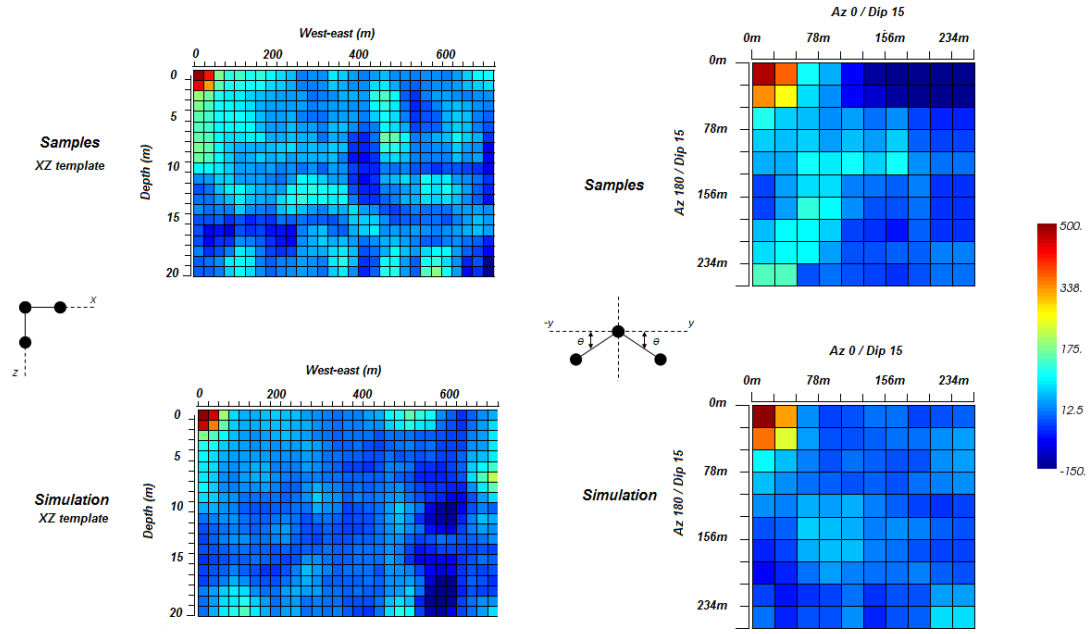

Figure 4.19 – Third-order cumulants maps of iron for both samples (top) and simulated models (bottom), with their respective spatial templates on the left.

One may note that, because the framework used herein aims to indirectely add some high-order complexity into the simulation process, by for example using unwrinkling for the simulation of the geological units and considering the spatial correlation of several variables, some high-order spatial features of the samples are honoured by the simulations (*see* Fig 18 and 19). However, many other high-order features are not well reprocuced, and these are specially notable for the third-order cumulant maps in Fig. 4.19.

4.3.4 Visualization of conditional simulations

Fig. 4.20 shows the example of a joint simulation at block support scale for the different lateritic zones and a joint simulation of Ni, Fe and SiO_2:MgO constrained by it. As suggested by the data set, the plan view of categorical simulation shows how saproltite tends to outcrop at the surface in many places where limonite was eroded because of the steep relief . The other plan views for the continuous elements split the simulations inside each of the lateritic zones. Thus, the most of the saprolite shown in those maps actually lies underneath the limonite layer. These maps highlight the spatial differences between limonite and saprolite and reinforce the previous validations, which suggest that the simulated models honour the spatial features from the dataset.

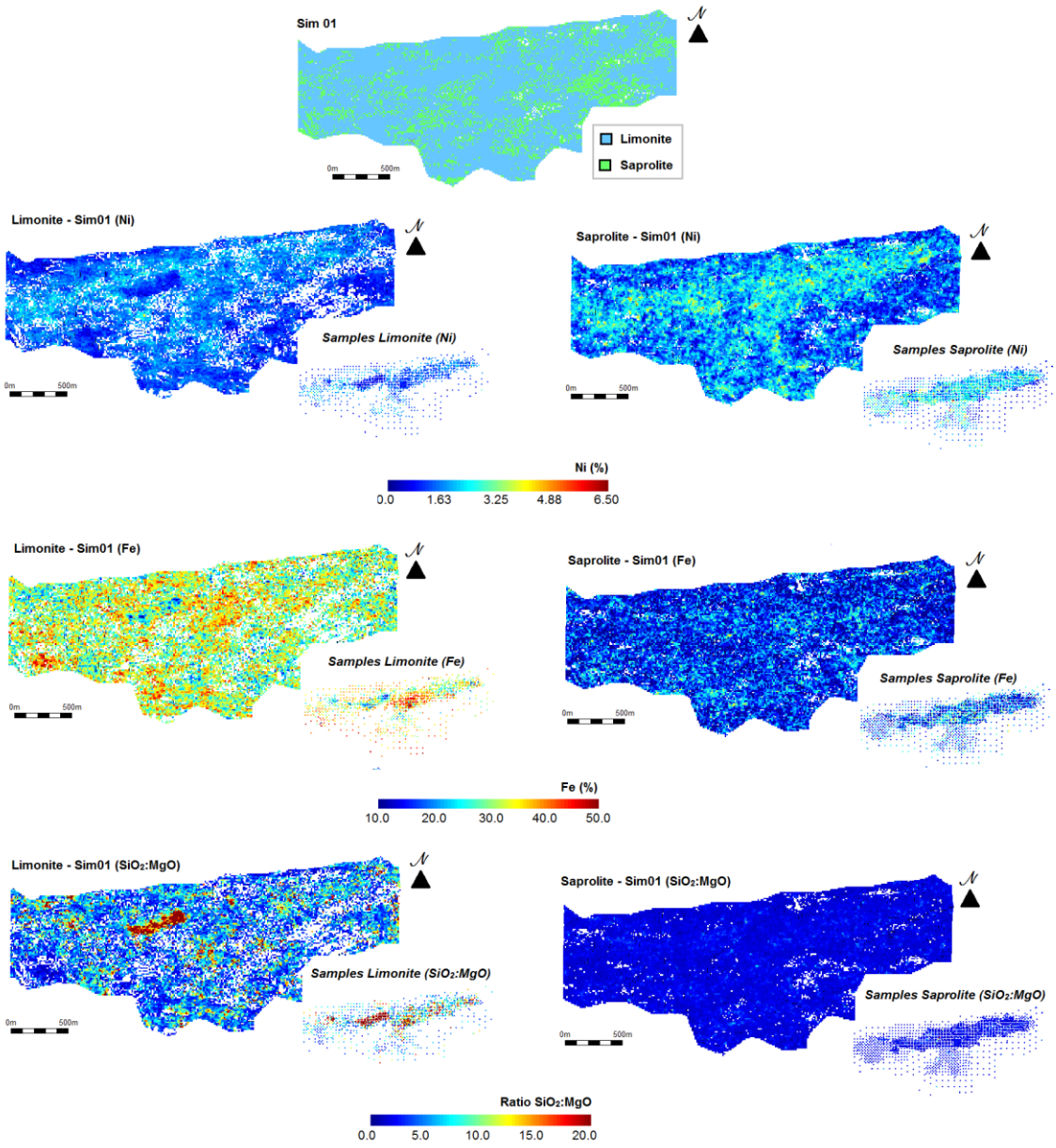

Figure 4.20 - Different plan views for one joint simulation at block support (12x12x3m3). The cattegorical simulation is shown on top followed by the continuous simulations constrained by their simulated lateritic zones.

4.3.5 Risk assessment

In lateritic nickel deposits, a strict control of SiO_2, MgO and Fe grades is required. The range of grades for those key elements may vary accordingly to the metallurgical route designed for the project. The entire mining project that includes the deposit considered in this study (Onça-Puma complex), represented a total investment of about $2.3 billion dollars. The operation produces ferronickel via rotary kiln-electric furnace process and because of the characteristics of this pyrometallurgical process, only saprolitic ore is processed (Vale S.A., 2014). The performance of the metallurgical plant is strongly influenced by the SiO_2:MgO ratio, which for this kind of operation ought to be usually kept between 1.5 and 2.0 depending on the operational conditions, and with iron grades between 12-16% (Xavier and Ciminelli, 2008; Goodfellow and Dimitrakopoulos, 2013). The high investment associated to the mineral asset and its metallurgical complexity highlights the importance of asessing the risks by means of the jointly simulated geological scenarios in order to ensure the viability of the project.

Although the mine currently does not process limonitic ore, it ought to be treated as opportunity material since it contains a significant amount of nickel. Therefore, for a better assessment of the uncertainty within the *in-situ* resources, this study considers both saprolitic and limonitic ore types.

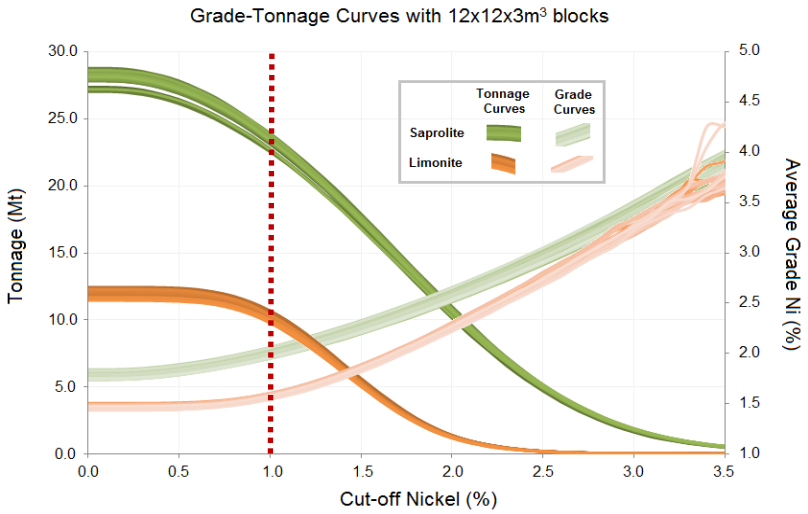

Figure 4.21 - Grade-tonnage curves for simulated block models (12x12x3m3).Tonnages and Ni average grades above given cut-off grades

Figure 4.21 highlights the relative importance of saprolitic ore in terms of its nickel content. Furthermore, the graph indicates that as the Ni cut-off grade increases, the uncertainty about the tonnage of material above the given cut-off decreases. In contrast, the uncertainty about the average grades of Ni and Fe such as the Si:Mg ratio increases for both saprolitic and limonitic ore types (*see* Fig. 4.22). It is noteworthy that in the approach presented here, the uncertainty regarding the tonnages incorporates both the lithological and Dry-Tonnange factor uncertainty modelled by the different geological realizations.

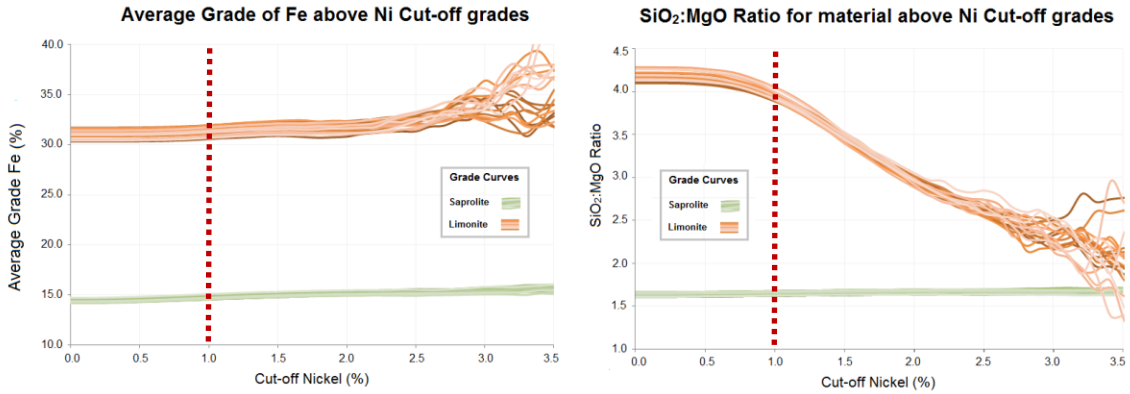

Figure 4.22 - Fe(%) average grades (left) and SiO2:MgO ratio (right) curves for simulated models as function of different Ni cut-off grades.

The graphs in Figs. 4.21 and 4.22 show that the assessment of the global uncertainty of the *in-situ* resources can be scrutinized by integrating all the main elements to keep high performance of the metallurgical plant. For instance, if one considers an operational Nickel cut-off grade of 1.0% Ni, Fig. 4.21 suggests that the tonnage of material above such thershold is likely to fall between 23-24Mt and 9.8-10.8Mt respectively for saprolitic and limonitic ore types, with nickel grades varying from 1.95-2.05% and 1.54-1.60% and so on. Fig. 4.22 shows that independently of the nickel cut-off grade saprolitic ore is very likely to have iron grade and Si:Mg ratio within the range required for a ferronickel plant. However, such observations are rather limited to an assessment of global uncertainty about the *in situ* resources since grade-tonnage curves do not bring any information about local uncertainty. Therefore, they do not allow the modelling of the uncertainty of the material to be fed in the metallurgical plant during the mining operation, since it depends on the spatial variability of the deposit. Such assessment is

only possible by explicitly applying the transfer-function on the stochastic simulations for the probabilistic assessment of its response parameters (e.g., stochastic mine production scheduling for assesing the uncertainty on Fe% and Si:Mg over the Life-Of-Mine as in Goodfellow and Dimitrakopoulos (2013)).

4.4 Conclusions

This paper showed the practical aspects of an efficient framework for joint simulation of multiple correlated variables, based on minimum/maximum autocorrelation factors in order to assess both the volumetric and multi-element uncertainty at a major nickel laterite deposit in northern Brazil.

The joint simulation of the limonitic and saprolitic weathered profiles is done by first extracting the influence of the topography though an unwrinkle process and modelling their true thicknesses. The joint simulation in two-dimensions is done with MAF, transforming spatially correlated geological attributes into uncorrelated service variables that can be independently simulated while avoiding the inference of a corregionalization model for the original variables. The different geological scenarios simulated for limonite and saprolite are used to constrain the joint simulation of nickel and five other correlated elements. For this purpose, the three-dimensional joint simulations are carried out by employing MAF directly at block support scale. The application of such an approach required fitting only 12 variograms for the uncorrelated factors (6 for each geological unit), instead of two sets of 21 variograms and cross-variograms needed for a full model of corregionalization inside each unit. It is clear that direct simulation at block support scale is computationally more efficient and simplifies memory management during simulation of large datasets.

The output of this study is a set of multiple equally probable scenarios of the nickel laterite deposit, validated by the statistics infered from the drillhole samples. Despite of the good reproduction up to second-order statistics, the simulations do not reproduce all the high-order features of the data samples. Even though *unwrinkling* and the consideration of multiple joint-spatial relationship among several variables help on the reproduction of some non-linear features of the deposit by the simulated models, they are

not sufficient. Such result highlights the limitation of simulation methods based on second-order statistics, such as the one tested herein, and the needs to pursuit the development of new methods which can incorporate

The stochastic realizations of the deposit can be further used for assessment of uncertainty of in-situ resources, such as revealed by the graphs of grade-tonnage. Results indicate that, in overall, uncertainty about nickel and iron grades, as well Si:Mg ratio, for the in-situ resources is quite low. However, such observations do not guarantee the uncertainty regarding the ore feed to the metallurgical plant, that depends on local uncertainty rather than global.

4.5 Chapter's Appendix A – Validation simulated limonite's thickness

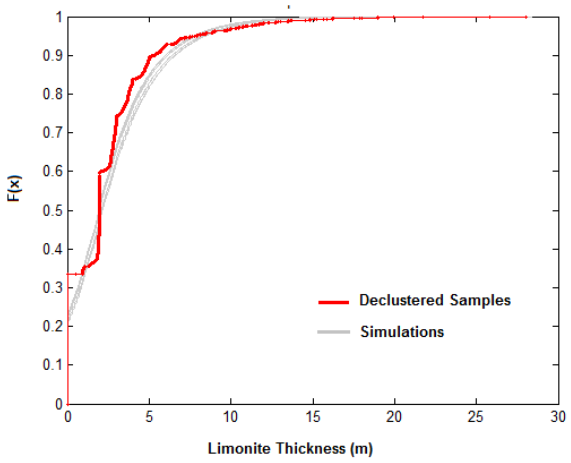

Figure 4.23 - Cumulative distributions of declustered samples in red and simulated models in gray for the limonite thickness.

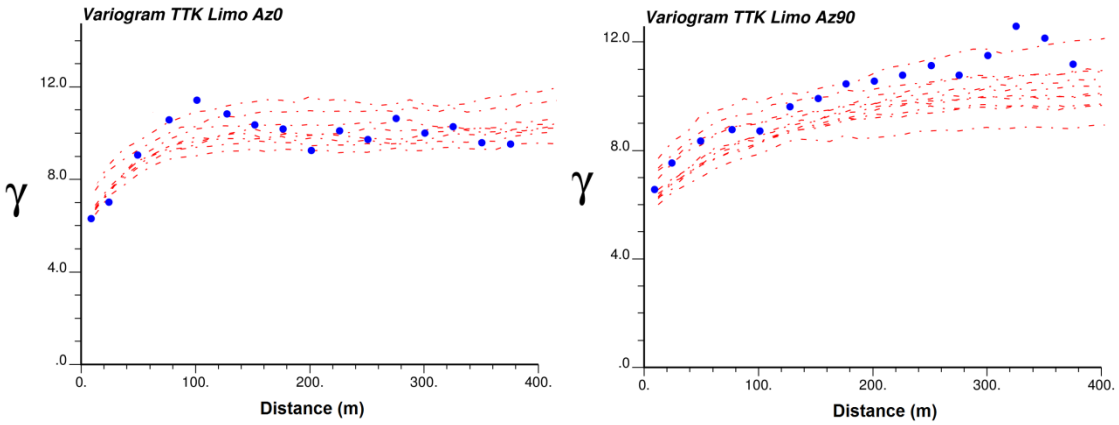

Figure 4.24 - Experimental variogram (blue dots) and simulated models (red dashed lines) for Limonite thickness along the main directions NS and EW.

4.6 Chapter's Appendix B – Modelling MAF variograms for saprolite and limonite

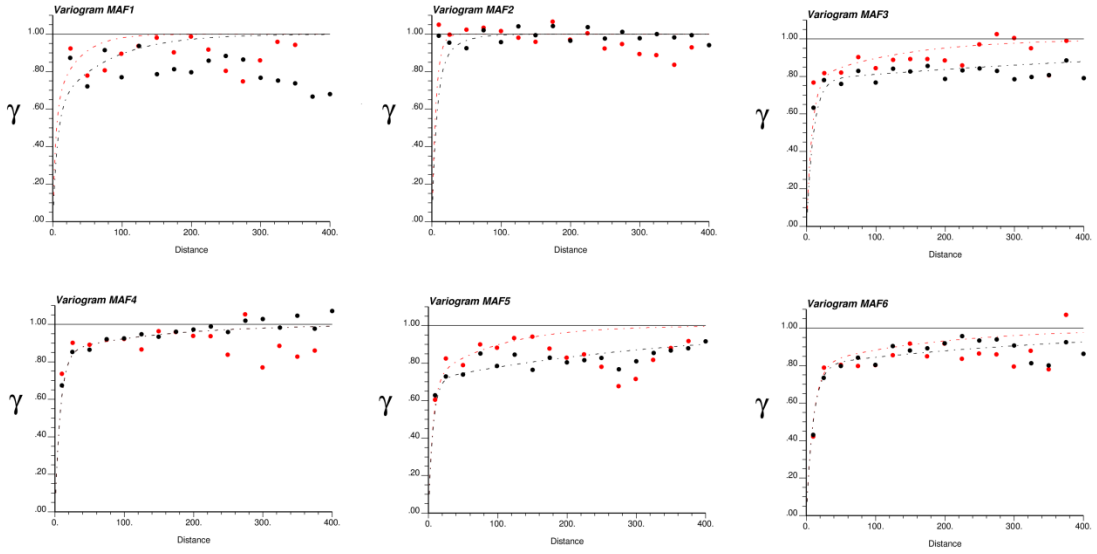

Figure 4.25 - Saprolite - Experimental variograms (dotted) and fitted models (dashed lines) for each MAF factor along the main directions, NS (red) and EW (black).

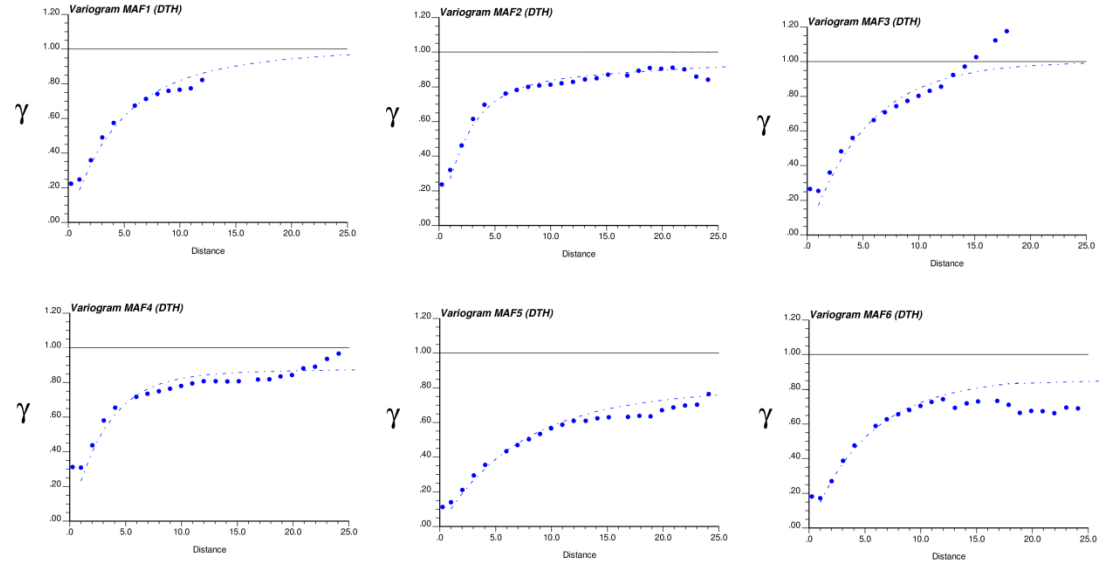

Figure 4.26 - Saprolite - Experimental variograms (dotted) and fitted models (dashed lines) for each MAF factor along the vertical direction (DTH: "Down the Hole").

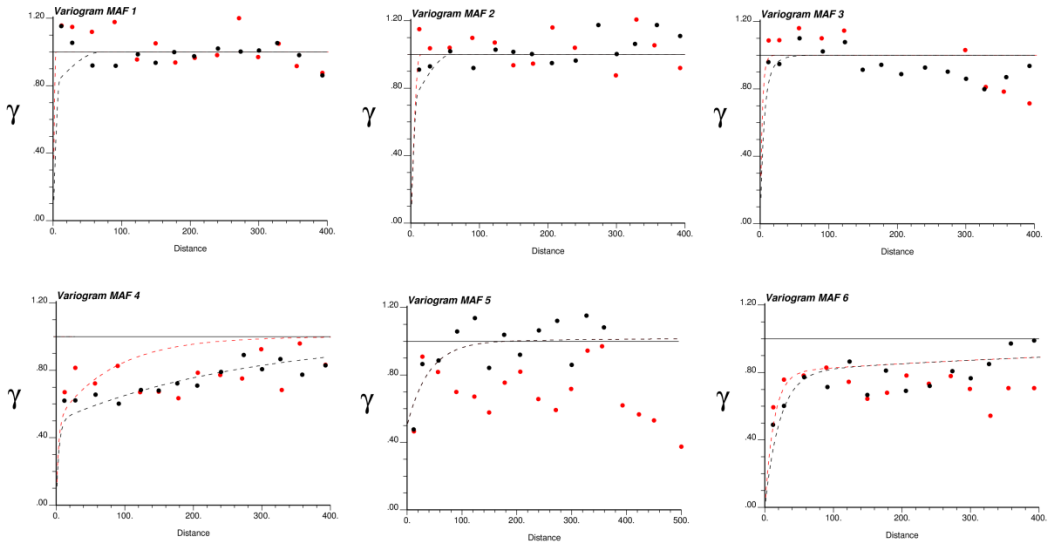

Figure 4.27 - Limonite - Experimental variograms (dotted) and fitted models (dashed lines) for each MAF factor along the main directions, NS (red) and EW (black).

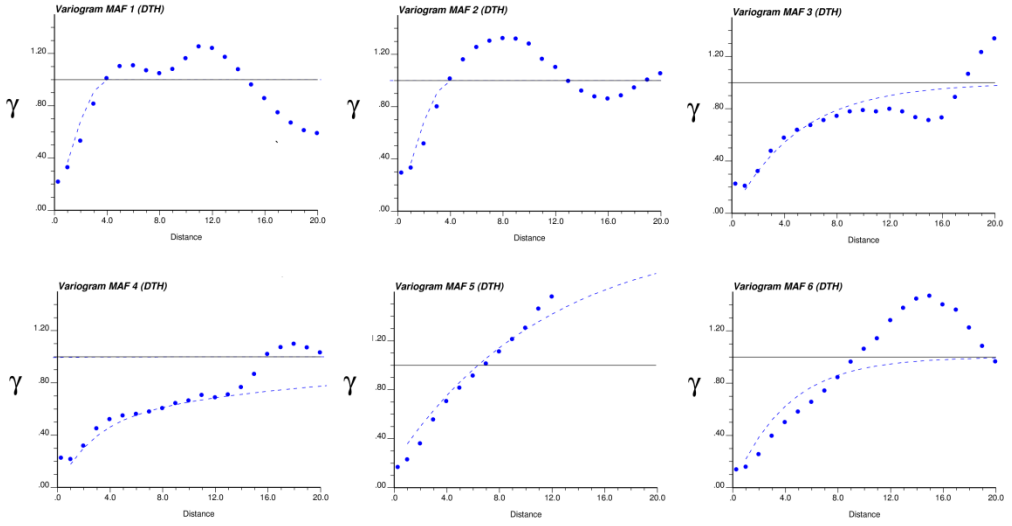

Figure 4.28 - Limonite - Experimental variograms (dotted) and fitted models (dashed lines) for each MAF factor along the vertical direction (DTH: "Down the Hole").

Chapter 5

Conclusions

"I am certain there is too much certainty in the world."
Michael Crichton

In this thesis, the main steps for a stochastic mine planning framework are shown. Two efficient methodologies are tested, one for the generation of joint stochastic simulation of coregionalized variables and the other for solving a SIP formulation of the OPMPS.

Chapter 2 starts by presenting a literature review on the main developments regarding stochastic mine planning, in particular to the OPMPS. Past works have converged to the conclusion that stochastic frameworks tend to provide robust solutions resilient to risks, and at the same time adding value to the project. (Meta-)Heuristic approaches allow for efficient implementations with high-quality solutions near to the optimality achieved by exact methods. Chapter 2 also reviews methodologies for modeling the geological uncertainty of multivariate mineral deposits, showing two mainstream approaches to achieve this goal: direct co-simulation of spatially correlated variables by explicitly modeling their coregionalization model or by factorization of original variables into uncorrelated variables. It was shown that the last approach tends to be significantly more efficient, because it relieves the modeling and inference of several coregionalization models and the solution of large cokriging systems.

Chapter 3 describes the application of a heuristic solution approach for a SIP formulation to the OPMPS. Such formulation accounts for the maximization of the discounted cash flow over the LOM and for the minimization of risks in not attending production targets of processing facilities. For a case study using a gold deposit comprising about 120 thousands blocks, the linear relaxation could not be solved by CPLEX after two weeks, but the heuristic solution approach could provide solutions in hours. The stochastic solutions provide feasible mine production schedules with high value, minimum risks on deviating from production targets. Results reinforce the efficiency of the methodology for solving real-size instances, and at the same time incorporating geological uncertainty.

Chapter 4 discusses the application of joint simulation techniques based on minimum/maximum autocorrelation factors (MAF) and direct block simulation. An application to a major nickel laterite deposit in Brazil was shown through the simulation of geological domains and the joint simulation of multi-elements that are deemed important for geological control and quality for the processing plant. The use of MAF overcome the need of laborious inference and modeling of multiple corregionalization models, and coupled to a direct simulation technique, it can provide multiple stochastic orebody models honoring the joint spatial distribution of the variables in a very efficient way, with low computational costs and better memory management. Validations shown that simulated models are able to reproduce well up to the second order statistics of the drill hole data. However, validations of high-order statistics have shown that, despite the complexity on generating the geological boundaries and considering the spatial correlation between several variables, the simulations are not able to reproduce well high-order spatial cumulants from the samples, which highlights the limitation of second-order simulation frameworks on reproducing complex and non-Gaussian structures of the deposit.

The methods presented in Chapter 3 and Chapter 4 show that efficient methods are available for the practical implementation of the stochastic OPMPS framework in the industry environment. However, there is still a large space for further improvements and developments:

- For the heuristic solution presented in Chapter 3: (a) consider a more efficient algorithm for solving the longest path problem other than using CPLEX; (b) exploration of alternative initial solution methods, such as the sequential heuristic proposed in Amina *et al.* (2014); (c) extend the formulation to incorporate market uncertainty, such as through stochastic price simulation.
- For joint stochastic simulation through factorization: (a) exploration of non-linear methods for decorrelation and dimensionality reduction such as non-linear PCA and independent component analysis, and kernel methods; (b) study the application of log-ratio transformation for dealing with compositional data; (c) develop algorithms to deal with heterotopic sampling configurations.

List of References

Afsari, B. (2008). Sensitivity analysis for the problem of matrix joint diagonalization. *SIAM Journal on Matrix Analysis and Applications*, 30, (3), 1148-1171.

Ahuja, R. K., Ergun, Ö., Orlin, J. B., & Punnen, A. P. (2002). A survey of very large-scale neighborhood search techniques. *Discrete Applied Mathematics*, 123, (1), 75-102.

Albor, F. R. & Dimitrakopoulos, R. (2009). Stochastic mine design optimisation based on simulated annealing: pit limits, production schedules, multiple orebody scenarios and sensitivity analysis. *Min. Technol. (Trans. Inst. Min. Metall. A)*, 118, (2), 80–91.

Albor, F. R., & Dimitrakopoulos, R. (2010). Algorithmic approach to pushback design based on stochastic programming: method, application and comparisons. *Min. Technol. (Trans. Inst. Min. Metall. A)*, 119, (2), 88-101.

Almeida A. S., & Journel A. G. (1994). Joint simulation of multiple variables with a Markov-type coregionalization. *Mathematical Geology,* 26, 565–588.

Arpat, G. B. (2005). *Sequential simulation with patterns*. Ph.D. thesis, Stanford University, Stanford, CA, USA.

Asad, M. W. A., & Dimitrakopoulos, R. (2012). Implementing a parametric maximum flow algorithm for optimal open pit mine design under uncertain supply and demand. *Journal of the Operational Research Society*, 64, 185–197. doi:10.1057/jors.2012.26,

Baker, C. K., & Giacomo, S. M. (2001). Resources and Reserves: Their Uses and Abuses by the Equity Markets. In Edwards, A. C. (Ed.), *Mineral Resource and Ore Reserve Estimation – The AusIMM Guide to Good Practice* (pp 666–676). Melbourne, Australia: AusIMM.

Bandarian, E. M. (2008). Linear transformation methods for multivariate geostatistical simulation, PhD thesis (unpublished), Edith Cowan University, Perth, Australia.

Bandarian, E. M., Bloom, L. M., & Mueller, U. A. (2008). Direct minimum/maximum autocorrelation factors within the framework of a two structure linear model of coregionalisation. *Computers & Geosciences*, 34, (3), 190-200.

Barnett, R. M., & Deutsch, C. V. (2012). Practical implementation of non-linear transforms for modeling geometallurgical variables. In P. Abrahamsen, R. Hauge & O. Kolbjornsen (Eds.), *Geostatistics Oslo 2012* (pp. 409-422). Oslo, Norway: Springer Netherlands.

Barnett, R. M., Manchuk, J. G., & Deutsch, C. V. (2014). Projection pursuit multivariate transform. *Mathematical Geosciences*, 46, (3), 337-359.

Benndorf, J., & Dimitrakopoulos, R. (2007). New efficient methods for conditional simulation of large orebodies. In R. Dimitrakopoulos (Ed.), *Orebody Modelling and Strategic Mine Planning - Uncertainty and Risk Management International Symposium* (pp. 103-109). Burwood: AusIMM.

Benndorf, J., & Dimitrakopoulos, R. (2013). Stochastic long-term production scheduling of iron ore deposits: Integrating joint multi-element geological uncertainty, *J. Mining Science*, 49, (1), 68-81.

Bienstock, D., & Zuckerberg, M. (2010). Solving LP relaxations of large-scale precedence constrained problems. in *Proc. 14th Int. Conf. on Integer Programming and Combinatorial Optimization* (pp. 1–14). Lausanne, Switzerland: Springer Verlag.

Birge, J. R., & Louveaux, F. (2011). *Introduction to Stochastic Programming* (2nd ed). Springer Verlag.

Boland, N., Dumitrescu, I., & Froyland, G. (2008a). A multistage stochastic programming approach to open pitmine production scheduling with uncertain geology. *Optimization Online*. Retrieved from www.optimizationonline.org/DBHTML/2008/10/2123.html

Boland, N., Dumitrescu, I., Froyland, G., & Gleixner, A. M. (2008b). LP-based disaggregation approaches to solving the open pit mining production scheduling problem with block processing selectivity. *Computers & Operations Research,* 36, (4), 1064–1089.

Boucher, A. & Dimitrakopoulos, R. (2009). Block simulation of multiple correlated variables. *Mathematical Geosciences,* 41, (2), 215-237.

Boucher, A., & Dimitrakopoulos, R. (2012). Multivariate block-support simulation of the Yandi iron ore deposit, Western Australia. *Mathematical Geosciences*, 44, (4), 449-468.

Canico Resource Corporation (2005). Technical report: Feasibility Study Resource Estimates for Onca Puma nickel laterite deposit. Retrieved from http://www.sedar.com

Caccetta, L., & Hill, S. P. (2003). An application of Branch and Cut to open pit mine scheduling. *Journal of Global Optimization,* 27, (2-3), 349-365.

Carr, J. R., & Myers, D. E. (1985). COSIM: a FORTRAN IV program for conditional simulation. *Computers & Geosciences*, 11, (6), 675-705.

Chiles, J. P. (1984). Simulation of a nickel deposit: problems encountered and practical solutions. In G. Verly, M. David, A. Journel & A. Marechal (Eds.), *Geostatistics for natural resources characterisation* (pp. 1015-1030), South Lake Tahoe: Reidel Publishing Company.

Chiles, J. P., & Delfiner, P. (2012). *Geostatistics, modelling spatial uncertainty* (2nd ed). New York: Wiley.

Dagdelen, K., & Johnson, T. B. (1986). Optimum open pit mine production scheduling by lagrangian parameterization. In *Proc. 19th Internat. Appl. Comput. Oper. Res. Mineral Indust. Sympos. (APCOM)* (pp. 127-142). Littleton, CO: SME.

Dantzig, G. (1955). Linear programming under uncertainty. *Management Sci.,* 1, 197-206.

David, M., Dowd, P., & Korobov, S. (1974). Forecasting departure from planning in open pit design and grade control. In *Proc. 12th Internat. Appl. Comput. Oper. Res. Mineral Indust. Sympos. (APCOM)* (pp. F131-F142). Golden, CO.

David M., Dagbert M., Sergerie G. & Cupcic F. (1984). Complete simulation of the tonnage, shape and grade of a Saskatchewan uranium deposit. *In Proc.27th International Geology congress* (pp. 154-186). VNU Science Press.

David, M. (1977). *Geostatistical ore reserve estimation*. Amsterdam: Elsevier.

David, M. (1988). *Handbook of applied advanced geostatistical ore reserve estimation*. Amsterdam: Elsevier.

Davis, M. D. (1987). Production of conditional simulations via the LU triangular decomposition of the covariance matrix. *Mathematical Geology,* 19, 91-98.

De Iaco, S., & Maggio, S. (2011). Validation techniques for geological patterns simulations based on variogram and multiple-point statistics. *Mathematical Geosciences*, 43, (4), 483-500.

Desbarats, A. J., & Dimitrakopoulos, R. (2000). Geostatistical simulation of regionalized pore-size distributions using min/max autocorrelation factors. *Mathematical Geology,* 32, (8), 919-942.

Deustch, C. V. (2005). Practical unfolding for geostatistical modeling of vein type and complex tabular mineral deposits. In *Proc. 32nd Internat. Appl. Comput. Oper. Res. Mineral Indust. Sympos. (APCOM)* (pp. 197-202). London: Taylor and Francis Group.

Dimitrakopoulos, R. (2011). Stochastic optimization for strategic mine planning: A decade of developments. *Journal of Mining Science*, 84, (2), 138-150.

Dimitrakopoulos, R., Farrelly, C. T. & Godoy, M. (2002). Moving forward from traditional optimization: grade uncertainty and risk effects in open pit design, *Min. Technol. (Trans. Inst. Min. Metall. A)*, 111, (1), 82–88

Dimitrakopoulos, R., & Foneca, M. (2003). Assessing risk in grade-tonnage curves in a complex copper deposit, northern Brazil, based on an efficient joint simulation of multiple correlated grades. In *Proceedings of the Application of Computers and Operations Research in the Minerals Industries* (pp. 373-382). Capetown: SAIMM.

Dimitrakopoulos, R., & Luo, X. (2004). Generalized sequential Gaussian simulation on group size n and screen-effect approximations for large field simulations. *Mathematical Geology,* 36, (5), 567-591.

Dimitrakopoulos, R., & Ramazan, S. (2004). Uncertainty based production scheduling in open pit mining. *SME Transactions*, 316, 106-112.

Dimitrakopoulos, R. & Ramazan, S. (2008). Stochastic integer programming for optimizing long-term production schedules of open pit mines: methods, application and value of stochastic solutions, *Min. Technol. (Trans. Inst. Min. Metall. A)*, 117, (4), 155–160.

Dimitrakopoulos, R., Martinez, L., & Ramazan, S. (2007). A maximum upside/minimum downside approach to the traditional optimization of open pit mine design. *Journal of Mining Science*, 43, (1), 73-82.

Dimitrakopoulos, R., Mustapha, H., & Gloaguen, E. (2010). High-order statistics of spatial random fields: Exploring spatial cumulants for modeling complex, non-Gaussian and non-linear phenomena. *Mathematical Geosciences*, 42, (1), 65-97.

Dimitrakopoulos, R., & Jewbali, A. (2013). Joint stochastic optimization of short- and long- term mine production planning: Method and application in a large operating gold mine. *Min. Technol. (Trans. Inst. Min. Metall. A)*, 122, (2), 110-123.

Dowd, P. A. (1984). Conditional simulation of inter related beds in an oil deposit. In G. Verly, M. David, A. Journel & A. Marechal (Eds.), *Geostatistics for natural resources characterisation* (pp. 1031-1043), South Lake Tahoe: Reidel Publishing Company.

Dowd, P. (1994). Risk assessment in reserve estimation and open pit planning, *Min. Technol. (Trans. Inst. Min. Metall. A)*, 103, 148–154

Dowd, P. (1997). Risk in minerals projects: analysis, perception and management, *Min. Technol. (Trans. Inst. Min. Metall. A)*, 106, 9–18

Eggins, R. G. (2006). *Modelling thickness in a stratiform deposit using joint simulation techniques*, M. Phil. Thesis (unpublished), University of Queensland, Brisbane, Australia.

Ferland, J. A., Amaya, J., & Djuimo, M. S. (2007). Application of a particle swarm algorithm to the capacitated open pit mining problem. In S. Mukhopadhyay & G. Sen Gupta (Eds.) *Autonomous Robots and Agents* (pp. 127-133). Springer Verlag.

Friedman, J. H. (1987). Exploratory projection pursuit. *Journal of the American statistical association*, 82, (397), 249-266.

Geman, S., & Geman, D. (1984). Stochastic relaxation, Gibbs distribution and the Bayesian restoration of images. *IEEE Trans. On Pattern Analysis and Machine Intelligence*, 6, (6), 721-741.

Gershon, M. (1983). Optimal mine production scheduling: evaluation of large scale mathematical programming approaches, *Geotechnical and Geological Engineering*, 1, (4), 315-329.

Gershon, M. (1987). Heuristic approaches for mine planning and production scheduling. *International Journal of Mining and Geological Engineering,* 5, (1), 1-13.

Gleixner, A. M. (2008). *Solving large-scale open pit mining production scheduling problems by integer programming,* (Master's thesis), Technische Universität Berlin, Berlin. http://opus.kobv.de/zib/volltexte/2009/1187/.

Godoy, M. (2003). *The effective management of geological risk in long-term production scheduling of open pit mines*, Ph.D. thesis (unpublished), University of Queensland, Brisbane, Australia.

Gómez-Hernández, J. J., & Journel, A. G. (1993). Joint sequential simulation of multiGaussian fields. In M. Armstrong & P. Dowd (Eds.), *Geostatistics Troia'92* (pp. 85-94). Fontainebleau, France: Springer Netherlands.

Goodfellow, R., Albor Consuegra, F., Dimitrakopoulos, & R., Lloyd, T. (2012). Quantifying multi-element and volumetric uncertainty, Coleman McCreedy deposit, Ontario, Canada. *Computers & Geosciences*, 42, 71-78.

Goodfellow, R. & Dimitrakopoulos, R. (2013). *Mining supply chain optimization under geological uncertainty*. Retrieved from Les Cahiers du GERAD website: http://www.gerad.ca/fichiers/cahiers/G-2013-54.pdf

Goodfellow, R., & Dimitrakopoulos, R. (2013). Algorithmic integration of geological uncertainty in pushback designs for complex multi-process open pit mines, *Min. Technol. (Trans. Inst. Min. Metall. A)*, 122, (2), 67-77

Goovaerts, P. (1993). Spatial orthogonality of the principal components computed from coregionalized variables. *Mathematical Geology*, 25, (3), 281-302.

Goovaerts, P. (1997). *Geostatistics for natural resources evaluation*. New York: Oxford University Press.

Grieco, N., & Dimitrakopoulos, R. (2007). Managing grade risk in stope design optimization: Probabilistic mathematical programming model and application in sublevel stoping. *Min. Technol. (Trans. Inst. Min. Metall. A),* 116, (2), 49–57.

Guardiano, F., Srivastava, R. (1993). Multivariate geostatistics: beyond bivariate moments. In A. Soares (Ed.), *Geostatistics Troia. Vol. 1* (pp. 133-144). Kluwer Academic Publications.

Hochbaum, D. S. & Chen, A. (2000). Performance analysis and best implementations of old and new algorithms for the open-pit mining problem. *Opererations Research,* 48, (6), 894-913.

Honarkhah, M. (2011). *Stochastic simulation of patterns using distance-based pattern modeling*. Ph.D. thesis, Stanford University, Stanford, CA, USA.

Huber, P. J. (1985). Projection pursuit. *The Annals of Statistics*, 435-475.

Hustrulid, W. A., & Kuchta, M. (2006). *Open pit mine planning & design (2nd ed.)*, London: Taylor and Francis.

Hyvärinen, A., Karhunen, J. & Oja, E. (2001). *Independent component analysis*. New York: Wiley Interscience Publication.

ILOG (2008). *ILOG CPLEX 11.2 User's Manual*. Armonk: IBM.

Jewbali, A. (2006). *Modeling geological uncertainty for stochastic short term production scheduling in open pit metal mines*, Ph.D. Thesis (unpublished), University of Queensland, Brisbane, Australia.

Jewbali, A., & Dimitrakopoulos, R. (2013). Joint stochastic optimization of short- and long- term mine production planning: Method and application in a large operating gold mine, *Min. Technol. (Trans. Inst. Min. Metall. A)*, 122, (2), 110-123.

Johnson, T. (1969). Optimum production scheduling. *In Proceedings of the 8th international symposium on computers and operations research* (pp. 539–562). Salt Lake City.

Johnson, R. A., & Wichern, D. W. (2007). *Applied multivariate statistical analysis (6th ed)*. Englewood Cliffs: Prentice-Hall.

Journel, A. G., & Huijbregts, C. J. (1978). *Mining geostatistics*. London: Academic Press.

Journel, A. G. (1974). Geostatistics for conditional simulation of ore bodies. *Economic Geology*, 69, (5), 673-687.

Journel, A. G. (1994). Modeling uncertainty: some conceptual thoughts. In R. Dimitrakopoulos (Ed.), *Geostatistics for the next century* (pp. 30-43). Springer Netherlands.

Journel, A. G. (1989). *Fundamentals of geostatistics in five lessons (Vol. 8)*. Washington, DC: American Geophysical Union.

Journel, A.G. (2007). Roadblocks to the evaluation of ore reserves - the simulation overpass and putting more geology into numerical models of deposits. In R. Dimitrakopoulos (Ed.), *Orebody Modelling and Strategic Mine Planning - Uncertainty and Risk Management International Symposium* (pp. 29–32). Burwood: AusIMM.

Kennedy, J., & Eberhart, R. (1995). Particle swarm optimization. *In Proceedings of IEEE international conference on neural networks*, 4, (2), 1942-1948.

Kim, Y. C. (1979), Production Scheduling: Technical Overview. In A. Weiss, (Ed.), *Computer Methods for the 80's* (pp. 610-614). New York : AIME.

King, A. J., & Wallace, S. W. (2012). *Modeling With Stochastic Programming. (Operations Research and Financial Engineering)*. Berlin: Springer.

Kirkpatrick, S., Gelatt, C. D., & Vecchi, M. P. (1983). Optimization by simulated annealing, *Science*, 220, 671-680.

Kolmogorov, A. N. (1956). *Foundations of the theory of probability*. New York: Chelsea Publishing Co.

Lamghari, A., & Dimitrakopoulos, R. (2012). A diversified tabu search approach for the open-pit mine production scheduling problem with metal uncertainty. *European Journal of Operational Research*, 222, 642-652.

Lamghari, A., & Dimitrakopoulos, R. (2013a). *A network-flow based algorithm for scheduling production in multi-processor open pit mines accounting for metal uncertainty*. Retrieved from Les Cahiers du GERAD website: www.gerad.ca/fichiers/cahiers/G-2013-63.pdf

Lamghari, A., Dimitrakopoulos, R., & Ferland, A. J. (2013b). A variable neighborhood descent algorithm for the open-pit mine production scheduling problem with metal uncertainty. *J Operational Research Society*. doi:10.1057/jors.2013.81.

Lamghari, A., Dimitrakopoulos, R., & Ferland, J. A. (2014). A hybrid method based on linear programming and variable neighborhood descent for scheduling production in open-pit mines. *Journal of Global Optimization*, 1-28. doi: 10.1007/s10898-014-0185-z.

Leite, A. (2008). *Application of stochastic mine design and optimization methods*. M. Eng. Thesis, McGill University, Montreal, QC, Canada.

Leite, A., and Dimitrakopoulos, R. (2007). Stochastic optimization model for open pit mine planning: application and risk analysis at a copper deposit. *Min. Technol. (Trans. Inst. Min. Metall. A)*, 116, (3), 109-118.

Leite, A., & Dimitrakopoulos, R. (2009). Production scheduling under metal uncertainty – Application of stochastic mathematical programming at an open pit copper mine and comparison to conventional scheduling. In R. Dimitrakopoulos (Ed.), *Orebody Modeling and Strategic Mine Planning* (pp. 35-39). AusIMM.

Lerchs, H., & Grossmann, I.F. (1965). Optimum design of open-pit mines. *Canad. Inst. Mining Bull.,* 58, 47-54.

Leuangthong, O., Lyall, G., & Deutsch, C. V. (2002). Multivariate geostatistical simulation of a nickel laterite deposit. In *Proc. 30th Internat. Appl. Comput. Oper. Res. Mineral Indust. Sympos. (APCOM)* (pp. 261-273). Littleton, CO: SME.

Lopes, J. A., Rosas, C. F., Fernandes, J. B., & Vanzela, G. A. (2011). Risk quantification in grade-tonnage curves and resource categorization in a lateritic nickel deposit using geologically constrained joint conditional simulation. *Journal of Mining Science*, 47, (2), 166-176.

Luster, G. (1985). *Raw Materials for Portland Cement: Applications of Conditional Simulation of Coregionalization*. PhD thesis, Stanford University, Stanford. Retrieved from https://pangea.stanford.edu/departments/ere/dropbox/scrf/documents/Theses/SCRF-Theses/1980-1989/1985_PhD_Luster.pdf

Mariethoz, G., Renard, P., & Straubhaar, J. (2010). The direct sampling method to perform multiple-point geostatistical simulations. *Water Resources Research,* 46, (11), 1-14.

Matheron, G. (1963). Principles of geostatistics. *Economic geology*, 58, (8), 1246-1266.

Matheron, G. (1971). *The theory of regionalized variables and its applications (Vol. 5)*. Ecole nationale supérieure des mines de Paris. Retrieved from http://cg.ensmp.fr/bibliotheque/public/MATHERON_Ouvrage_00167.pdf

Matheron, G. (1973). The intrinsic random functions and their applications. *Advances in Applied Probability,* 5, (3), 439-468.

Meagher, C., Abdel Sabour, S. A., & Dimitrakopoulos, R. (2009). Pushback design of open pit mines under geological and market uncertainties. In R. Dimitrakopoulos (Ed.), *Orebody Modeling and Strategic Mine Planning* (pp. 291-298). AusIMM.

Menabde, M., Froyland, G., Stone, P., & Yeates, G. (2007). Mining schedule optimisation for conditionally simulated orebodies. In R. Dimitrakopoulos (Ed.), *Orebody Modelling and Strategic Mine Planning - Uncertainty and Risk Management International Symposium* (pp. 379–384). Burwood: AusIMM.

Montiel, L., & Dimitrakopoulos, R. (2013a). Stochastic mine production scheduling with multiple processes: Application at Escondida Norte, Chile. *Journal of Mining Science,* 49, (2), 583-597.

Montiel, L., & Dimitrakopoulos, R. (2013b). A*n extended stochastic optimization method for multi-process mining complexes*. Retrieved from Les Cahiers du GERAD website: www.gerad.ca/fichiers/cahiers/G-2013-56.pdf.

Morales, N., & Rubio, E. (2010). Robust open-pit planning under geological uncertainty. *In MININ 2010 Proceeding of the 4th International Conference on Mining Innovation* (pp. 235-244). Santiago, Chile.

Morton, J., & Lim, L. (2009), *Principal Cumulant Component Analysis*, Working Paper, Standford University, Stanford, CA. Retrieved from http://www.stat.uchicago.edu/~lekheng/work/pcca.pdf

Mueller, U. A., & Ferreira, J. (2012). The U-WEDGE transformation method for multivariate geostatistical simulation. *Mathematical Geosciences*, 44, (4), 427-448.

Mustapha, H., & Dimitrakopoulos, R. (2010). High-order stochastic simulation of complex spatiallydistributed natural phenomena. *Mathematical Geosciences*, 42, (5), 457-485.

Myers, D. E. (1989). Vector conditional simulation. In M. Armstrong (Ed.), *Geostatistics* (pp. 283-292). Avignon, France: Kluwer Academic Publishers.

Peattie, R., & Dimitrakopoulos, R. (2013). Forecasting recoverable ore reserves and their uncertainty at Morila gold deposit, mali: an efficient simulation approach and future grade control drilling. *Mathematical Geosciences*, 45, (8), 1005-1020.

Picard, J. C. (1976). Maximal Closure of a Graph and Applications to Combinatorial Problems. *Management Science*, 22, (11), 1268-1272.

Ramazan, S., & Dimitrakopoulos, R. (2004a). Recent applications of operations research and efficient MIP formulations in open pit mining. *SME Transactions,* 316, 73-78.

Ramazan, S., & Dimitrakopoulos, R. (2004b). Traditional and new MIP models for production scheduling with in-situ grade variability. *International Journal of Surface Mining, Reclamation and Environment*, 18, (2), 85-9.

Ramazan S., (2007). The new fundamental tree algorithm for production scheduling of open pit mines. *European Journal of Operational Research,* 177, (2), 1153–1166.

Ramazan S., & Dimitrakopoulos R. (2007). Stochastic optimization of long term production scheduling for open pit mines with a new integer programming formulation. In R. Dimitrakopoulos (Ed.), *Orebody Modelling and Strategic Mine Planning - Uncertainty and Risk Management International Symposium* (pp. 359–365). Burwood: AusIMM.

Ramazan S., & Dimitrakopoulos R. (2013). Production scheduling with uncertain supply: A new solution to the open pit mining problem. *Optimization and Engineering*, 14, (2), 361–380.

Ravenscroft, P., (1992). Risk analysis for mine scheduling by conditional simulation. *Min. Technol. (Trans. Inst. Min. Metall. A)*, 101, 104–108.

Rondon, O. (2012). Teaching aid: minimum/maximum autocorrelation factors for joint simulation of attributes. *Mathematical Geosciences*, 44, (4), 469-504.

Rosenblatt, M. (1952). Remarks on a multivariate transformation. *The Annals of Mathematical Statistics*, 470-472.

Sarker, R. A., & Gunn, E. A. (1997). A simple SLP algorithm for solving a class of nonlinear programs. *European Journal of Operational Research*, 101, (1), 140-154.

Seymour, F. (1995). Pit limit parametrization from modified 3D Lerchs-Grossmann algorithm. *SME Transactions,* 298, 1860-1864.

Soares, A. (2001). Direct sequential simulation and cosimulation. *Mathematical Geology,* 33, 911–926

Strebelle, S. (2002). Conditional simulation of complex geological structures using multiple-point statistics. *Mathematical Geology,* 34, (1), 1-22.

Strebelle, S., & Cavelius, C. (2014). Solving speed and memory issues in multiple-point statistics simulation program snesim. *Mathematical Geosciences,* 46, (2), 171-186.

Switzer, P., & Green, A. (1984). *Min/Max autocorrelation factors for multivariate spatial imaging: Technical Report No. 6, Department of Statistics*, Stanford University, Stanford, CA, USA.

Tercan, A. E., & Sohrabian, B. (2013). Multivariate geostatistical simulation of coal quality data by independent components. *International Journal of Coal Geology*, 112, 53-66.

Tichavsky, P., & Yeredor, A. (2009). Fast approximate joint diagonalization incorporating weight matrices. *Signal Processing, IEEE Transactions*, 57, (3), 878-891.

Tolwinski, B., & Underwood, R. (1996). A scheduling algorithm for open pit mines. *IMA Journal of Mathematics Applied in Business & Industry,* 7, 247-270.

Vale S.A., (2014). Annual report 2013. Retrieved from www.vale.com/EN/investors/Quarterly-results-reports/20F/20FDocs.

Vallee, M. (2000). Mineral resource + engineering, economic and legal feasibility. *CIM bulletin*, 93, (1038), 53-61.

Verly, G. W. (1993). Sequential Gaussian cosimulation: a simulation method integrating several types of information. In M. Armstrong & P. Dowd (Eds.), *Geostatistics Troia'92* (pp. 543-554). Fontainebleau, France: Springer Netherlands.

Xavier, F. M. R. S., & Ciminelli, V. S. T. (2008). Development of technical and economic parameters affecting process selection to treat nickel laterite ores. In Young, C. A., Tay, P. R., & Anderson, C. G. (Eds.), *Hydrometallurgy 2008: Proceedings of the Sixth International Symposium* (pp. 532-540). Littleton, CO: SME.

Yeredor, A. (2000). Approximate joint diagonalization using non-orthogonal matrices. *In Proc. International Workshop on Independent Component Analysis and Blind Source Separation* (pp. 33-38). Helsinki, Finland: University of Technology

Wackernagel, H., Petitgas, Y., & Touffait, Y. (1989) Overview of methods for coregionalization analysis. In M. Armstrong (Ed.), *Geostatistics* (pp. 409–420). Avignon, France: Kluwer Academic Publishers.

Wackernagel, H. (2003). *Multivariate geostatistics: An introduction with applications (3rd ed.)*. Berlin: Springer.

Whittle, J. (1988) Beyond optimization in open-pit design. In K. Fytas (Ed.), *Proc. Computer Applications in the Mineral Industries* (pp. 331– 337. 115). Quebec City: Balkema,.

Whittle, J. (1998). *Four-X user manual, Whittle Programming Pty Ltd.*, Melbourne, Australia.

Whittle, J., (1999). A decade of open pit mine planning and optimization — The craft of turning algorithms into packages. In *Proc. 28th Internat. Appl. Comput. Oper. Res. Mineral Indust. Sympos. (APCOM)* (pp. 15-24). Golden, CO: SME.

Whittle, D., & Bozorgebrahimi, A., (2007). Hybrid pits - linking conditional simulation and lerchs-grossmann through set theory. In R. Dimitrakopoulos (Ed.), *Orebody Modelling and Strategic Mine Planning - Uncertainty and Risk Management International Symposium* (pp. 323–328). Burwood: AusIMM.

Wolcott, D. S., & Chopra, A. K. (1993), Incorporating reservoir heterogeneity with geostatistics to investigate waterflood recoveries. *SPE Formation Evaluation*, 8, (1), 26-32.

Zhang, T. (2006). *Filter-based training pattern classification for spatial pattern simulation*. PhD thesis, Stanford University, Stanford. Retrieved from https://pangea.stanford.edu/departments/ere/dropbox/scrf/documents/Theses/SCRF-Theses/2000-2009/2006_PhD_Zhang.pdf

Zhang T., Switzer P., & Journel A. (2006). Filter-based classification of training image patterns for spatial simulation. *Mathematical Geology,* 38, (1), 63–80.

Zhao, Y., & Kim, Y. C. (1991) A New Graph Theory Algorithm for Optimal Pit Design. *SME Transactions*, 290, 1832-1838.

Appendix A – Complete validation of (cross)variograms, Saprolite unit

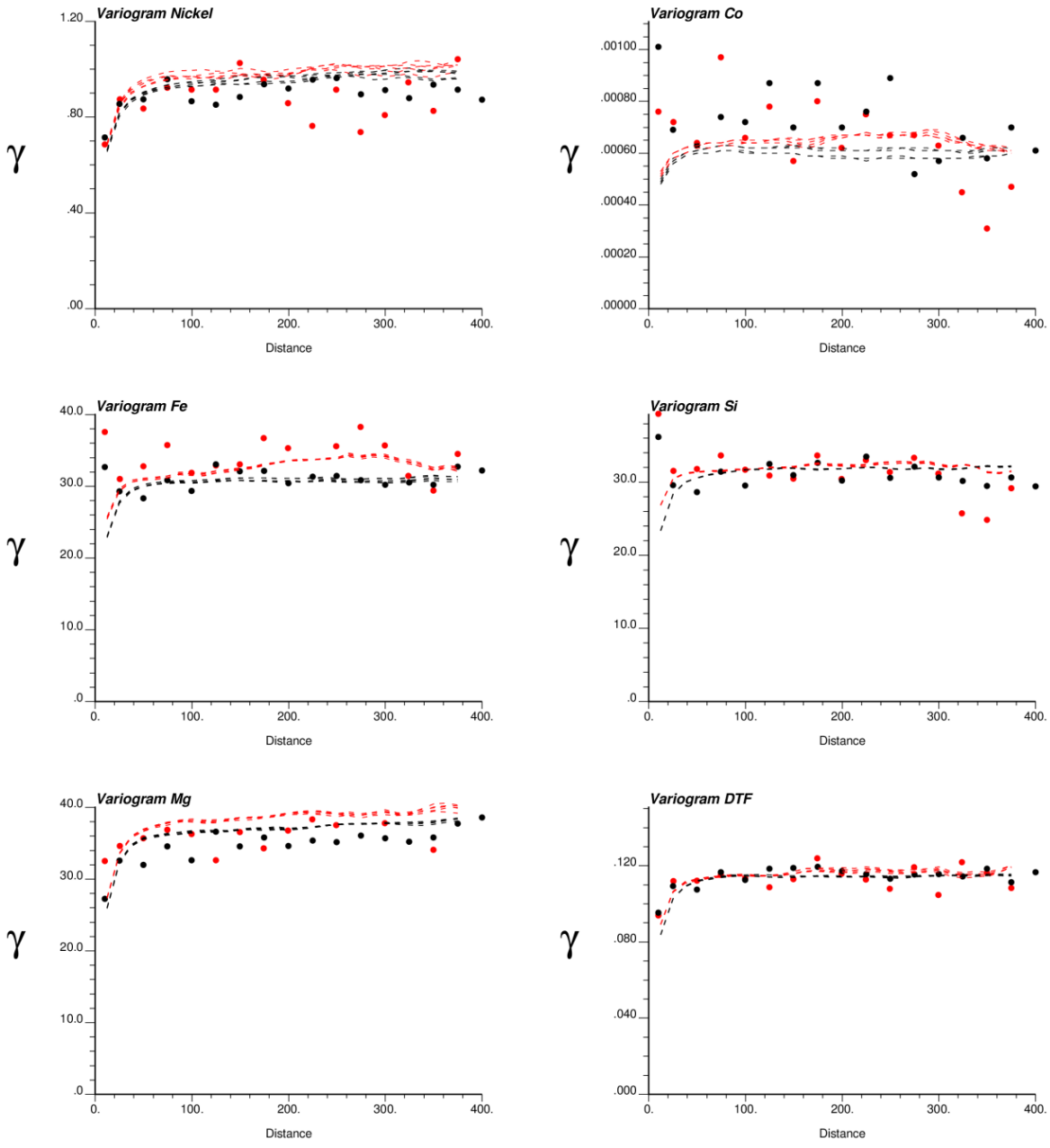

Figure A.1 - Saprolite - Experimental direct variograms (dotted) and point-support simulated models (lines) for each element in data space over the horizontal direction (NS in red and EW in black).

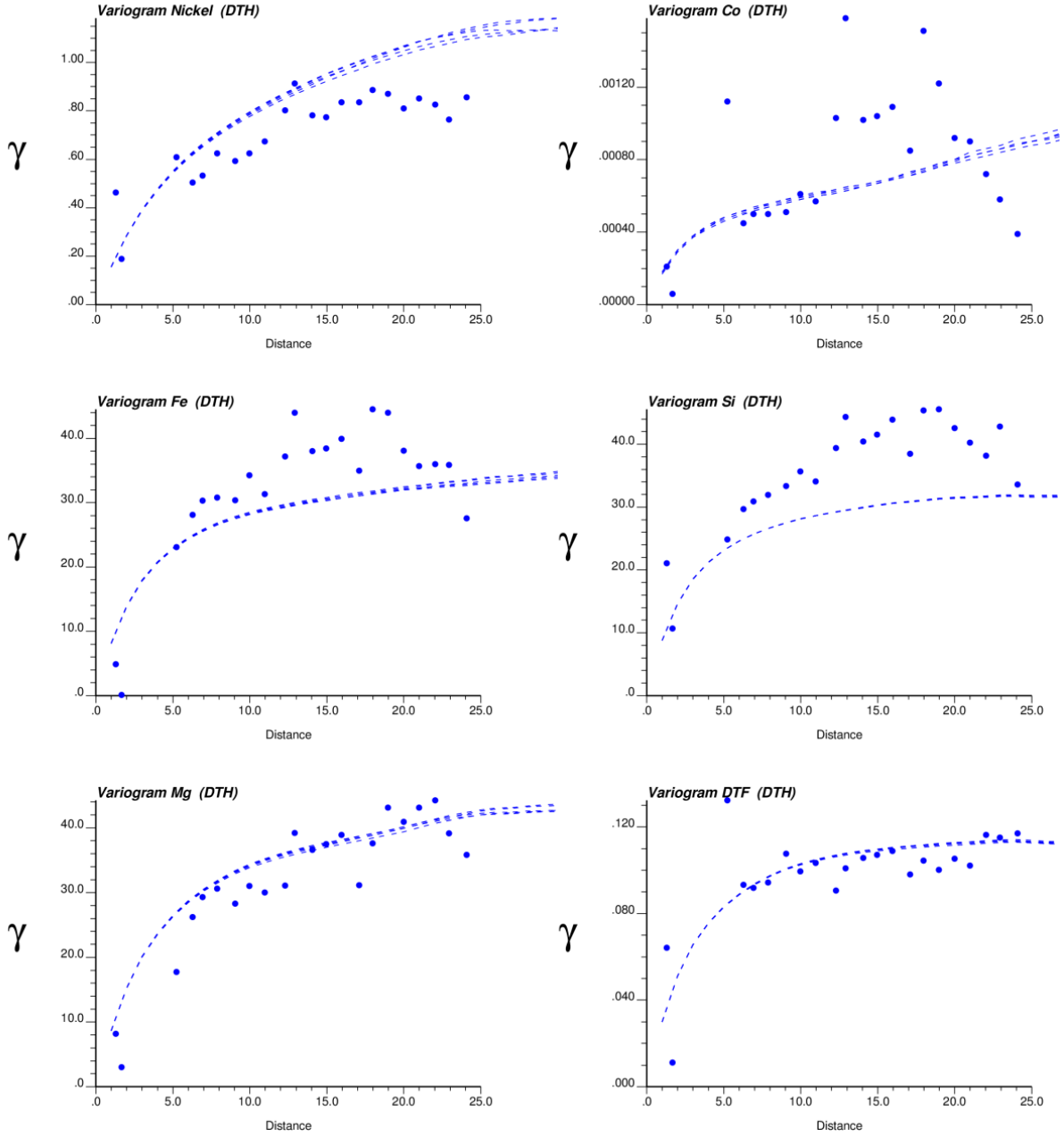

Figure A.2 - Saprolite - Experimental direct variograms (dotted) and (point-support) simulated models (lines) for each element in data space along the vertical direction.

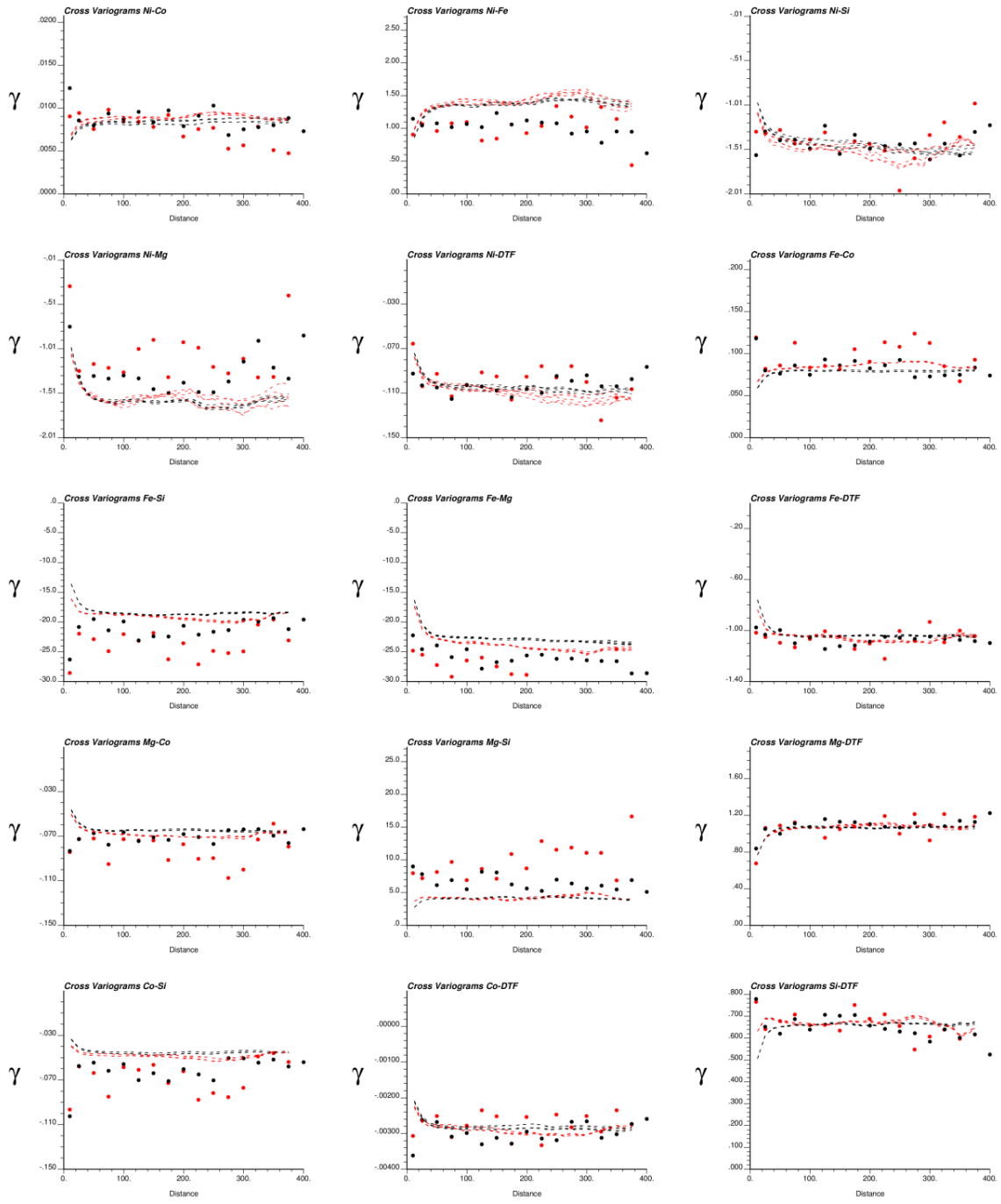

Figure A.3 - Saprolite - Experimental cross-variograms (dotted) and point-support simulated models (dashed lines) for nickel and other five elements, in data space, over the horizontal direction (NS in red and EW in black).

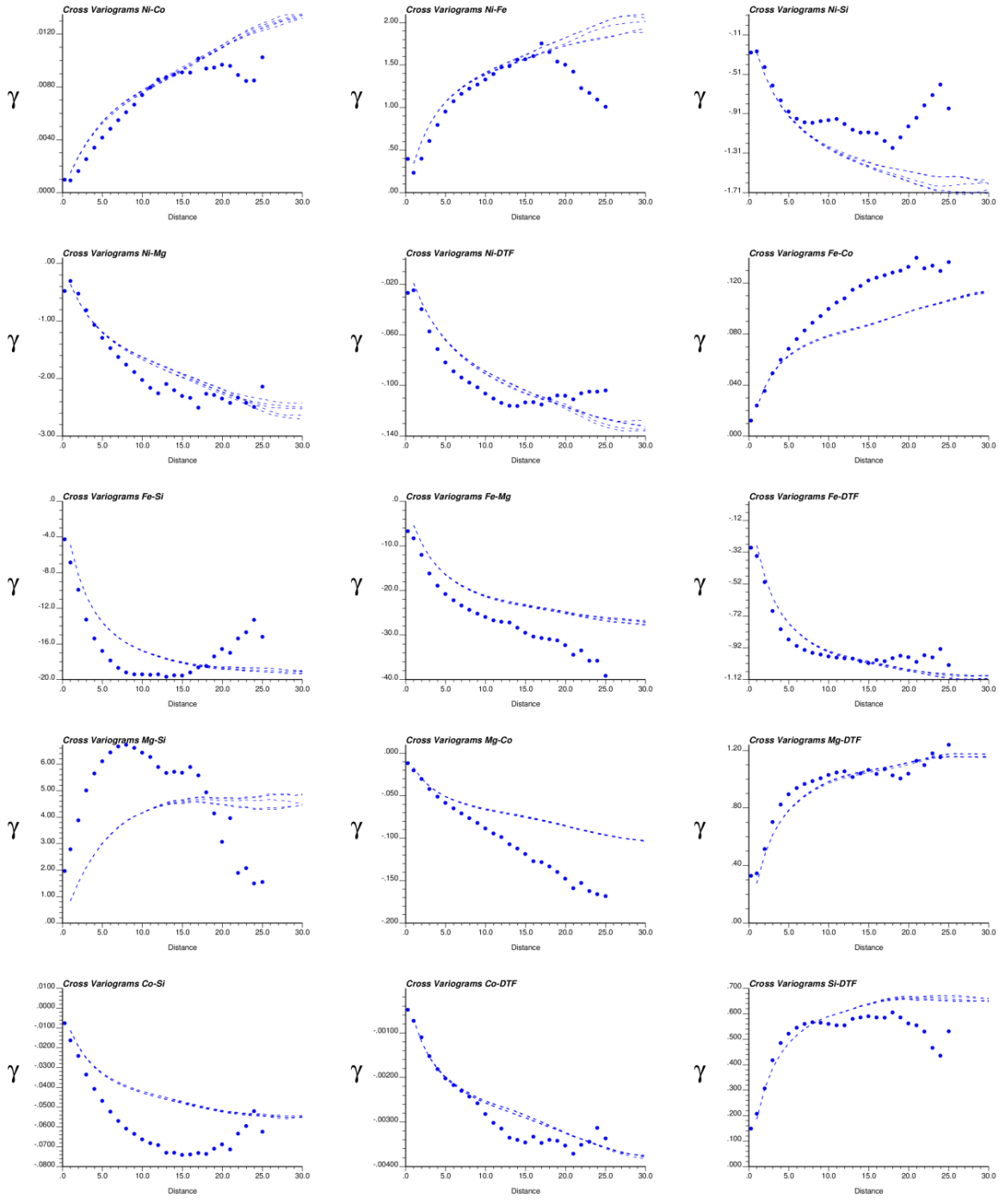

Figure A.4 - Saprolite - Experimental cross-variograms (dotted) and point-support simulated models (dashed lines) for nickel and other five elements, in data space, along the vertical direction.

Appendix B – Complete validation of (cross)variograms, Limonite unit

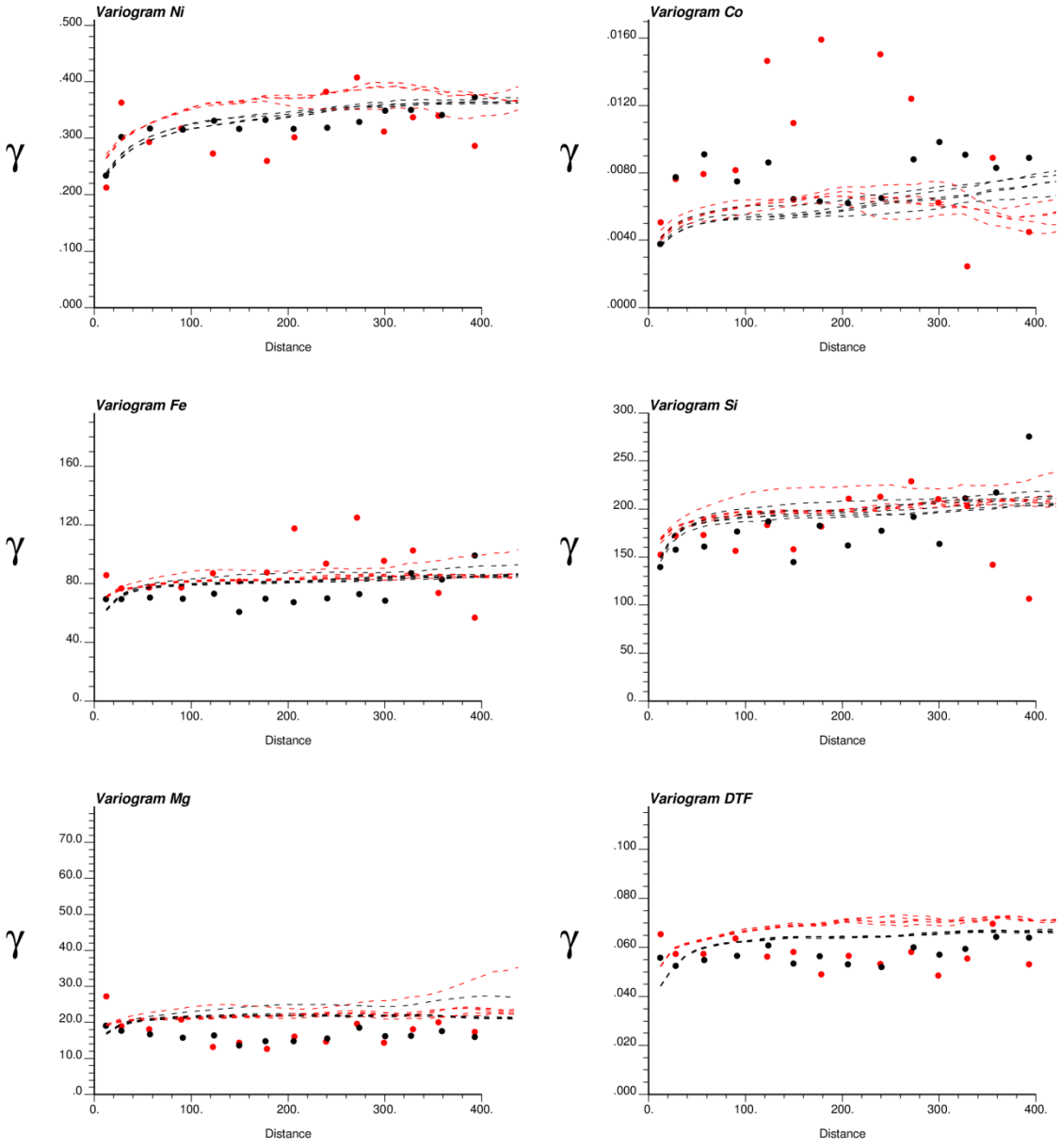

Figure B.1 - Limonite - Experimental direct variograms (dotted) and point-support simulated models (lines) for each element in data space over the horizontal direction (NS in red and EW in black).

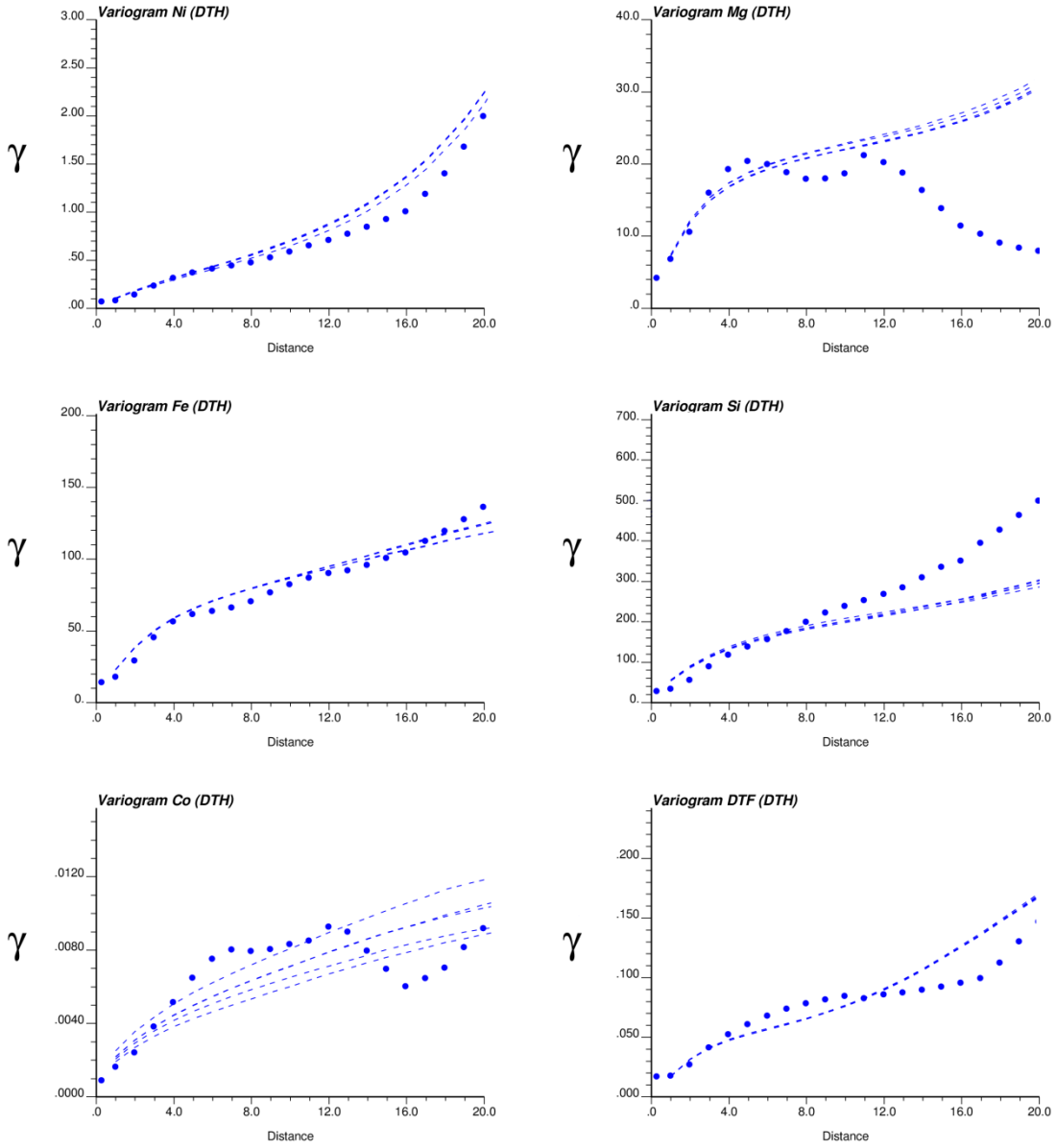

Figure B.2 - Limonite - Experimental direct variograms (dotted) and (point-support) simulated models (lines) for each element in data space along the vertical direction.

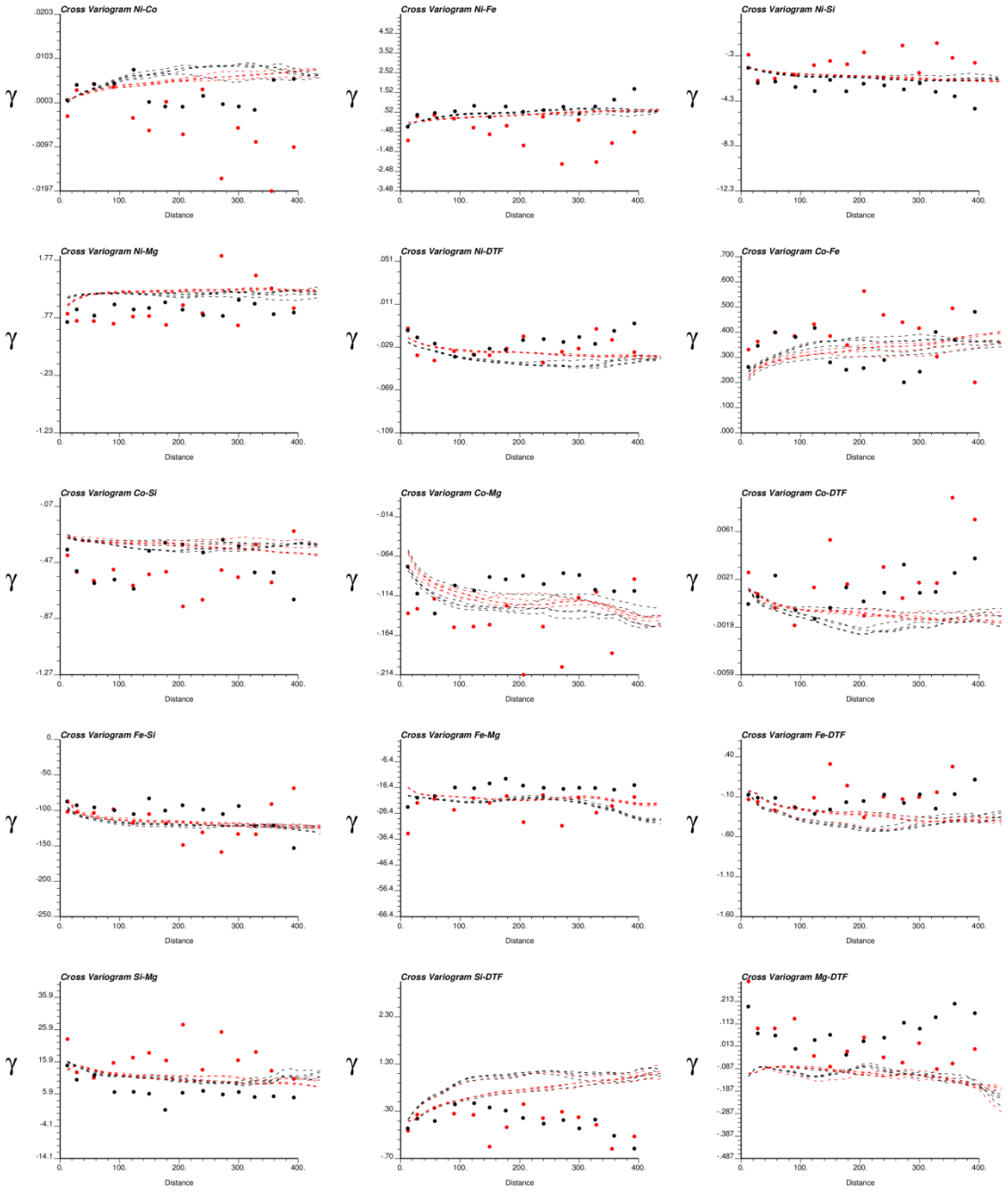

Figure B.3 - Limonite - Experimental cross-variograms (dotted) and point-support simulated models (dashed lines) for nickel and other five elements, in data space, over the horizontal direction (NS in red and EW in black).

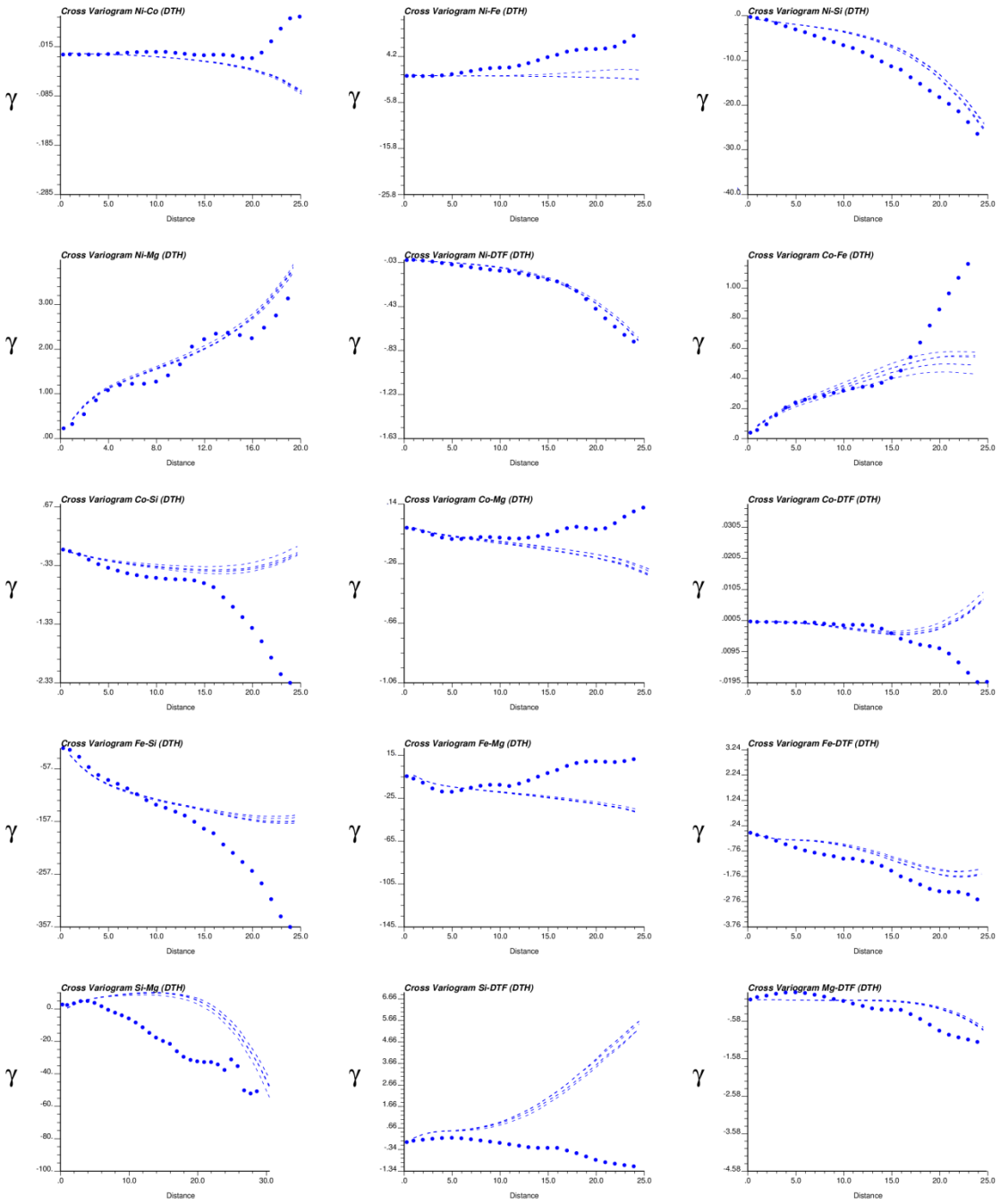

Figure B.4 - Limonite - Experimental cross-variograms (dotted) and point-support simulated models (dashed lines) for nickel and other five elements, in data space, along the vertical direction.